UNIVERSITÀ
DEGLI STUDI
DI PADOVA

Sede Amministrativa: Università degli Studi di Padova

Dipartimento di Geoscienze

SCUOLA DI DOTTORATO DI RICERCA IN SCIENZE DELLA TERRA
CICLO XXIV

Biochronologic and evolutionary study of calcareous nannofossil assemblages during the Middle Eocene Climatic Optimum

Direttore della Scuola : Ch.mo Prof. Gilberto Artioli
Supervisore : Dott.ssa Claudia Agnini

Dottorando : Dott.ssa Federica Toffanin

TABLE OF CONTENTS

SUMMARY

In my PhD project, I've studied calcareous nannofossil assemblages from three different sites during the Middle Eocene Climatic Optimum (MECO). The MECO is a global transient short-lived hyperthermal episode characterized by a global prominent perturbation both in oxygen and carbon stable isotopes, it occurred at Chron C18r-C18n transition (ca. 40 Ma) and lasted ca. 500-600 kyr (Bohaty et al., 2009). It represents a significant climate reversal during the Middle-Late Eocene long-term cooling trend. The MECO event is one of several hyperthermal events occurred in the Paleogene, after the well known Paleocene Eocene Thermal Maximum (Kennett and Stott, 1991). Actually, interest in these issues is raising because they are considered potential analogues in the past of the expected global warming we are going to experience in the next future. The most accredited hypothesis regarding the onset of the MECO warming involves a huge CO_2 degassing event, linked to major plate tectonic reorganization, occurred during the Eocene (Bohaty et al., 2009).

The study sections are located in different depositional settings and geographical areas. In particular, the first study succession, the Alano section, is set in north-eastern Southern Alps of the Veneto region and spans the middle to late Eocene. From a paleogeographic point of view, the section has a paleodepth of 600-1000 m and belongs to the Belluno Basin in the central-western Tethys; the second study section was recovered from IODP Site 1333 during Exp.320 in the Equatorial Pacific. The paleodepth estimate for this Site is ca. 3800 m, while the modern water depth is ca. 4800. The third study section was recovered during ODP Leg 171B located in the Blake Nose (NW Atlantic) with a paleodepth of ca. 1500 m.

The first aim of this study is to verify if there is a unique and global change of calcareous nannofossil assemblages in response to the MECO event. A wide spectrum of paleodepositional settings and locations (Alano section, Site 1051A and U1333C) has been analyzed during this extreme paleoclimatic phase eventually providing paleoenviromental reconstructions based on modifications observed in calcareous nannofossil assemblages. The second aim of this study is focused on biostratigraphic and biochronologic issues related to Middle Eocene to Early Oligocene interval, with a special emphasis on the MECO. Standard and additional biohorizons have been tested and compared with previous data available from literature, providing estimates of the degree of reliability of considered bioevents and of their calibrations.

The first chapter of this thesis is a brief general overview of the early Paleogene paleoclimatic evolution, followed by a description of the study materials and common methods and strategies adopted in this work.

In the second chapter of this thesis, a high resolution study on calcareous nannofossil across the MECO event is presented. Our data from the middle-bathial Alano section indicate that the MECO interval seems to coincide with significant changes in calcareous nannofossil assemblages. Eutrophic/cold taxa and reworked specimens show an overall increase in abundance during the warming event. Conversely, oligotrophic/warm taxa are characterized by a peculiar anticovariant trend with respect to meso-eutrophic taxa, decreasing significantly during the MECO and post-MECO intervals. These results are interpreted as a transient enrichment in dissolved nutrients in warmer sea surface waters and suggest that the enhanced availability of nutrient in the water column overrides other environmental factors in the make-up of calcareous nannofossil assemblage. Morevover, the increase in reworking is consistent with an augment in terrigenous input, likely due to accelerated chemical weathering triggered by the enhanced hydrological cycle.

In the third chapter of this thesis, I provide results of sediments recovered from IODP Exp. 320 (U1333C - Pacific Equatorial Ocean) in a time interval comprised from the Middle Eocene to Early Oligocene. These data show dramatic changes in preservation state, with the number of specimens counted on a specific area (1 mm^2) virtually collapsing to zero during the MECO event. In the same interval, we also observed changes in calcareous nannofossil assemblages that are consistent with strong dissolution phenomena. As already said, a strong decrease of specimens/mm^2 is clear, but a even stronger argument for pervasive dissolution conditions is based on the fact that if we consider the relative abundance (%) of the most resistant genus, *Discoaster*, there is a remarkable increase of this taxon, as it is expected if the pristine assemblages were altered/biased by preferential dissolution. At Site U1333C, the MECO can be considered a semi-barren interval and thus any paleoenviromental inference is definitively hindered. For this reason, I decided to focus on a longer interval with the purpose of providing biostratigraphic and biochronologic datums from one of the rare carbonate successions available for the Middle Eocene to Early Oligocene in the Equatorial Pacific. We used this refined framework to analyze the mode and tempo of evolution of some calcareous nannofossil taxa (i.e., sphenoliths and *Dictycoccites*).

The fourth chapter of this thesis provides a highly resolved documentation of the MECO as recorded from the ODP Site 1051A (NW Atlantic). Our results evidence changes in calcareous nannoflora assemblages during this transient episode of global warming that are consistent with an increase in nutrient availability. Small reticulofenestrids, typically thriving in eutrophic environments and stressed conditions, show a long-term gradual increase in their relative abundance thus suggesting increased nutrient availability of the sea surface waters at ODP Site 1051A. A similar trend is also recorded by eutrophic large *Dictyococcites* which sharply increase in abundance at the same stratigraphic level (LCO) providing a further evidence of a shift toward more eutrophic conditions. This scenario is also supported by the slight decline showed by *Sphenolithus* and *Discoaster*. These genera are considered as k-specialist warm-oligotrophic taxa and their decrease in abundance during a phase of gradual warming is clearly related to an increase of nutrient availability. Finally, if we go into detail on genus *Sphenolithus*, a profound reorganization was found to take place: *S. furcatolithoides* goes extinct, *S. predistentus* and *S. obtusus* firstly appear and most of the other species temporary increase/decrease their abundance. Overall, our data from ODP Site 1051A indicate that changes in calcareous nannofossil assemblages started well after the onset of the MECO and before the peak warming following two different modes, a first type has been defined as abrupt (e.g., the LCO of *Dictyococcites,* the HO of *S. furcatolithoides*) while the second as gradual (the increase of small *Reticulofenestra*).

RIASSUNTO

Durante il mio progetto di dottorato ho studiato le associazioni a nannofossili calcarei provenienti da tre siti nell'intervallo corrispondente al Middle Eocene Climatic Optimum (MECO). Il MECO è un episodio ipertermale transitorio e di breve durata, caratterizzato da un'importante perturbazione a livello globale degli isotopi stabili sia dell'ossigeno che del carbonio, osservato alla transizione tra Chron C18r-C18n (ca. 40 Ma) ha una durata di circa 500-600 kyr (Bohaty et al., 2009). Esso rappresenta un'inversione significativa del clima durante il trend di raffreddamento di lunga durata dell'Eocene medio e superiore. Il MECO è uno tra gli eventi ipertermali, assieme al meglio conosciuto Paleocene Eocene Thermal Maximum, riconosciuti nel Paleogene (PETM, Kennett and Stott, 1991). Attualmente l'interesse verso questi argomenti è crescente perché essi sono considerati potenziali analoghi nel passato dell'atteso riscaldamento globale che sarà in atto nel prossimo futuro. L'ipotesi più accreditata riguardo le cause del MECO è connessa ad un enorme evento di degassazione di CO_2, legato a una importante riorganizzazione delle placche tettoniche avvenuta durante l'Eocene (Bohaty et al., 2009).

Le sezioni studiate sono situate in diversi setting deposizionali e aree geografiche. In particolare la prima successione, la sezione di Alano, è localizzata nelle Alpi nord orientali del Veneto e comprende l'Eocene medio e superiore. Dal punto di vista paleogeografico, la sezione ha una paleoprofondità di 600-1000 m ed è parte del bacino di Belluno, entro la Tetide centro occidentale; la seconda sezione di studio è stata recuperata nell'IODP Site 1333 durante l'Exp.320 svoltasi nel Pacifico Equatoriale. La paleoprofondità stimata per questo Site è di 3800 m, mentre la profondità attuale è ca. 4800 m. La terza sezione di studio è stata recuperata dal Leg ODP 171B nell'area del Blake Nose (Atlantico nord occidentale) ed ha paleoprofondità stimata di ca. 1500 m.

Il primo obiettivo di questo studio è verificare se c'è un cambiamento unico e globale nelle associazioni a nannofossili calcarei in risposta al MECO. Un ampio spettro di setting paleodeposizionali e aree diverse (sezione di Alano, Site 1051A and U1333C) è stato analizzato durante questa fase paleoclimatica estrema e sono state fornite ricostruzioni paleoambientali basate su modificazioni osservate nelle associazioni a nannofossili calcarei. Il secondo obiettivo di questo studio è centrato sulla biostratigrafia e biocronologia dell'intervallo Eocene medio a Oligocene inferiore, con particolare attenzione al MECO. Biorizzonti standard e addizionali sono stati testati e confrontati con

dati precedenti presenti in letteratura, fornendo stime del grado di affidabilità dei bioeventi considerati e delle loro calibrazioni.

Il primo capitolo della tesi è una breve presentazione generale dell'evoluzione paleoclimatica del Paleogene inferiore, seguita dalla descrizione dei materiali di studio e dei metodi e strategie adottate in questo lavoro.

Nel secondo capitolo di questa tesi viene presentato uno studio sui nannofossili calcarei ad alta risoluzione attraverso il MECO. I nostri dati dalla sezione medio batiale di Alano indicano che l'intervallo riguardante il MECO sembra coincidere con cambiamenti significativi nelle associazioni a nannofossili calcarei. Taxa che preferiscono acque eutrofiche/fredde e forme rimaneggiati mostrano un aumento nelle abbondanze durante l'evento ipertermale. Al contrario, taxa con preferenze per acque oligotrofiche/calde mostrano un trend peculiare anticovariante rispetto ai taxa meso-eutrofici, diminuendo in modo significativo durante gli intervalli del MECO e post-MECO. Questi risultati possono essere interpretati come un arricchimento temporaneo dei nutrienti disciolti nelle acque più calde superficiali, e suggeriscono che la aumentata disponibilità di nutrienti nella colonna d'acqua ricopre un'importanza maggiore rispetto ad altri fattori ambientali nel determinare l costituzione dell'associazione a nannofossili calcarei. Inoltre il maggior rimaneggiamento è coerente con un aumentato input di terrigeno, probabilmente dovuto all'accelerato weathering (alterazione) chimico, scatenato dall'aumentato ciclo idrologico.

Nel terzo capitolo di questa tesi, fornisco i risultati dei sedimenti recuperati dall'IODP Site 1333 durante l'Exp.320 nel Pacifico Equatoriale, in un intervallo di tempo compreso tra l'Eocene medio e l'Oligocene inferiore. Questi dati evidenziano un importante cambiamento nello stato di preservazione, con il numero di individui contati entro un'area specifica (1 mm^2) che si avvicinano allo zero durante il MECO. Nello stesso intervallo abbiamo osservato modifiche nelle associazioni a nannofossili calcarei coerenti con un evento di intensa dissoluzione. Oltre alla evidente forte diminuzione di individui/mm^2 già citata, un argomento ancora più forte a favore di condizioni di dissoluzione pervasiva è basato sul fatto che, se consideriamo l'abbondanza relativa (%), *Discoaster*, il genere più resistente, aumenta considerevolmente, come atteso nel caso in cui l'associazione originaria sia alterata da dissoluzione preferenziale. Al Site U1333C, il MECO si può considerare un intervallo semi sterile, quindi nessuna interpretazione paleoambientale è possibile. Per questo motivo ho deciso di focalizzarmi su un intervallo più lungo, con l'obiettivo di ottenere dati biostratigrafici e biocronologici da una delle rare successioni carbonatiche disponibili dall'Eocene medio all'Oligocene inferiore nel Pacifico equatoriale.

Abbiamo usato questo modello per analizzare il modo e tempo dell'evoluzione di alcuni taxa di nannofossili calcarei (i.e., sfenoliti e *Dictycoccites*).

Il quarto capitolo della tesi fornisce una serie di dati ad alta risoluzione del MECO, ottenuti dal Site 1051A (Atlantico nordoccidentale). I nostri risultati evidenziano cambiamenti nelle associazioni a nannofossili calcarei durante questo episodio transitorio di riscaldamento globale coerenti con un aumento nella disponibilità di nutrienti. I reticulofenestridi di piccole dimensioni, che tipicamente prosperano in ambienti eutrofici e in condizioni di stress, mostrano un aumento graduale di lunga durata nelle loro abbondanze relative, suggerendo quindi una aumentata disponibilità di nutrienti nelle acque superficiali dell'ODP Site 1051A. Un andamento simile si registra anche nei *Dictyococcites* di grandi dimensioni, eutrofici, che aumentano bruscamente in abbondanza allo stesso livello stratigrafico (LCO), fornendo una ulteriore evidenza di uno shift verso condizioni più eutrofiche. Questo scenario è supportato anche dal lieve declino che si evidenza in *Sphenolithus* e *Discoaster*. Questi generi sono considerati taxa di acque calde ed oligotrofiche, K-specialisti, e la loro diminuzione in abbondanza durante una fase di graduale riscaldamento è chiaramente correlabile ad un aumento dei nutrienti disponibili. Infine, entrando all'interno del genere *Sphenolithus*, si è osservata una profonda riorganizzazione, *S. furcatolithoides* si estingue, *S. predistentus* e *S. obtusus* fanno la loro prima comparsa, e molte delle altre specie subiscono aumenti o diminuzioni temporanee delle loro abbondanze. Nel complesso, i dati provenienti dal Site ODP 1051A indicano che i cambiamenti nelle associazioni a nannofossili calcarei sono iniziati molto dopo l'inizio del MECO e prima del picco di riscaldamento, presentando due diversi andamenti: un primo tipo può essere definito brusco (ad es. la LCO di *Dictyococcites*, la HO di *S. furcatolithoides*), mentre un secondo tipo è graduale (ad es. l'aumento delle *Reticulofenestra* di piccole dimensioni).

References

Bohaty, S.M., Zachos, J.C., Florindo, F., Delaney, M.L. 2009. Coupled greenhouse warming and deep-sea acidification in the middle Eocene Paleoceanography 24 , PA2207.

Kennett, J.P., Stott, L.D., 1991. Abrupt deep-sea warming, palaeoceanographic changes and benthic extinctions at the end of the Palaeocene. Nature 353, 225–229.

CHAPTER 1 - Introduction

During the Cenozoic Earth's climate has undergone major modifications. The early Paleogene, namely the interval between the K-Pg (ca. 66.0 Ma; Charles et al., 2011) and the Eocene/Oligocene boundary (ca. 33.4 Ma, O1 event, Miller et al., 1991), represents the transition from a world without any permanent ice-sheet at the poles to a world with a well established Antarctic ice-sheet. During this time, a 5 Myr long global warming trend began in the late Paleocene and climaxed in the early Eocene climatic optimum (EECO; ca. 50 Ma) was followed by ca.15 Myr cooling trend that eventually led to the modern icehouse world. This long transition in the Earth climatic system is referred to as the doubthouse world (Zachos et al., 2001), its mode and tempo are still poorly known, but it is becoming more and more evident that the middle-late Eocene transition was not gradual or monotonic, as evidenced by previous works (e.g., Diester Haas and Zahn, 1996), but instead characterized by multiple episodes of extreme climates (e.g., Bohaty and Zachos, 2003; Sexton et al, 2006, Edgar et al., 2007; Bohaty et al., 2009).

One prominent episode of significant climatic instability during this interval is the hyperthermal event referred to as the Middle Eocene Climatic Optimum (MECO). The MECO event was recently revisited by Bohaty and co-authors (2009), who define its timing and nature. It is now commonly accepted that the MECO is a global short-lived warming episode aged ca. 40 Ma, within Chron C18r. It is characterized by a temperature raise of ca. 4-6 °C both of surface and deep waters and a total duration of ca. 500 kyr. A direct link was also proposed between the increase in temperature and changes in ocean chemistry, and the augment in greenhouse gas concentration (Bohaty et al., 2009; Spofforth et al., 2010).

Foraminiferal and bulk oxygen isotope data from several sections indicate 4-6 °C raising temperatures of both surface and deep waters and altered ecological conditions during the MECO (Agnini et al., 2011; Bohaty et al., 2009; Luciani et al., 2010; Spofforth et al., 2010) that lasted for ca. 500 kyr. One of the causes suggested to explain the onset of this warming phase is a massive influx of CO_2 in the ocean-atmosphere system (Bohaty et al., 2009; Spofforth et al., 2010). If it is the case, the MECO as some other short–lived episodes of global warming documented in the geological record, may represent good analogues of the ongoing CO_2 antropogenic emission and could be thus used to improve our understanding of causes, mode and tempo of these extreme climates in prespecting of predicting/modeling what we are going to experience in the near future. The Earth's

climate evolution results from a complex interaction between biological (biotic) and chemo-physical (abiotic) factors. The undestanding of the mechanisms determining the relationship between biotic evolution and Earth's environmental system represents a key point for a better comprehension of global changes through time (Erba, 2006). Solving this issue obviously needs a multi-approach effort and, in this contest, I decided to focus on the fossil assemblages of one of the main players of the sea-surface waters, the calcareous phytoplankton.

Calcareous nannofossils are the external calcified scales (coccoliths) produced by unicellular phytoplanctonic algae mainly belonging to Haptophyta (Edvardsen et al., 2000). These organisms secrete calcitic plates comprised between 1 and 30 μm in size. Every single cell has an extracellular cover made up of numerous (10-100) coccoliths, that is called coccosphere. Following the death of the organism, the coccosphere breaks up and disarticolated coccoliths sink through the water column finally reaching the sea floor (Winter and Siessier, 1994; Young et al., 1997).

Calcareous nannofossils are the most important components of deep-sea oozes and chalks, and thus have great potential for providing key floral, isotopic and biomarker signals that can be used to analyze and interpret global changes in the geological record. Their rapid evolutionary rates make them exceptionally valuable as a biostratigraphic tool and provide huge potential for testing evolutionary hypotheses (Thierstein and Young, 2004).

Prominent changes in calcareous nannofossils assemblages are routinely used to integrate parallel modifications in the physical paleoenvironmental proxies trying to interpret paleoclimatic and paleoceanographic conditions. Calcareous nannoplankton have played a vital role in the global carbon cycle since the Mesozoic Era by supplying organic carbon and calcium carbonate to the deep ocean (Hay, 2004). The distribution of nannoplankton in modern oceans is controlled by factors such as temperature, nutrients, light and salinity, and their ecological preferences go to sea surface waters with low nutrient availability and warm temperatures even if some taxa are able to thrive also in more eutrophic/cold environments, where they are usually overridden by siliceous phytoplankton (Okada and Honjo, 1973; Hallock et al., 1987). Their sensitivity to enviromental changes is used as an excellent proxy resource, with a number of taxa having become established as paleotemperature and/or paleofertility indicators (Haq and Lohmann, 1976 Haq et al., 1977; Lees et al., 2005). In this context, the study of calcareous nannofossil assemblages before, during and after the MECO in different areas and

depositional settings, that is the topic of this work, points out any possible change in the phytoplankton community and eventually correlates these modifications with changes in the physical enviroment. Our micropaleontological data have been integrated with geochemical proxies, when available, in order to provide more reliable paleoenvironmental reconstructions of the MECO event.

Materials

This PhD thesis is based on data generated from three sedimentary successions in which the MECO interval is recorded:

The marine on-land section of the Alano di Piave (Southern Alps, NE Italy), which is located in the Veneto region, a classical area for the study of the early Paleogene (e.g. Bolli, 1975; Channell et al., 1979; Channell and Grandesso, 1987; Channell et al., 1987; Giusberti et al., 2007);

The IODP Site U1333C recovered in the Pacific Equatorial Ocean during Exp. 320, which represents one the rare successions with carbonates in the Equatorial Pacific during this time interval;

The ODP Site 1051A recovered in the Blake Nose (NW Atlantic Ocean) during Leg171B, which consists of well preserved carbonate sediments and are used as a reference section for this interval.

Methods

Smear slides were prepared for all the studied samples following standard methods from unprocessed material and examined by an optical microscope at a 1250X magnification. Overall, the taxonomy used is that illustrated in Perch-Nielsen (1985) and Aubry (1984; 1988; 1989; 1990; 1999), except when it is differently specified.

During this study, I have adopted several different counts depending on the information I would like to achieve. In particular, relative abundances of species and genera, expressed in percentage, were calculated on at least 300 specimens for all the three datasets. Semiquantitative data are also determined counting all calcareous nannofossil specimens present in a prefixed area of 1 mm^2 or 9 mm^2. In addition, I have calculated the species abundance within a genus, counting a total of 100 specimens belonging to same genus (Rio et al., 1990). Resulting data were put in graphic form in order to investigate if any relationship between abundance variations in paleoecological groups and changes in paleoecological conditions may exist.

Work strategy and plan

The first year of work was devoted to analyze samples (ca. 100) from the Alano section (Italy), where we performed a high resolution micropaleontological analysis spanning the MECO interval. From the biostratigraphic point of view, the section is all comprised within calcareous nannofossil Zone NP16 or CP14a (Martini, 1971; Okada and Bukry, 1980). In the second year of work, I analyzed ca. 109 samples recovered in 2009 from IODP Expedition 320 in the Pacific Equatorial. The study succession encompasses nannofossil Zones NP16–NP21 (Martini, 1971), that is from the Middle Eocene to the Early Oligocene. At this site I performed calcareous nannofossil analysis with a particular emphasis on biostratigraphy. During the third year I completed analyzes of ca. 72 samples recovered from ODP Site 1051A (NW Atlantic). The study interval spans calcareous nannofossil Zone NP16 or CP14a (Martini, 1971; Okada and Bukry, 1980) and was chosen to document the response of calcareous nannofossil assemblages to the MECO event in the Blake Nose reference section.

The studies carried out at these three sites have been reported in the following chapters:

-In Chapter 2, the results from the Alano section are described, the nannofossil dataset has been compared with geochemical proxies available for the MECO interval of this section, and eventually points out interesting relations between biotic evolution and abiotic changes.

-In Chapter 3, a high resolution biostratigraphic study on calcareous nannofossil assemblages at the Pacific Equatorial site is presented. This dataset is affected by strong dissolution, which results in a very badly preserved nannofossil assemblages at this deep ocean site.

-In Chapter 4, I reported results from NW Atlantic Blake Nose site. Once again, our data indicate that major variations seem to occur in the calcareous nannofossil assemblage. The peculiarity of this site lies in its early response to the MECO. Changes in calcareous nannofossil assemblages start well before the peak warming of the MECO and likely correlate with the gradual negative oxygen shift within Chron C18r.

References

Agnini C., Fornaciari E., Giusberti L., Grandesso P., Lanci L., Luciani V., Muttoni G., Rio D., Stefani C., Pälike H. and Spofforth D.J.A, 2011 Integrated bio-magnetostratigraphy of the Alano section (NE Italy): a proposal for defining the Middle-Late Eocene boundary, Geological Society of America Bulletin.

Aubry, M.-P., 1984. Handbook of Cenozoic Calcareous Nannoplankton, book 1, Ortholithae (Discoaster). Am. Mus. of Nat. Hist. Micropaleontol. Press, New York. 263 pp.

Aubry, M.-P., 1988. Handbook of Cenozoic Calcareous Nannoplankton, book 2, Ortholithae (Holococcoliths, Ceratoliths, Ortholiths and Other). Am. Mus. of Nat. Hist.Micropaleontol. Press, New York. 279 pp.

Aubry, M.-P., 1989. Handbook of Cenozoic Calcareous Nannoplankton, book 3, Ortholithae (Pentaliths and Other), Heliolithae (Fasciculiths, Sphenoliths and Others). Am. Mus. of Nat. Hist. Micropaleontol. Press, New York. 279 pp.

Aubry, M.-P., 1990. Handbook of Cenozoic Calcareous Nannoplankton, book 4, Heliolithae (Helicoliths, Cribriliths, Lopadoliths and Other). Am. Mus. of Nat. Hist.Micropaleontol. Press, New York. 381 pp.

Aubry, M.-P., 1999. Handbook of Cenozoic Calcareous Nannoplankton, book 5, Heliolithae (Zygoliths and Rhabdoliths). Am. Mus. of Nat. Hist.Micropaleontol. Press, New York. 368 pp.

Bohaty S. M., and Zachos, J. C., 2003. Significant Southern Ocean warming event in the late middle Eocene, Geology, 31(11), 1017– 1020, doi:10.1130/G19800.1

Bohaty S. M., Zachos J. C., Florindo F., Delaney M. L. 2009, Coupled greenhouse warming and deep-sea acidification in the middle Eocene, Paleoceanography, 24, PA2207.

Bolli, H.M., ed., 1975, Monografia Micropaleontologica sul Paleocene e l'Eocene di Possagno, Provincia di Treviso, Italia: Schweizerische Palaeontologische Abhandlungen, v. 97, 222 p.

Channell, J.E.T., D'Argenio, B., and Horvath, F., 1979, Adria, the African promontory in Mesozoic Mediterranean palaeogeography: Earth-Science Reviews, v. 15, p. 213–292, doi: 10.1016/0012-8252(79)90083-7.

Channell, J.E.T., and Grandesso, P., 1987. A revised correlation of Mesozoic polarity chrons and calpionellid zones.Earth Planetary Science Letters, v. 85, pp. 222-240.

Channell, J.E.T., Bralower, T.J., and Grandesso, P., 1987. Biostratigraphic correlation of Mesozoic polarity chrons CM1 to CM23 at Capriolo and Xausa (Southern Alps, Italy). Earth and Planetary Science Letters, v. 85, pp. 203-221.

Charles, A.J., Condon, D.J., Harding, I.C., Pälike, H. Marshall, J.E.A., Cui, Y., Kump, L., Croudace, I. W. and WUN PACE Group (2011) Constraints on the numerical age of the Paleocene/Eocene boundary, Geochemistry, Geophysics, Geosystems, 12, Q0AA17. (doi:10.1029/2010GC003426).

Diester-Haass, L., and Zahn, R., 1996, Eocene–Oligocene transition in the Southern Ocean: History of water mass circulation and biological productivity: Geology, v. 24, p. 163–166.

Edgar, K.M., Wilson, P.A., Sexton, P.F. and Suganuma, Y., 2007. No extreme bipolar glaciation during the main Eocene calcite compensation shift. Nature, 448:908-911.

Edvardsen, B., Eikrem, W., Green, J.C., Andersen, R.A., Monn-Van der Staay, S.Y., Medlin, LK, 2000. Phylogenetic reconstructions of Haptophyta inferred from 18S ribosomal DNA sequence and available morphological data. Phycologia 39, 19-35.

Erba, E., 2006 The first 150 million years history of calcareous nannoplankton: Biosphere–geosphere interactions. Palaeogeography, Palaeoclimatology, Palaeoecology 232 (2006) 237–250.

Giusberti, L., Rio, D., Agnini, C., Backman, J., Fornaciari, E., Tateo, F. and Oddone, M. 2007, Mode and tempo of the Paleocene Eocene thermal maximum in an expanded section from the Venetian pre-Alps, Geol. Soc. Am. Bull., 119, 391–412, doi:10.1130/B25994.1.

Hallock, P., 1987 Fluctuations in the trophic resource continuum: A factor in global diversity cycles? Paleoceanography, vol. 2, no. 5, 457-471, doi:10.1029/PA002i005p00457

Haq, B.U. and Lohmann, G.P., 1976. Early Cenozoic Calcareous nannoplankton biogeography of the Atlantic Ocean: Marine Micropaleo., v. 1, p. 120-197.

Haq, B.U., Premoli Silva, I., Lohmann, G.P., 1977. Calcareous plankton paleobiogeographic evidence for major climatic fluctuations in the Early Cenozoic Atlantic Ocean. J. Geophys. Res. 82, 3861–3876.

Hay, W.W., 2004. Carbonate fluxes and calcareous nannoplankton. In: Thierstein, H.R., Young, J.R. (Eds.), Coccolithophores. From Molecular Processes to Global Impact. Springer-Verlag, Berlin, pp. 509–528.

Lees, J.A., and Bown, P.R., 2005. Upper Cretaceous calcareous nannofossil biostratigraphy, ODP Leg 198 (Shatsky Rise, northwest Pacific Ocean). *In* Bralower, T.J., Premoli Silva, I., and Malone, M.J. (Eds.), Proc. ODP, Sci. Results, 198 [Online]. Available from World Wide Web: <http://www-odp.tamu.edu/publications/198_SR/114/114.htm>.

Luciani, V., Giusberti, L., Agnini, C. Fornaciari, E., Rio, D., Spofforth, D.J.A., Pälike, H.. 2010. Ecological and evolutionary response of Tethyan planktonic foraminifera to the middle Eocene climatic optimum (MECO) from the Alano section (NE Italy), Palaeogeography, Palaeoclimatology, Palaeoecology 292 (2010) 82–95.

Martini E., 1971, Standard Tertiary and Quaternary calcareous nannoplankton zonation, in Farinacci, A., ed., Proceedings, International Conference on Planktonic Microfossils, second, Rome, Volume 2: Rome, Italy, Tecnoscienza Editzione, p. 739-785.

Miller, K.G., Wright, J.D., and Fairbanks, R.G., 1991. Unlocking the Ice House: Oligocene–Miocene oxygen isotopes, eustasy, and margin erosion. J. Geophys. Res., 96:6829–6848.

Okada, H. and Honjo, S., 1973. The distribution of oceanic coccolithophorids in the Pacific. Deep Sea Research, 20: 55–374.

Okada, H., and Bukry, D., 1980. Supplementary modification and introduction of code numbers to the low-latitude Coccolith biostratigraphic zonation, (Bukry, 1973; 1975). Mar. Micropaleontol., 5:321-325

Perch-Nielsen, K. 1985, Cenozoic calcareous nannofossils. In Bolli H.M., Saunders J.B., Perch-Nielsen K. Plankton Stratigraphy. Cambridge University Press, pp.427-554.

Rio, D., Raffi, I., Villa, G., 1990. Pliocene–Pleistocene calcareous nannofossil distribution patterns in the western Mediterranean. Proc. Ocean Drill. Program Sci. Results 107, 513–533.

Sexton, P. F., Wilson, P. A., and Norris, R. D., 2006. Testing the Cenozoic multisite composite δ18O and δ13C curves: New monospecific Eocene records from a single locality, Demerara Rise (Ocean Drilling Program Leg 207), Paleoceanography, 21, PA2019, doi:10.1029/2005PA001253.

Spofforth D.J.A., Agnini C., Pälike H., Rio D., Fornaciari E., Giusberti L:, Luciani V., Lanci L., and Muttoni G., 2010. Organic carbon burial following the middle Eocene climatic optimum in the central western Tethys, Paleoceanography, 25, PA3210, doi:10.1029/2009PA001738.

Thierstein and Young, 2004 Winter, A., Siesser, W.G. editors. Coccolithophores. ix, 242p. Cambridge University Press, 1994

Young, J.R., Bergen, J.A., Bown, P.R., Burnett, J.A., Fiorentino, A., Jordan, R.W., Kleijne, A., Niel, B.E. van, Romein, A.J.T. and Salis, K. von, 1997. Guidelines for coccolith and Calcareous nannofossil terminology. Palaeontology: [Journal of the Palaeontological Association], 40/4, 875-912.

Zachos, J., Pagani, M., Sloan, L., Thomas, E., and Billups, K., 2001, Trends, rhythms, and aberrations in global climate 65 Ma to present: Science, v. 292, p. 686–693.

CHAPTER 2 - Changes in calcareous nannofossil assemblages during the Middle Eocene Climatic Optimum: Clues from the central-western Tethys (Alano section, NE Italy).

Abstract

We present a study focused on changes in calcareous nannofossil assemblages of the Alano section during the Middle Eocene Climatic Optimum (MECO). This warming event is characterized by a prominent perturbation both in oxygen and carbon stable isotopes around the Chron C18r-C18n transition (ca. 40 Ma) and lasting ca. 500-600 kyr. Semi-quantitative analyses on calcareous nannofossil assemblages have been carried out. Our results show that the MECO interval coincides with a significant shift in the relative abundance of calcareous nannofossil taxa, suggesting a relationship between biotic changes and stable isotope shifts. Paleoecological studies at species level and/or based on morphometric criteria (i.e., small placoliths) sometimes show the opposite behaviour between changes observed at the genus level and those observed at lower taxonomic levels. For instance, a taxon thought to be better adapted to oligotrophic/warm waters, e.g. *Sphenolithus*, shows a prominent decrease if analyzed at genus level, but an increase was instead recorded for *S. spiniger.* Moreover, taxa preferentially thriving in eutrophic/cold waters, as for instance small reticulofenestrids, increase remarkably in abundance during this warming phase, while medium-large placoliths do not show any significant trend. An increase in reworked, mainly Cretaceous, specimens is also observed during the MECO. These lines of evidence are consistent with a transient enrichment in dissolved nutrients in warmer sea surface waters suggesting that an enhanced nutrient availability could have driven the make-up of the calcareous nannofossil assemblages. The increase in reworking may indicate an increase in terrigenous input, due to increased chemical weathering likely produced by an enhanced hydrological cycle.

1. Introduction

The global deep-sea oxygen isotope compilation available for the Cenozoic indicates that the Earth climate has fluctuated widely during Earth's history (Zachos et al., 2008). The middle to late Eocene, i.e. the interval between the Early Eocene Climatic Optimum (EECO; ca. 50 Ma) and the Eocene/Oligocene boundary (33.4 Ma, O1 event, Miller et al., 1991), represents the transition from a world without any permanent ice-sheet at the poles to one with a permanent Antarctic ice cap.

A 5 Myr long global warming trend that began in the late Paleocene and climaxed during the EECO was followed by a ca. 15 Myr cooling trend that eventually resulted into an icehouse world. The mode and tempo of this important transition of the Earth's climatic system remains still poorly known, but it is becoming more and more evident that the middle-late Eocene transition was not gradual or monotonic, but instead characterized by a succession of episodes with extreme climates (Diester Haas and Zahn; 1996; Wade and Kroon, 2002; Bohaty and Zachos; 2003; Tripati et al., 2005a; b; Edgar et al., 2007).

Recent deep-sea drilling has paid considerable attention to Paleogene climate evolution, including several expeditions in the Atlantic and Pacific Oceans in the last decade (ODP Legs 199, 207, 208; IODP Exp. 320-321; Lyle at al., 2002; Erbacher et al., 2004; Zachos et al., 2004; Pälike et al., 2010; Lyle et al., 2010). Detailed paleoclimate records generated from this new material reveal significant high frequency (10-100kyrs) climate variability superimposed on the long-term cooling trend.

First, there is a long lasting temporal reversal in the cooling trend observed between 44 and 42 Ma in benthic foraminiferal oxygen isotope records from the equatorial Atlantic (Sexton et al. 2006). At shorter timescales (10-100kyrs), there are a number of marked warming and cooling events that punctuate the middle and late Eocene. A bipolar glaciation, albeit controversial, was thought to have taken place in concomitance with a deepening of the CCD at ca. 41.6 Ma (Tripati et al., 2005a; b; Edgar et al., 2007; Burgess et al., 2008; Dawber et al., 2011; Dawber and Tripati, in press). Immediately preceding this cooling, Edgar et al. (2007) identified a rapid transient warming event within Chron 19r. Subsequent to this, the longer and more prominent, Middle Eocene Climatic Optimum (MECO) event has now been documented at many localities, with a peak warming around ~40.0Ma (Bohaty et al., 2009). There is also a reversal to the general late Eocene cooling trend, the late Eocene warming event, at ~36Ma (Bohaty and Zachos, 2003).

The MECO event was recently revisited by Bohaty and co-authors (2009), who carefully tried to address a number of unresolved questions regarding the timing and

nature of this peculiar paleoceanographic event. Their compilation of existing and new data indicates that the MECO is a global event of ~500kyr duration, expressed as a temperature rise of ca. 4-6ºC in both surface and deep-waters. A direct link was also proposed between the increase in temperature and changes in ocean chemistry, and a rise in greenhouse gas concentrations (Bohaty et al., 2009; Spofforth et al, 2010).

High resolution geochemical datasets are available from multiple sites located in both the Northern and Southern hemispheres, but direct comparisons between geochemical and paleontological signals are rare. One of the specific goals of this study consists in integrating geochemical proxies and calcareous nannofossil data achieved from a middle-bathyal succession, the Alano section, located in north-eastern Italy (Agnini et al., 2011). Calcareous nannofossils are an excellent proxy resource with a number of taxa showing distinct responses to paleoenvironemental change, including to temperature and paleofertility (e.g. Bralower 2002; Gibbs et al., 2006; Dunkley Jones et al., 2008).

We have performed a high resolution study of calcareous nannoflora assemblages before, during, and after the MECO to investigate their response to this transient episode of global warming. These paleontological data have been integrated with geochemical proxies in order to provide a more reliable paleoenviromental reconstruction of the MECO interval.

2. Geological setting, bio-magnetochronostratigraphic framework and geochemistry of the Alano section

2.1. Geological setting

The Alano section is located in the Southern Alps of NE Italy (latitude 45°54'51.10"N, longitude 11°55'4.87"E; Fig. 1). This area belongs to the Belluno Basin, a paleogeographic domain formed in the Jurassic by the regional rifting that eventually led to the break up and consequent collapse of Triassic shallow water carbonate platforms (Winterer and Bosellini, 1981). From that time on, hemipelagic sedimentation persisted until the late Eocene in this part of the Southern Alps (Grandesso, 1976, Stefani and Grandesso, 1991; Agnini et al., 2011). The section crops out for ca. 500 m near the Alano di Piave village along the Calcino creek. It consists of monotonous greyish hemipelagic marls with intercalated silty-sandy layers or bio-calcarenite-rudite beds. Between the 17 and 25 m stratigraphic level, we observed a prominent change in the lithology from grey marls to laminated organic-enriched sediments. This interval is divided into two subintervals, the ORG1 and ORG2 of

Spofforth et al. (2010), by a ca. 2 m-thick grey marl bed. The measured section is about 105 m thick (Agnini et al, 2011). In the present work, we will focus on the lower part of the section, from 10 to 30m, which spans the MECO (Spofforth et al. 2010; Agnini et al. 2011). An estimate based on benthic foraminifera suggests a mid-bathyal paleodepth for the lower part of the Alano section (Agnini et al., 2011).

2.2. Biomagnetostratigraphic framework

Previous data produced for the Alano section provide the integrated bio-magnetostratigraphy used in this work (Agnini et al., 2011), which is summarized below. The study interval spans Chrons C18r and C18n. In terms of calcareous nannofossils, the simultaneous presence of *Chiasmolithus solitus, Cribrocentrum reticulatum* and *Reticulofenestra umbilicus* allows an assignment to nannofossil Zones NP16/CP14a (Martini, 1971, Okada and Bukry, 1980; Fig. 2). With regard to planktic foraminifera, the basal part of the section up to 14.40 m level is assigned to the upper part of the combined Zones E10/E11, whereas the interval from 14.40 to 19.50 m level belongs to Zone E12, and the interval between 19.5 and 57.52 m is assigned to Zone E13 (Berggren and Pearson, 2005, Fig. 2).

2.3. Geochemical data

Geochemical data from the Alano section are provided by Spofforth et al. (2010). A characteristic pattern of gradually decreasing oxygen isotope values at the top of C18r, followed by a more rapid recovery back to more positive values, allows for the reliable identification of the MECO interval (Bohaty et al. 2009). At Alano, the MECO is also characterized by a prominent decrease in $CaCO_3$ content, a significant increase in the concentration of sulphur and redox-sensitive trace metals, very low concentrations of Mn and occurrence of pyrite (Spofforth et al., 2010).

From ~17 to ~25 m, the sedimentation of monotonous grayish marls is suddenly interrupted by a 8 m-thick dark and laminated sapropel-like sediments, which, in turn, consist of two organic-enriched intervals, the ORG1 and ORG2 of Spofforth et al. (2010).

The MECO event was originally defined on the basis of a transient negative excursion in $\delta^{18}O$ (Bohaty and Zachos, 2003), with the peak warming conditions corresponding to lowest $\delta^{18}O$ values at Chron C18r/C18n.2n transition (Bohaty et al., 2009). Similarly with data available for the Southern Ocean, a rapid return to pre-excursion conditions is also observed in $\delta^{18}O$ values (Bohaty et al., 2009). Superimposed on this $\delta^{18}O$ shift, $\delta^{13}C$

shows more variability at Alano, which includes a negative shift, coincident with an oxygen isotope excursion, followed by a rapid increase in $\delta^{13}C$ values at the base of the ORG1 interval. At the Alano section maximum positive $\delta^{13}C$ values are associated with the sedimentation of organic-rich intervals, that represent the lithologic expression of what is named the post-MECO event after Luciani et al. (2010).

3. Materials and methods

The study interval spans from the 10 to 30 m level, with a sampling resolution of 20 cm represented by ca. 100 samples. Samples were prepared from unprocessed sediment as smear slides for nannofossil analysis using standard techniques (Bown and Young, 1998). Smear slides were then analyzed with an optical microscope, at 1250 magnification. Calcareous nannofossils were determined using taxonomic concepts of various authors (Aubry, 1984; 1988; 1989; 1990; 1999; Perch-Nielsen, 1985; Bown, 2005), except for sphenoliths that were classified following Fornaciari et al. (2010) and *Reticulofenestra* and *Dictyococcites* that were grouped by size. The biostratigraphic schemes adopted are those of Martini (1971) and Okada and Bukry (1980).

A qualitative approach was firstly used in each sample to evaluate the state of preservation of calcareous nannofossil assemblages (Table 1 supplementary data, see attached CD for Alano supplementary data). Overall, the preservation varies throughout the succession. The critical interval, the MECO and post-MECO, is characterized by a decrease in the degree of preservation, that ranges from moderate below and above the critical interval to moderate to poor during the core of the event.

Quantitative analyses were then carried out by determining the relative abundances of species and genera, expressed in percentage, based on at least 300 specimens. The relative frequencies of species belonging to the genera *Discoaster* and *Sphenolithus* were determined by counting a prefixed number of taxonomically related forms: 100 sphenoliths and 30 discoasterids (Rio et al. 1990). Additional counts were carried out in a prefixed area of 1 mm^2 (50 fields) or 9 mm^2 (three transects). In particular, we determined all the calcareous nannofossils present in 1 mm^2. A further counting was also performed on very rare taxa, such as species belonging to the genus *Chiasmolithus*, in order to provide a more reliable biostratigraphic framework, which is essentially based on the presence of *C. solitus*.

The calcareous nannofossil dataset was integrated with independent geochemical/mineralogical proxies that document modified environmental conditions

during the MECO. Changes in relative abundance of calcareous nannofossil taxa are thus correlated with changes in ecological factors. Although there is a certain degree of uncertainness, there is a general agreement that some nannofossil species can be interpreted as reflecting distinct paleoecological conditions (e.g., Haq and Lohmann, 1976; Wei and Wise, 1990a; Aubry, 1998; Bralower, 2002). Prominent changes in calcareous nannofossils assemblages are routinely used to corroborate parallel modifications in the physical paleoenvironmental proxies, in an attempt to interpret changes in paleoclimatic and paleoceanographic conditions (Agnini et al, 2006, 2007a; 2007b; Tremolada and Bralower, 2004; Raffi et al., 2005; Gibbs et al., 2006; Mutterlose et al, 2007).

3.1. Paleoecological affinities and significant modifications in calcareous nannofossil assemblages during the MECO

There have been many efforts during the past three decades to disentangle the role of temperature and nutrient supply on the relative abundance fluctuations in Cenozoic calcareous nannoplankton assemblages (e.g. Haq and Lohmann, 1976; Haq et al., 1976; Wei and Wise, 1990; Chepstow-Lusty et al., 1991; Aubry, 1992; Winter et al., 1994; Aubry, 1998). The assignment of environmental preferences for individual taxa is difficult to establish. Until today, no comprehensive paleotemperature and paleofertility model has been proposed, essentially because the environmental factors influencing the biogeographical distribution of taxa through time are interconnected with each other in highly complex ways (Agnini et al., 2007a). Here, we try to interpret changes in calcareous nannofossil assemblages observed in the Alano section in terms of environmental modifications. Variations in lithology and $\delta^{18}O$, that are thus used as independent geochemical/mineralogical proxies, provide a starting point. In particular, oxygen isotope measurements on bulk sediments from the Alano section suggest raised temperatures and altered ecological conditions during the MECO and post-MECO (Spofforth et al., 2010), and the relative increase in terrigenous components likely indicates an enhanced sediment supply from the mainland. In principle, increase or decrease in relative abundance of calcareous nannofossil taxa is directly correlated with modifications of physical environment indicators archived in sediments. The comparison between the two datasets permits us to interpret modifications in relative abundance of calcareous nannofossil taxa in terms of paleoecological preferences. These results are eventually compared with

ecological preferences suggested in the literature in order to perform a consistency check between our interpretation and previous paleoenviromental assignments.

4. Results

4.1. Geochemical results

Geochemical results of bulk carbon and oxygen isotopes and $CaCO_3$ content for the Alano section are from Spofforth et al. (2010; Figs. 2-4). We specifically focused on the interval, from 10 to 30 m level, recording the MECO and post-MECO event. This dataset shows a prominent transient isotope excursions beginning at the ~13 m level, where the bulk $\delta^{18}O$ curve evidences a negative shift by about 1.8‰. The minimum $\delta^{18}O$ value is reached at ~17 m, virtually coincident with the beginning of ORG1 (Spofforth et al., 2010). $\delta^{13}C$ and $CaCO_3$ records also show their minimum values, 0.2‰ and 20% respectively, at the same level (Fig. 2).

$\delta^{18}O$ values gradually recover to pre-event values at the 25 m level, whereas the $\delta^{13}C$ and $CaCO_3$ records are more variable, tending to co-vary with lithological changes (Fig. 2). The $\delta^{13}C$ negative excursion is followed by two positive excursions interrupted by temporary lighter $\delta^{13}C$ values. The two positive carbon-isotope excursions are comparable in magnitude (~1.25‰) and coincident with remarkable peaks in TOC content (up to 3%).

4.2. Calcareous nannofossil results

4.2.1. Preservation

Calcareous nannofossil assemblages can be substantially altered because of different degrees of preservation. Dissolution can occur in the water column, at the sediment-water interface, and in the sediment (e.g., Honjo, 1976; Steinmetz, 1994) eventually resulting in an impoverished fossil record. Our qualitative approach indicates no extensive changes in the preservation of calcareous nannofossils, with only limited indications for etching (E1) and overgrowth (O1) in the MECO and post- MECO intervals (Roth and Thierstein, 1972; Roth, 1983). Diagenetically altered assemblages should show low numbers of species accompanied by high abundances of dissolution resistant taxa (Bornemann and Mutterlose, 2008). If dissolution would severely have affected nannofossils from the Alano section, the assemblage should be dominated by dissolution-resistant taxa, such as for instance *Discoaster* (Adelseck et al., 1973). However, this is not the case. Moreover, a high specific diversity is maintained even in most of the more impoverished samples, inside ORG1 and ORG2. These lines of evidence support the idea that modifications

observed in calcareous nannofossil assemblages are genuine and paleocologically meaningful.

Dissolution in carbonate during the MECO has been recorded in ODP-IODP pelagic records, due to a rise in the CCD in response to an increased CO_2 input in the ocean-atmosphere system (Bohaty et al., 2009); a lack of pervasive dissolution in sediments of the middle bathyal Alano section suggests that the assumed CCD shoaling has only affected deeper depositional settings.

4.2.2. Calcareous nannofossil fluctuations

Throughout the study section, the calcareous nannofossil assemblage is dominated by placoliths, among which *Reticulofenestra, Cyclicargolithus* and *Dictyococcites* are prominent (together up to ca. 75-80% of the total assemblage).

In Figures 2-4, we report paleontological data from the Alano section plotted against bulk oxygen isotope values. Overall, the MECO and post-MECO are characterized by significant changes in calcareous nannofossil assemblages that concide with prominent modifications in geochemical proxies. The apparent correlation of the two datasets can be inferred by careful observations. During the MECO and post- MECO, a relative increase in abundance of small reticulofenestrids (Fig. 2) is associated with a decrease in *Sphenolithus*. Finally, reworked specimens of mainly Cretaceous taxa (e.g., *Watznaueria* or *Micula*), show an increase. Other prominent assemblage modifications include (Figs. 2-4):

- The genus *Reticulofenestra* shows a marked increase during the MECO and post- MECO with two peaks in the ORG1 and ORG2 intervals. If we consider different groups, based on size, within this genus, smaller specimens, that is <4µm and ranging between 4-5.9µm, show a more prominent increase (Fig. 3);
- A slight increase can be noted for *Helicosphaera* at the basis of ORG1 (Fig. 3)*;*
- Although *Coccolithus* and *Ericsonia* are among the main constituents of the Alano assemblage, they do not seem to show a remarkable decrease or an unambiguous increase of abundance (Fig. 3).
- *Sphenolithus* evidences a clear decrease in relative abundance during the MECO and post-MECO (Fig. 4). This decrease is temporary interrupted between organic-enriched ORG1 and ORG2, where $CaCO_3$ content shows a rapid, although transient, recovery to pre and post perturbation values.

- Small specimens of *Dicyococcites* (4-5.9µm) show an increase during the MECO and post-MECO interval (Fig. 3).
- *Cyclicargolithus floridanus* is one of the dominant placoliths of the assemblage and its abundance shows an overall, though highly irregular, decrease during the MECO and post-MECO with a temporary recovery between the organic-enriched ORG1 and ORG2 (Fig. 3).
- *Cribrocentrum reticulatum* decreases during the MECO and first part of the post-MECO (Fig. 3).
- A slight increase in the relative abundance of reworked specimens was found in coincidence with the negative oxygen isotope shift at the onset of the MECO (Fig. 2).

Sphenoliths

- Counts of 100 sphenoliths were performed during this study. *Sphenolithus* evidences a clear decrease in its relative abundance during the MECO and post-MECO (Fig. 4). This decrease is temporary interrupted between organic-enriched ORG1 and ORG2, where $CaCO_3$ content shows a rapid, although transient, recovery to pre and post perturbation values. Overall, we observed a dramatic change in the sphenolith assemblage during the event. Moreover, this genus has a peculiar trend, if observed at species level, with two species, *S. moriformis* and *S. spiniger*, showing an opposite behavior during this stressed interval. In particular, we recorded a marked decrease in the abundance of *S. moriformis*, the most common species among sphenoliths, occurring just before the onset of the MECO (Fig. 4). By contrast, *Sphenolithus spiniger* group, which also includes specimens with an outline similar to *S. spiniger,* but without spine or with a short spine and triangular outline, increases during the MECO and post-MECO interval (Fig.4). Our definition of this group is larger than the strict taxonomic concept of Bukry (1971). This informal taxonomic group increases remarkably in abundance during the MECO and post-MECO. A decrease in abundance of the *S. spiniger* group occurs virtually in coincidence with the appearance of *S. obtusus* in the very final part of the perturbed interval. *Sphenolithus predistentus* and intermediate specimens between *S. predistentus* and *S. distentus* have been observed during the event. These taxa are no longer recorded after the event (Fig. 4).

4.3. Previous paleoecological assignments

Most of the taxa that are investigated and discussed have paleoecological preferences suggested in the literature based on data and interpretations of variable quality. There is not always a consistent assignment of ecological preferences for whole genera and/or individual species. Nevertheless, literature data are commonly used to interpret changes in calcareous nannofossil assemblages in terms of paleoenviromental changes. Earlier published interpretations are thus reported with the intent of giving a broad idea of environmental preferences, and to verify these assignments with our outcomings.

Coccolithus pelagicus was a major constituent of middle and high latitude nannoflora assemblages during the Eocene. It is generally considered to prefer warm waters in the early Paleogene (Haq and Lohmann, 1976), changing its preferences to mid and high latitude settings in the Oligocene (Wei and Wise, 1990a). Aubry (1998) suggested a eurytopic affinity, but other authors consistently reported a temperate dependance for this taxon (Persico and Villa; 2004; Villa and Persico, 2006; Villa et al., 2008). Species ascribed to the genus *Reticulofenestra* are abundant at mid to high latitudes and are thought to be mesotrophic temperate water taxa (e.g., Wei and Wise, 1990a; Persico and Villa, 2004; Villa et al. 2008). The genus *Cyclicargolithus* is reported to be more abundant at the mid latitudes, and is referred as to a temperate water taxon (e.g., Wei and Wise, 1990a), even if some high latitude studies suggest the absence of a temperature affinity (Persico and Villa, 2004; Villa and Persico, 2006). Species ascribable to genus *Sphenolithus* are usually interpreted as K-mode specialists, adapted to warm/oligotrophic environments (Bralower, 2002; Wei and Wise, 1990a; Gibbs et al., 2004; Gibbs at al., 2006; Agnini et al., 2007a; Persico and Villa, 2004; Villa and Persico, 2006 and Villa et al. 2008), even if Dunkley Jones et al. (2008) have recently challenged this interpretation inferring a more eutrophic affinity.

5.Discussion

The studied section can be subdivided in three lithological/geochemical intervals, as shown in figures 2-4: 1) the pre-isotope excursion interval (background conditions), 2) the perturbed interval, that includes the MECO *strictu sensu* and post-MECO interval and 3) the return to stable conditions (background conditions) above ORG1 and ORG2.

5.1.Main modifications of calcareous nannofossil assemblages

The decrease in $CaCO_3$ content observed during the MECO and post-MECO intervals is likely to be attributable to an enhanced discharge of terrigenous material to the ocean (Ravizza et al., 2001; Schmitz et al., 2001; Crouch et al., 2003; Hollis et al., 2005; Zachos et al., 2005; Giusberti et al., 2007; Nicolo et al., 2007; Agnini et al., 2009). This would suggest a higher nutrient availability in this marginal setting during the MECO and post-MECO.

The decrease of *C. floridanus* during the MECO is anticorrelated with small placoliths ascribed to *Reticulofenestra* and *Dictyococcites* (Fig. 3). *Cyclicargolithus floridanus* is thought to be a cosmopolitan taxon, thriving in warm-temperate waters and high nutrient levels (Haq et al., 1977; Wei and Wise, 1990a,b; Aubry, 1992), but our data suggest a meso-oligotrophic affinity.

Among reticulofenestrids we have distinguished several subgroups based on size. The abundance pattern of individuals smaller than 4µm or ranging between 4–5.9 µm shows a significant increase during the MECO and post-MECO event (Fig. 3). Small reticulofenestrids are considered to be adapted to eutrophic conditions, because in recent ecosystems, small placoliths typically flourish in high-productivity areas (Okada and Honjo, 1973; Winter et al., 1994; Okada, 2000; Hagino and Okada, 2001), where rapid population growth occurs (Young, 1994). Moreover, since the dissolution rate of carbonate grains is inversely related to their size (Walter and Morse, 1984), we can infer that small placoliths are more affected by dissolution (Andruleit et al., 2004; Dunkley Jones and Bown, 2007). At Alano, the increase in abundance of small reticulofenetrids provides evidence of good preservation and support a scenario of enhanced nutrient availability.

The genus *Dictyococcites* consists of dissolution resistant taxa (Bukry, 1971) commonly considered to live in temperate waters (Haq and Lohmann, 1976; Villa and Persico, 2006). A detailed analysis within the genus, essentially based on a morphometric approach, points out a remarkable increase in the relative abundance of specimens ranging from 4–5.9 µm (Fig. 3). The increase in abundance of small placoliths suggests a good preservation. This peculiar feature virtually mirrors that observed for small reticulofenestrids, further supporting the idea of an increased eutrophication of sea surface water during the event.

The abundance pattern of sphenoliths has been commonly utilized as a paleoecological proxy in order to interpret changes in environmental conditions and they surely deserve a special attention. They will be treated in the next paragraph.

Sphenolithus moriformis and *S. spiniger* are anticorrelated during the event. During the MECO *Sphenolithus spiniger* became predominant within sphenoliths at the expense of *S. moriformis* (Fig. 4). Overall, sphenoliths are thought to be adapted to oligotrophic, warm-water conditions (e.g., Aubry, 1998; Young, 1994; Bralower, 2002). In particular, *S. moriformis* was interpreted as an oligotrophic taxon (Agnini et al., 2007a), thus suggesting that the low abundance of this taxon during the MECO and post- MECO was driven by enhanced eutrophy. The different response of *S. moriformis* and *S. spiniger* can probably be explained by a species specific adaptation to more eutrophic conditions. We suspect the *S. spiniger* increased its abundance in coincidence with an enhanced terrigenous input likely producing higher nutrient availability in sea surface waters. This change in paleoenviromental conditions would have favored the flourishing of more eutrophic taxa. If true, it shows that different species of the same genus can thrive in different ecological niches along a trophic resource continuum.

Analyzing the abundance patterns of taxa ascribed to *Sphenolithus*, we thus recognize a distinct episode of important biotic modifications embedded in a relatively stable interval. In particular, the genus *Sphenolithus* displays an interesting series of disappearances/appearances, which in particular include *S. spiniger* (Highest Occurrence)*, S. predistentus* (Lowest Occurrence - LO) and *S. obtusus* (LO)*.* Perch-Nielsen (1985, in Fig. 69) proposed that possible linkages exist between these species. In fact, *S. furcatholitoides* is thought to be the common ancestor of *S. predistentus* and *S. obtusus*, which thus represent two distinct divergent branches without any phyletic relationship*.* Our data, instead, seem to provide for a different story: the consistent presence of specimens that morphologically resemble the *Sphenolithus predistentus-distentus* group *sensu* Huang (1977), associated with morphotypes with intermediate characters between *S. predistentus* and *S. obtusus* suggests a linear phyletic relationship between the two taxa. This finding contrasts with the hypothesis of Perch-Nielsen (1985) that inferred no relationship between *S. predistentus* and *S. obtusus*. Unfortunately, the evolutionary relationship between *S. furcatholitoides* and *S. predistentus* remains obscure, because we have been unable to document intermediate forms between these two species. It is, however, interesting to note that *S. predistentus-S. obtusus* lineage observed during the middle Eocene shows a similar morphological evolution (e.g., the development through time of a V-shaped extinction line between the upper quadrants and the apical spine) compared to *S. predistentus-S. distentus* lineage evolving later in the Oligocene time, (Huang, 1977).

5.2. Clues on paleo-oceanographic reconstruction

Several lines of evidence suggest that episodes of global transient warming are associated with carbon cycle perturbations in the early Eocene (e.g., Zachos et al., 2001; Lourens et al., 2005). The recovery of pre-event conditions is likely to be related to enhanced siliciclastic weathering and a stronger hydrological cycle implying, in turn, increased runoff and nutrient delivery to the ocean (Ravizza et al., 2001; Schmitz et al., 2001; Crouch et al., 2003; Hollis et al., 2005; Pagani et al., 2006; Zachos et al., 2006; Agnini et al., 2007a; Giusberti et al., 2007, Luciani et al., 2007; Nicolo et al., 2007).

The productivity model proposed by Gibbs et al. (2006) for the PETM could provide a theoretical framework for understanding changes occurred during the MECO in a more global perspective. The authors infer a possible decoupling in the marine domain between open ocean settings, that are generally indicative of lower productivity, and shelf or more proximal settings, which seem to be characterized by increased nutrient availability. At the middle bathyal Alano section, the shift towards an increased eutrophication of the surface waters was documented by the appearance and/or marked increase in abundance of eutrophic calcareous plankton taxa (i.e., calcareous nannofossil and planktic foraminifera) during the MECO and post-MECO interval, and the presence of radiolaria confined to the two sapropel-like intervals (Luciani et al., 2010; Spofforth et al., 2010). These lines of evidence suggest that high productivity conditions are not restricted to shelf–slope areas but are possibly extended to deep water marine settings affected by continental runoff during the MECO. The MECO occurred in a doubthouse climate regime at ca. 40 Ma, that is after the Early Eocene Climatic Optimum (EECO), but the way in which the Earth's system responds to episodes of global warming seems to be very similar to that recorded during the Early Eocene time. The return to pre-event conditions is likely achieved thanks to accelerated chemical weathering, strengthened by an enhanced hydrological cycle. These mechanisms would eventually cause an increase in terrigenous input, especially in the marginal settings (Spofforth et al. 2010). The decrease in $CaCO_3$ content during the MECO would be explained by an increased terrestrial input from mainland, diluting the carbonate produced in-situ and taking account for a good preservation. The increase in reworked specimens as well as the relative increase of eutrophic taxa, and the obvious decrease of oligotrophic taxa, is consistent with an enhanced productivity, which may be caused by terrigenous components discharged to the sea.

At Alano, the MECO interval is characterized by remarkable changes in lithology, geochemistry and micropaleontological assemblages. These modifications are not unidirectional, but show variable trends throughout the study section. For instance, the presence of two organic-rich layers, ORG1 and ORG2 of Spofforth et al. (2010), represents the lithologic expression of the post-MECO interval in our section. These sapropel-like intervals, which interrupt a monotonous deposition of gray hemipelagic marls, are divided by ca. 2m of marls very similar to pre-MECO sediments. The possible subdivision of the MECO into several phases is also evident looking at some geochemical/mineralogical proxies ($CaCO_3$, $\delta^{18}O$, $\delta^{13}C$, TOC; Fig. 2). Calcareous nannofossil data are strongly correlated with carbonate content and stable isotope curves, and may provide a useful tool to understand the increase of organic carbon (TOC) during the study interval (Figs. 3-4).

The preservation of organic carbon in rocks and sediments is still attracting the attention of many scientists. During the past decades, the formation of the Cretaceous black shales (Schlanger and Jenkyns, 1976) and late Cenozoic sapropels (Kidd et al., 1978) had sparked a hot debate based on two opposite hypotheses: the stagnation model, explaining the elevated TOC levels by enhanced organic matter preservation under oxygen-deficient deep-water conditions; and the productivity model, linking the occurrence of organic-enriched sediments to increased marine biological production in the photic zone (see also Rohling, 1994 for an overview).

At Alano, the presence of ORG1 and ORG2 is coupled with an increase in sedimentation rates driven both by increased input of terrestrial carbon and increased primary production stimulated by weathering derived nutrients (Luciani et al., 2010). Moreover, an increase in sulphur and redox-sensitive trace metals and the occurrence of pyrite together with marked changes in benthic foraminiferal communities give evidence that dysoxic conditions occurred at the sea floor during the MECO interval (Spofforth et al., 2010). The increased organic carbon stored in sediments may be interpreted as a result of both increased productivity and low-oxygen content at the seafloor, suggesting a complex interaction between net production and preservation of organic carbon.

The transient shift of planktic foraminiferal assemblages and the presence of radiolaria indicate conditions of enhanced marine productivity in marine microplankton that, in turn, suggest a net increase of export productivity (Luciani et al., 2010). Calcareous nannofossil data show a more ambiguous scenario: (1) There is an increase in relative abundance of eutrophic taxa paired with a decrease in oligotrophic taxa (2) but also a decrease in the

number of specimens per mm^2 in ORG1 and ORG2 (Fig. 2). Coccolithophorids are thought to be very well adapted to oligotrophic environments (Hallock, 1981; 1985), while they are outcompeted by less heavily calcified or noncalcareous organisms, e.g. diatoms, in eutrophic enviroments (Birkeland, 1987; Brock and Smith, 1983; Hallock 1987; Egge and Aksnes, 1992). The contraction of the Trophic Resource Continuum (TRC) implies the elimination of habitats at the oligotrophic end of the continuum and a simultaneous expansion of eutrophic and mesotrophic environments. Consequently, an increase in nutrient availability in the surface waters can result in oligotrophic habitat elimination (Hallock, 1987). The relative increase of eutrophic and decrease of oligotrophic taxa corroborates an enhanced nutrient supply. The expected increase in phytoplankton productivity is contradicted by the decrease observed in the number of specimens per mm^2 (Fig. 2). This finding can be possibly related to the passing of a nutrient supply threshold that eventually results in more eutrophic conditions that favor eutrophic taxa. Alternatively, the lower coccolith density and the simultaneous replacement of oligotrophic forms by more eutrophic ones are convincingly explained by enhanced eutrophic conditions. However, lower coccolith densities can also be explained as a dilution effect due to increased sediment delivery.

5.3. Calcareous nannoplankton evolution

Our data show that the MECO interval is characterized by several modifications of the calcareous nannofossil assemblages. Some of these changes, which essentially consist in changes of the relative abundances of individual taxa, are confined to the event. For instance, the increase in abundance of small placoliths represents an important modification in calcareous nannofossil assemblages likely triggered by pronounced climatic changes and ending with the return to pre-event background conditions.

6. Conclusions

At Alano, the MECO and post-MECO intervals coincide with prominent changes in several geochemical proxies such as oxygen and carbon isotopes, carbonate content, TOC %, etc. During this time, calcareous nannofossil data show significant modifications that correlate with geochemical and paleoenviromental indicators. Changes in the relative abundance of calcareous nannofossil taxa are interpreted as a temporary shift toward more eutrophic conditions in warmer sea surface waters during the MECO and especially post-MECO events. An increase in nutrient availability is consistent with the increased

terrigenous input likely related to an enhanced hydrological cycle and may also indicate that, during the MECO and post-MECO, the increased food availability, and not temperature, was the main factor driving the modification of the calcareous nannofossil assemblage.

Our results are very similar to those recorded during early Eocene hyperthermals in the same marginal setting of the central-western Tethys (Giusberti et al., 2007; Agnini et al., 2009), suggesting that similar mechanisms might be active during these warming phases. Further studies from different areas and/or depositional settings are needed to eventually provide a more global perspective of the event and better understand the response of calcareous nannoplankton.

Figures

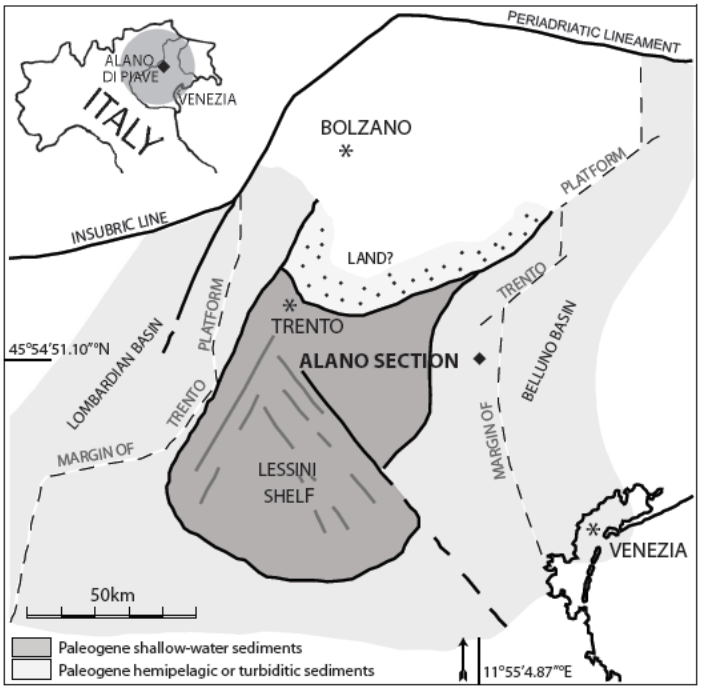

Figure 1. Paleogeographic reconstruction of main elements of the Southern Alps during the Paleogene (modified from Bosellini and Papazzoni, 2003). The location of the Alano section is also reported.

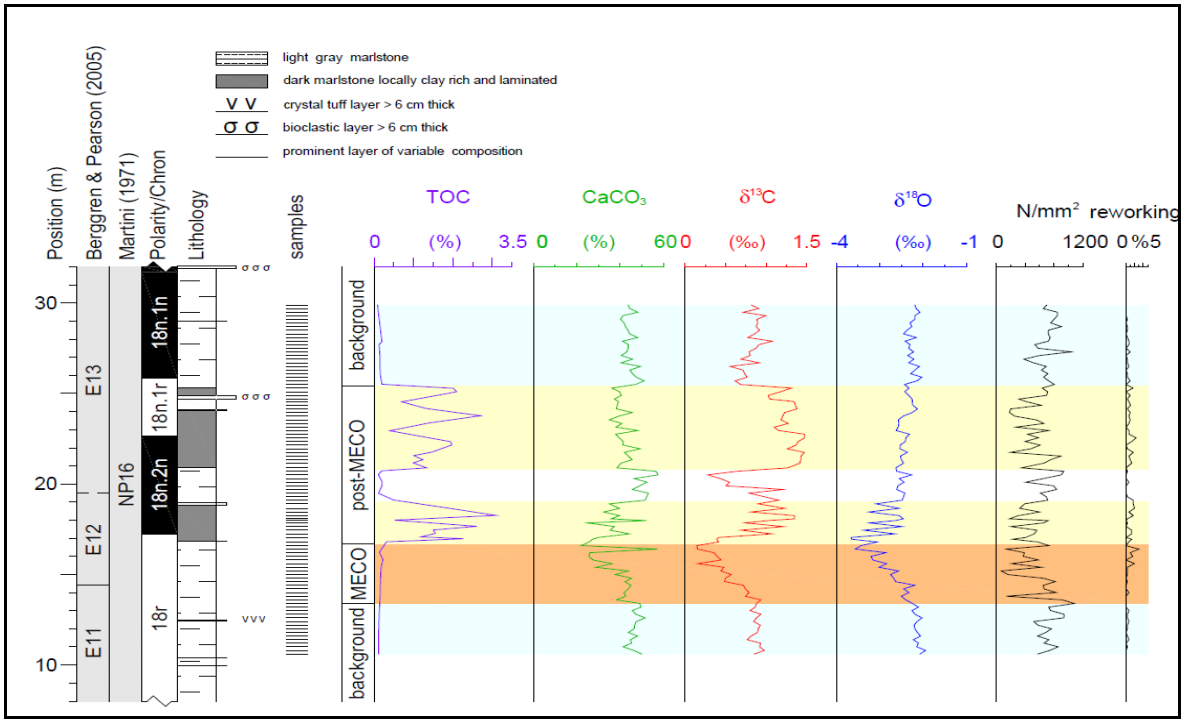

Figure 2. Relative abundance of reworked forms and number of specimens per mm^2 are reported against lithology, magnetostratigraphy and calcareous plankton biostratigraphy over the Alano section. Shown here are also $\delta^{18}O$, $\delta^{13}C$, $CaCO_3$ (%) and TOC (%) records and stratigraphic position of samples. A legend for lithologies is provided in the upper part of the figure. The shaded dark grey (orange) band indicates the position of the MECO. Pale grey (yellow) overlaid bands indicate organic rich intervals during the post-MECO.

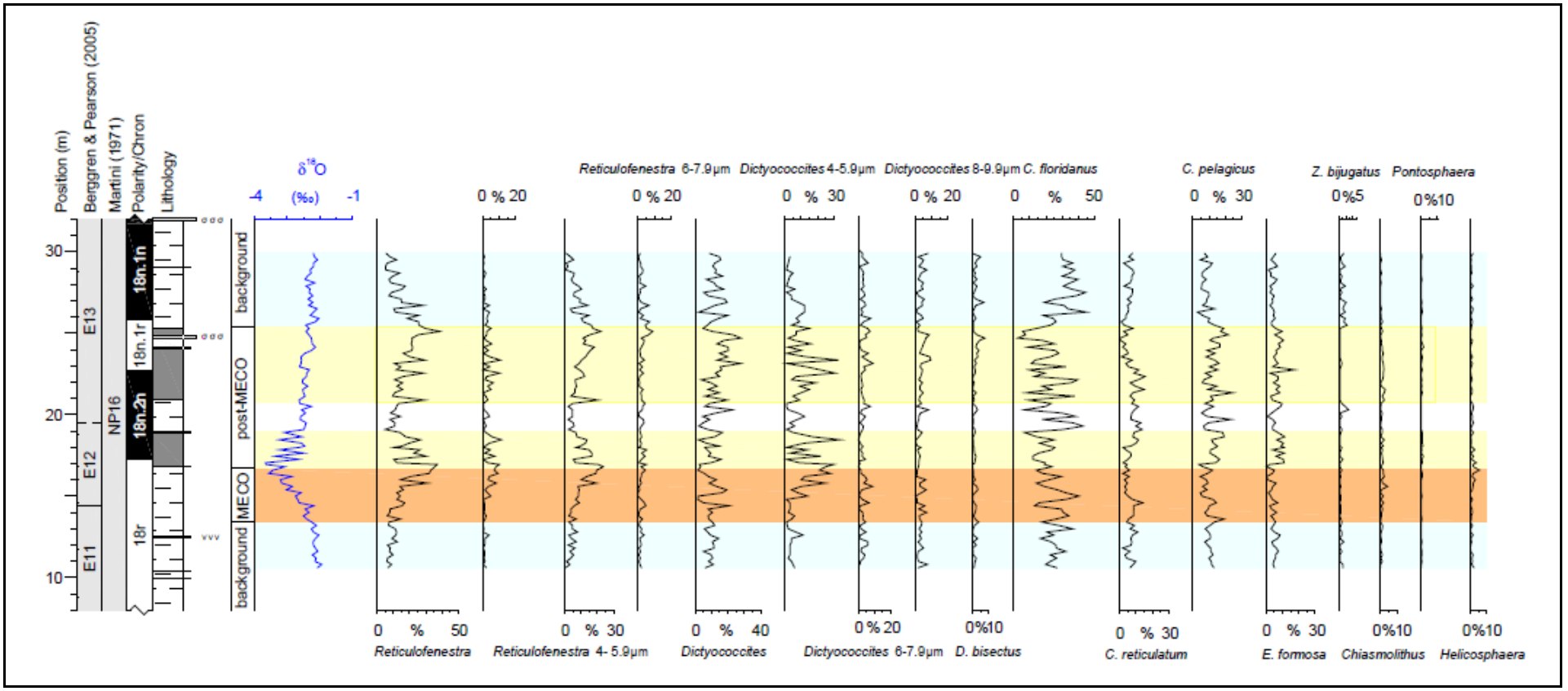

Figure 3. Abundance of selected calcareous nannofossil taxa are reported against lithology, magnetostratigraphy and calcareous plankton biostratigraphy in the Alano section. Shown here is also $\delta^{18}O$, record. The shaded dark grey (orange) band indicates the position of the MECO. Pale grey (yellow) overlaid bands indicate organic rich intervals during the post-MECO.

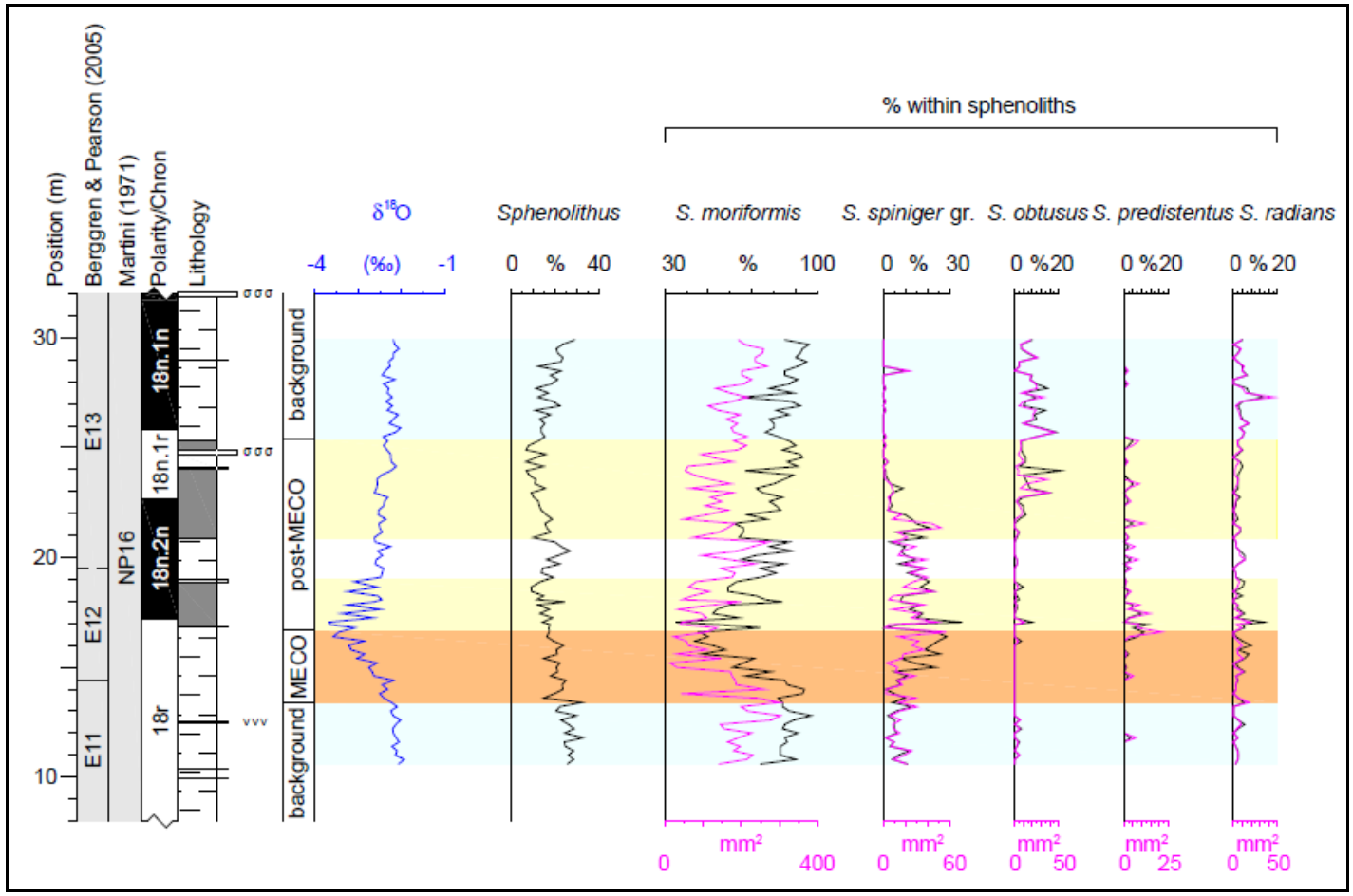

Figure 4. Relative abundance of selected sphenolith species among sphenolith assemblage and number of specimens per mm^2 over the Alano section. Data are plotted against lithology, $\delta^{18}O$ record, magnetostratigraphy and calcareous plankton biostratigraphy. The shaded dark grey (orange) band indicates the position of the MECO. Pale grey (yellow) overlaid bands indicate organic rich intervals during the post-MECO.

References

Adelseck, C.G. Jr., Geehan, G.W. and Roth, P.H., 1973. Experimental Evidence for the Selective Dissolution and Overgrowth of Calcareous Nannofossils During Diagenesis, Geological Society of America Bulletin 84, 2755-2762.

Agnini, C., Muttoni, G., Kent, D.V., and Rio, D., 2006, Eocene biostratigraphy and magnetic stratigraphy from Possagno, Italy: The calcareous nannofossil response to climate variability, Earth Planet. Sci. Lett. 241, 815–830, doi:10.1016/j.epsl.2005.11.005.

Agnini, C., Fornaciari, E., Rio, D., Tateo, F., Backman, J. and Giusberti, L, 2007a. Responses of calcareous nannofossil assemblages, mineralogy and geochemistry to the environmental perturbations across the Paleocene/Eocene boundary in the Venetian pre-Alps, Mar. Micropaleontol. 63, 19 – 38, doi:10.1016/j.marmicro.2006.10.002.

Agnini, C., Fornaciari, E., Raffi, I., Rio, D., Röhl, U., Westerhold, T., 2007b. High resolution nannofossil biochronology of middle Paleocene to early Eocene at ODP Site 1262: Implications for calcareous nannoplankton evolution, Mar. Micropaleontol. 64, 215 – 248, doi:10.1016/j.marmicro. 2007.05.003.

Agnini, C., Macrì, P., Backman, J., Brinkhuis, H., Fornaciari, E., Giusberti, L., Luciani, V., Rio, D., Sluijs, A., Speranza, F., 2009. An early Eocene carbon cycle perturbation at ~ 52.5 Ma in the Southern Alps: Chronology and biotic response Paleoceanography 24, PA2209, doi:10.1029/2008PA001649.

Agnini C., Fornaciari E., Giusberti L., Grandesso P., Lanci L., Luciani V., Muttoni G., Rio D., Stefani C., Pälike H., Spofforth D.J.A , 2011. Integrated bio-magnetostratigraphy of the Alano section (NE Italy): a proposal for defining the Middle-Late Eocene boundary, Geological Society of America Bulletin, 123, (5/6) 841-872. doi:10.1130/B30158.1.

Andruleit, H., Rogalla, U., Stäger, S., 2004. From living communities to fossil assemblages: origin and fate of coccolithophores in the northern Arabian Sea. Micropaleontology 50(1), 5-21, DOI: 10.2113/50.Suppl_1.5.

Aubry, M.-P., 1984. Handbook of Cenozoic Calcareous Nannoplankton, book 1, Ortholithae (Discoaster). Am. Mus. of Nat. Hist. Micropaleontol. Press, New York. 263 pp.

Aubry, M.-P., 1988. Handbook of Cenozoic Calcareous Nannoplankton, book 2, Ortholithae (Holococcoliths, Ceratoliths, Ortholiths and Other). Am. Mus. of Nat. Hist.Micropaleontol. Press, New York. 279 pp.

Aubry, M.-P., 1989. Handbook of Cenozoic Calcareous Nannoplankton, book 3, Ortholithae (Pentaliths and Other), Heliolithae (Fasciculiths, Sphenoliths and Others). Am. Mus. of Nat. Hist. Micropaleontol. Press, New York. 279 pp.

Aubry, M.-P., 1990. Handbook of Cenozoic Calcareous Nannoplankton, book 4, Heliolithae (Helicoliths, Cribriliths, Lopadoliths and Other). Am. Mus. of Nat. Hist. Micropaleontol. Press, New York. 381 pp.

Aubry, M.-P., 1992. Late Paleogene calcareous nannoplankton evolution: a tale of climatic deterioration, in Eocene–Oligocene climatic and biotic evolution. In: Prothero, D.R., Berggren, W.A. (Eds.), Eocene–Oligocene Climatic and Biotic Evolution. Princeton Univ. Press, Princeton, NJ, pp. 272–309.

Aubry M.-P.,1998, Early Paleogene calcareous nannoplankton evolution: a tale of climatic amelioration, in late Paleocene and early Eocene climatic and biotic evolution. In: M.-P. Aubry, S. Lucas and W. Berggren, Editors, Late Paleocene–early Eocene climatic and biotic events in the marine and terrestrial record, Columbia University Press (1998), pp. 158–203.

Aubry, M.-P., 1999. Handbook of Cenozoic Calcareous Nannoplankton, book 5, Heliolithae (Zygoliths and Rhabdoliths). Am. Mus. of Nat. Hist.Micropaleontol. Press, New York. 368 pp.

Berggren, W.A., Pearson, P.N., 2005. A revised tropical to subtropical Paleogene planktonic foraminiferal zonation. Journal of Foraminiferal Research 35, 279-298, doi: 10.2113/35.4.279.

Birkeland, C. 1987. Nutrient availability as a major determinant of differences among coastal hard-substratum communities in different regions of the tropics. In: Comparisons between Atlantic and Pacific tropical coastal marine ecosystems: community structure, ecological processes, and productivity, Birkeland, C. (ed.), UNESCO Reports in Marine Science 46, pp. 45-97.

Bohaty, S.M., Zachos, J.C., 2003. Significant Southern Ocean warming event in the late middle Eocene. Geology 31(11), 1017– 1020, doi:10.1130/G19800.1

Bohaty, S.M., Zachos, J.C., Florindo, F., Delaney, M.L. 2009. Coupled greenhouse warming and deep-sea acidification in the middle Eocene Paleoceanography 24 , PA2207.

Bornemann, A., Mutterlose, J., 2008. Calcareous Nannofossil and $\delta^{13}C$ Records from the Early Cretaceous of the Western Atlantic Ocean: Evidence for Enhanced Fertilization across the Berriasian–Valanginian Transition. Palaios 23, 821-832.Bosellini, F.R.

Papazzoni, C.A., 2003. Palaeoecological significance of coral-encrusting foraminifera associations. A case study from the late Eocene of the Nago Limestone (Northern Italy). Acta Pal. Polonica 48 (2), 279-292.

Bown, P.R., 2005. Paleogene calcareous nannofossils from the Kilwa and Lindi areas of coastal Tanzania: Tanzania Drilling Project Sites 1 to 10. Journal of Nannoplankton Research 27, 21-95.

Bown, P.R., and Young, J.R., 1998. Techniques. In Bown, P.R. (Ed.), Calcareous Nannofossil Biostratigraphy: London, Chapman & Hall, pp. 16–28.

Bown, P.R., Dunkley Jones, T., 2006, New Paleogene calcareous nannofossil taxa from coastal Tanzania. Journal of Nannoplankton Research 28, 17-34.

Bralower, T.J., 2002. Evidence for surface water oligotrophy during the Paleocene-Eocene Thermal Maximum: Nannofossil assemblage data from Ocean Drilling Program Site 690, Maud Rise, Weddell Sea Paleoceanography 17(2), 1023, doi:10.1029/2001PA000662.

Brock, R.E. Smith, S.V., 1983. Response of coral reef cryptofaunal communities to food and space. Coral Reefs 1, 179–183.

Bukry, D., 1971. Cenozoic calcareous nannofossils from the Pacific Ocean. Transactions of the San Diego Society of Natural History 16, 303–328.

Burgess, C.E., Pearson, P.N, Lear, C.H., Morgans; H.E.G., Handley, L., Pancost, R.D., Schouten, S., 2008. Middle Eocene climate cyclicity in the southern Pacific: Implications for global ice volume. Geology 36, 651-654, doi:10.1130/G24762A.1

Crouch, E.M., Dickens, G.R., Brinkhuis, H., Aubry, M.-P., Hollis, G. J., Rogers, K. M., Visscher, H., 2003. The Apectodinium acme and terrestrial discharge during the Paleocene-Eocene thermal maximum: New palynological, geochemical and calcareous nannoplankton observations at Tawanui, New Zealand, Palaeogeogr. Palaeoclimatol. Palaeoecol. 194, 387–403, doi:10.1016/S0031-0182(03)00334-1.

Dawber, C.F., Tripati, A.K., 2011. Constraints on Glaciation in the Middle Eocene (46–37 Ma) from Ocean Drilling Program (ODP) Site 1209 in the Tropical Pacific Ocean. Paleoceanography 26, PA2208, doi:10.1029/2010PA002037.

Dawber, C.F., Aradhna K. Tripati, A.K., Gale, A.S., MacNiocaill, C.Hesselbo, S.P., 2011. Glacioeustasy during the middle Eocene? Insights from the stratigraphy of the Hampshire Basin, UK Palaeogeography, Palaeoclimatology, Palaeoecolog 300, 84–100.

Diester-Haass, L., Zahn, R., 1996, Eocene–Oligocene transition in the Southern Ocean: History of water mass circulation and biological productivity. Geology 24, 163–166.

Dunkley Jones, T., Bown, P.R., 2007. Post-sampling dissolution and the consistency of nannofossil diversity measures: A case study from freshly cored sediments of coastal Tanzania. Mar. Micropaleontology 62, 254-268.

Dunkley Jones, T., Bown, P.R., Pearson, P.N., Wade, B.S., Coxall, H.K., Lear, C.H. 2008. Major shifts in calcareous phytoplankton assemblages through the Eocene-Oligocene transition of Tanzania and their implications for low-latitude primary production. Paleoceanography 23, PA4204, doi:10.1029/2008PA001640.

Edgar, K.M., Wilson, P.A., Sexton, P.F. Suganuma, Y., 2007. No extreme bipolar glaciation during the main Eocene calcite compensation shift. Nature, 448:908-911.

Egge, J.K., Aksnes, D.L., 1992. Silicate as regulating nutrient in phytoplankton competition. Mar. Ecol. Prog. Ser. 83, 281–289.

Erbacher, J., Mosher, D.C., Malone, M.J., et al., 2004. *Proc. ODP, Init. Repts.,* 207: College Station, TX (Ocean Drilling Program), 1-89, doi:10.2973/odp.proc.ir.207.2004

Fornaciari, E., Agnini, C., Catanzariti, R., Rio, D., Bolla, E.M., Valvasoni, E., 2010, Mid-latitude calcareous nannofossil biostratigraphy, biochronology and evolution across the middle to late Eocene transition. Stratigraphy 7, (4) 229-264.

Gibbs, S.J., Shackleton, N.J., Young, J.R., 2004, Orbitally forced climate signals in mid-Pliocene nannofossil assemblages, Mar. Micropaleontol. 51, 39–56, doi:10.1016/ j.marmicro.2003.09.002.

Gibbs, S.J., Bralower, T.J., Bown, P.R., Zachos, J.C., Bybell, L.M., 2006. Shelf and open-ocean calcareous phytoplankton assemblages across the Paleocene–Eocene thermal maximum: implications for global productivity gradients. Geology 34 (4), 233–236.

Giusberti, L., Rio, D., Agnini, C., Backman, J., Fornaciari, E., Tateo, F., Oddone, M. 2007, Mode and tempo of the Paleocene Eocene thermal maximum in an expanded section from the Venetian pre-Alps, Geol. Soc. Am. Bull. 119, 391–412, doi:10.1130/B25994.1.

Grandesso, P., 1976, Biostratigrafia delle formazioni terziarie del Vallone Bellunese: Bollettino 1292 Società Geologica Italiana 94, 1323–1348.

Hagino, K., Okada, H., 2001. Morphological observations of living Gephyrocapsa crassipons, J. Nannoplankton Res. 23, 3–7.

Hallock, P., 1981. Algal symbiosis: A mathematical analysis. Marine Biology 62, 249-255.

Hallock, P., 1985. Why are larger foraminifera large? Paleobiology 11, 195-208.

Hallock, P., 1987 Fluctuations in the trophic resource continuum: A factor in global diversity cycles? Paleoceanography, 2(5), 457-471, doi:10.1029/PA002i005p00457

Haq, B.U., Lohmann, G.P., 1976. Early Cenozoic Calcareous nannoplankton biogeography of the Atlantic Ocean. Marine Micropaleo. 1, 120-197.

Haq, B.U., Premoli Silva, I., Lohmann, G.P., 1977. Calcareous plankton paleobiogeographic evidence for major climatic fluctuations in the Early Cenozoic Atlantic Ocean. J. Geophys. Res. 82, 3861–3876.

Hollis, C.J., Dickens, G.R., Field, B.D., Jones, C.M., Strong, C.P., 2005. The Paleocene-Eocene transition at Mead Stream, New Zealand: A southern Pacific record of early Cenozoic global change, Palaeogeogr. Palaeoclimatol. Palaeoecol. 215, 313–343, doi:10.1016/j.palaeo.2004.09.011.

Honjo, S., 1976, Coccoliths—Production, transportation and sedimentation. Mar. Micropaleont. 1. 65-79.

Huang, T.C , 1977. Calcareous nannoplankton stratigraphy of the upper Wulai Group (Oligocene) in northern Taiwan. Petroleum Geology of Taiwan 14, 147-179.

Kidd, R.B., Cita, M.B., and Ryan, W.B.F., 1978. Stratigraphy of eastern Mediterranean sapropel sequences recovered during DSDP Leg 42A and their paleoenvironmental significance. *In* Hsü, K.J., Montadert, L., et al., Init. Repts*. DSDP,* 42 (Pt. 1): Washington (U.S. Govt. Printing Office), 421-443.

Lourens, L.J., Sluijs, A., Kroon, D., Zachos, J.C., Thomas, E., Röhl, U., Bowles, J., Raffi, I., 2005. Astronomical pacing of late Palaeocene to early Eocene global warming events. Nature 435, 1083–1087.

Luciani, V., Giusberti, L., Agnini, C., Backman, J., Fornaciari, E., Rio, D., 2007, The Paleocene-Eocene thermal maximum as recorded by Tethyan planktonic foraminifera in the Forada section (northern Italy), Mar. Micropaleontol., 64, 189–214, doi:10.1016/j.marmicro. 2007.05.001.

Luciani, V., Giusberti, L., Agnini, C. Fornaciari, E., Rio, D., Spofforth, D.J.A., Pälike, H.. 2010. Ecological and evolutionary response of Tethyan planktonic foraminifera to the middle Eocene climatic optimum (MECO) from the Alano section (NE Italy), Palaeogeogr., Palaeoclimatol., Palaeoecol. 292, 82–95.

Lyle, M., Liberty, L., Moore, T.C., Jr., Rea, D.K., 2002. Development of a seismic stratigraphy for the Paleogene sedimentary section, central tropical Pacific Ocean. *In* Lyle, M., Wilson, P.A., Janecek, T.R., et al., Proc. ODP, Init. Repts*.,* 199: College Station, TX (Ocean Drilling Program), 1–21.

Lyle, M., Palike, H., Nishi, H, Raffi, I., Gamage, K., Klaus, A. and the IODP Expedition320/321 Scientific Party, 2010. The Pacific Equatorial Age Transect, IODP Expeditions 320 and 321: Building a 50-million-year-long environmental record of the Equatorial Pacific. Sci. Drill. 9, 4-15.

Martini E., 1971, Standard Tertiary and Quaternary calcareous nannoplankton zonation, in Farinacci, A., ed., Proceedings, International Conference on Planktonic Microfossils, second, Rome, Volume 2: Rome, Italy, Tecnoscienza Edizione, p. 739-785.

Miller, K.G., Wright, J.D., Fairbanks, R.G., 1991. Unlocking the Ice House: Oligocene–Miocene oxygen isotopes, eustasy, and margin erosion. J. Geophys. Res. 96, 6829–6848.

Mutterlose, J., Linnert, C., Norris, R.D., 2007 Calcareous nannofossils from the Paleocene-Eocene Thermal Maximum of the equatorial Atlantic (ODP Site 1260B): Evidence for tropical warming. Marine Micropaleontology 65, 13-31. doi:10.1016/j.marmicro.2007.05.004.

Nicolo, M.J., Dickens, G.R., Hollis, C.J., Zachos, J.C., 2007, Multiple early Eocene hyperthermals: Their sedimentary expression on the New Zealand continental margin and in the deep sea, Geology 35(8), 699–702, doi:10.1130/G23648A.1.

Okada, H., 2000. Neogene and Quarternary calcareous nannofossils from the Blake Ridge, Sites 994, 995, and 997. In Paull, C.K., Matsumoto, R., Wallace, P.J., and Dillon, W.P. (Eds.), Proc. ODP, Sci. Results, 164: College Station, TX (Ocean Drilling Program), 331-341.

Okada, H., Honjo, S., 1973. The distribution of oceanic coccolithophorids in the Pacific. Deep Sea Research 20, 355–374.

Okada, H., Bukry, D., 1980. Supplementary modification and introduction of code numbers to the low-latitude Coccolith biostratigraphic zonation, (Bukry, 1973; 1975). Mar. Micropaleontol. 5, 321-325

Pagani, M., Pedentchouk, N., Huber, M., Sluijs, A., Schouten, S., Brinkhuis, H., Sinninghe Damste, J.S., Dickens, G.R. and the IODP Expedition 302 Scientists, 2006. Arctic hydrology during global warming at the Palaeocene/Eocene thermal maximum, Nature 442, 671– 675, doi:10.1038/nature05043.

Pälike, H., Nishi, H., Lyle, M., Raffi, I., Gamage, K., Klaus, A., and the Expedition 320/321 Scientists, 2010. Proc. IODP, 320/321: Tokyo (Integrated Ocean Drilling Program Management International, Inc.). doi:10.2204/iodp.proc.320321.101.2010.

Perch-Nielsen, K. 1985, Cenozoic calcareous nannofossils. In Bolli H.M., Saunders J.B., Perch-Nielsen K. Plankton Stratigraphy. Cambridge University Press, p. 427-554.

Persico, D., Villa G., 2004. Eocene-Oligocene calcareous nannofossils from Maud Rise and Kerguelen Plateau (Antarctica): palaeoecological and palaeoceanographic implications. Mar. Micropaleontol. 52, 153-179.

Raffi, I., Backman, J., Pälike, H., 2005 Changes in calcareous nannofossil assemblages across the Paleocene/Eocene transition from the paleo-equatorial Pacific Ocean. Palaeogeogr., Palaeoclimatol., Palaeoecol. 226(1–2), 93-126.

Ravizza, G., Norris, R.N., Blusztajn, J., Aubry, M.-P., 2001. An osmium isotope excursion associated with the Late Paleocene thermal maximum: Evidence of intensified chemical weathering. Paleoceanography 16(2), 155-163, doi:10.1029/2000PA000541.

Rio, D., Raffi, I., Villa, G., 1990. Pliocene–Pleistocene calcareous nannofossil distribution patterns in the western Mediterranean. Proc. Ocean Drill. Program Sci. Results 107, 513–533.

Rohling, E.J., 1994. Review and new aspects concerning the formation of eastern Mediterranean sapropels. Mar. Geol. 122, 1–28.

Roth, P.H., 1983. Jurassic and Lower Cretaceous calcareous nannofossils in the Western North Atlantic (Site 534): biostratigraphy, preservation, and some observations on biogeography and paleoceanography. Initial Reports of the Deep Sea Drilling Project 76, 587-621.

Roth, P.H., Thierstein, H.R. 1972. Calcareous nannoplankton: Leg XIV of the Deep Sea Drilling Project. In D. E. Hayes & A. C. Pimm (Eds.), Initial Reports of the Deep Sea Drilling Project 14, :421-486.

Schlanger, S.O., Jenkins, H.C., 1976, Cretaceous anoxic events: Causes and consequences: Geologie en Mjinbouw. 55, 179-184.

Schmitz, B., Pujalte, V., Núñez-Betelu, K., 2001, Climate and sea-level perturbations during the initial Eocene thermal maximum: Evidence from siliciclastic units in the Basque Basin (Ermua, Zumaia and Trabakua Pass), northern Spain: Palaeogeogr., Palaeoclimatol., Palaeoecol. 165, 299–320, doi: 10.1016/S0031-0182(00)00167-X.

Sexton, P.F., Wilson, P.A., Norris, R.D., 2006. Testing the Cenozoic multisite composite $\delta^{18}O$ and $\delta^{13}C$ curves: New monospecific Eocene records from a single locality, Demerara Rise (Ocean Drilling Program Leg 207). Paleoceanography 21, PA2019, doi:10.1029/2005PA001253.

Spofforth D.J.A., Agnini C., Pälike H., Rio D., Fornaciari E., Giusberti L:, Luciani V., Lanci L., and Muttoni G., 2010. Organic carbon burial following the middle Eocene climatic optimum in the central western Tethys. Paleoceanography 25, PA3210, doi:10.1029/2009PA001738.

Stefani, C., Grandesso, P., 1991, Studio preliminare di due sezioni del Flysch bellunese: Rend. Soc. Geol. It. 14, 157–162.

Steinmetz, J.C., 1994. Sedimentation of coccolithophores: In A. Winter and W.G. Siesser, W.G., Editors, Coccolithophores, Cambridge University Press, Cambridge, UK, pp. 179–197.

Tremolada, F., Bralower, T.J., 2004. Nannofossil assemblage fluctuations during the Paleocene–Eocene Thermal Maximum at Sites 213 (Indian Ocean) and 401 (North Atlantic Ocean): palaeoceanographic implications. Mar. Micropaleontol. 52, 107–116.

Tripati, A., Elderfield, H., 2005a. Deep-Sea Temperature and Circulation Changes at the Paleocene-Eocene Thermal Maximum. Science 308(5729), 1894-1898.

Tripati, A., Backman J., Elderfield H., Ferretti P. 2005b. Eocene bipolar glaciations associated with global carbon cycle changes. Nature. 436(21), 341-346.

Villa G. Persico D., 2006. Late Oligocene climatic changes: Evidence from calcareous nannofossils at Kerguelen Plateau Site 748 (Southern Ocean). Palaeogeogr., Palaeoclimatol., Palaeoecol. 231(1-2), 110-119.

Villa, G., Fioroni, C., Pea, L., Bohaty, S. M., Persico, D., 2008. Middle Eocene– late Oligocene climate variability: Calcareous nannofossil response at Kerguelen Plateau, Site 748. Mar. Micropaleontol. 69, 173–192, doi:10.1016/ j.marmicro.2008.07.006.

Wade, B.S., Kroon, D. 2002 Middle Eocene regional climate instability: Evidence from the western North Atlantic. Geology 30 (11), 1011-1014.

Walter, L.M., Morse, J.W., 1984. Reactive surface area of skeletal carbonates during dissolution: effect of grain size. J. Sediment. Petrol. 54, 1081–1090.

Wei, W., Wise, S.W., 1990a, Biogeographic gradients of middle Eocene-Oligocene calcareous nannoplankton in the South Atlantic Ocean. Palaeogeogr. Palaeoclimatol. Palaeoecol. 79, 29– 61.

Wei W., Wise, S.W. Jr.; 1990b Middle Eocene to Pleistocene calcareous nannofossils recovered by Ocean Drilling Program Leg 113 in the Weddel Sea. Proceedings of the Ocean Drilling Program. Scientific Results 113. 639–666.

Winter, A., Jordan, R.W., Roth, P.H., 1994. Biogeography of living coccolithophores in ocean waters. In: Winter, A, Siesser, W.G., Eds., Coccolithophores, p. 161-177. Cambridge: Cambridge University Press.

Winterer, E.L., Bosellini, A., 1981. Subsidence and sedimentation on Jurassic passive continental margin, Southern Alps, Italy. Amer. Ass. Petr. Geol. Bull. 65(3), 394-421.

Young, J.R., 1994. Functions of coccoliths. In: Winter, A, Siesser, W.G., Eds., *Coccolithophores*, p. 63–82. Cambridge: Cambridge University Press.

Zachos, J.C., Pagani, M., Sloan, L., Thomas, E., Billups, K., 2001, Trends, rhythms, and aberrations in global climate 65 Ma to present: Science 292, 686–693.

Zachos, J.C., D. Kroon, P. Blum, et al., 2004. Proc. ODP, Init. Repts., 208 [Online]. Available from World Wide Web: http://www-odp.tamu.edu/publications/208_IR/208ir.htm

Zachos, J.C., Röhl, U., Schellenberg, S.A., Sluijs, A., Hodell, D.A., Kelly, D.C., Thomas, E., Nicolo, M., Raffi , I., Lourens, L.J., McCarren, H., Kroon, D., 2005, Rapid acidification of the ocean during the Paleocene-Eocene thermal maximum: Science 308, 1611–1615, doi: 10.1126/science.1109004.

Zachos, J.C., Schouten, S., Bohaty, S., Sluijs, A., Brinkhuis, H., Gibbs, S., Bralower, T., Quattlebaum, T., 2006. Extreme warming of mid-latitude coastal ocean during the Paleocene-Eocene Thermal Maximum: Inferences from TEX_{86} and Isotope Data. Geology 34, 737–740.

Zachos, J.C., Dickens, G.R., Zeebe, R.E., 2008. An early Cenozoic perspective on greenhouse warming and carbon-cycle dynamics. Nature 451, 279-283.

CHAPTER 3 – Middle Eocene to Early Oligocene calcareous nannofossil biostratigraphy at Site U1333c (Pacific Equatorial)

Abstract

We present a biostratigraphic and biochronologic study of calcareous nannofossils of Middle Eocene - Early Oligocene age recovered during IODP Expedition 320, at Site U1333c in the Pacific Equatorial Ocean. The study succession encompasses nannofossil Zones NP16–NP21 (equivalent to CP13–CP16) and Chrons C20r–C12r. The distribution patterns of calcareous nannofossil taxa are studied by means of relative abundance and semiquantitative countings with the final aim to test the reliability of biohorizons used in the Paleogene standard biozonations (Martini, 1971; Okada and Bukry, 1980) and check alternative bioevents included in a more recent biostratigraphic scheme (Fornaciari et al., 2010). Biochronologic data are also provided. The study sediments cover the crucial time period following the maximum Cenozoic warmth and going through the initial major glaciation on Antarctica. During this 15-16 Myr interval two important climatic events, the Middle Eocene Climatic Optimum (MECO), a transient episode of global warming during a long-term cooling trend, and the Oi-1 event, the onset of a permanent ice-sheet on Antarctica, were found to occur. The peculiar regime in sedimentation observed in the Equatorial Pacific, which roughly consists in alternated phases of Carbonate Accumulation Events (CAE) and crashes in carbonate abundances, are correlated with increases and decreases in calcareous nannofossil abundance. A more detailed comparison points out that the MECO corresponds to a very low carbonate interval in between CAE3 and CAE4.

1. **Introduction**

The Eocene time was an intriguing interval because it represents the transition between Greenhouse conditions, that lasted up to the Early Eocene, with its climax in the Early Eocene Climatic Optimum (EECO; ca. 50 Ma), and Icehouse conditions (Zachos et al., 2001; 2008), considered established at the base of the Oligocene ca. 33.8 Ma, with the O1 event (Miller et al., 1991), that is correlated with the South Pole permanent glaciation. The long-term cooling trend initiated after the EECO was not monotonic, but instead studded by several transient warming and cooling episodes (Bohaty and Zachos 2003; Bohaty et al., 2009; Edgar et al., 2007; Sexton et al., 2006; 2011; Tripati et al., 2005a; Vonhof et al., 2000). The Eocene was a time of extremely warm climates, reaching the warmest temperature of the past 80 Myr, but also of progressive deterioration, during the Middle to Late Eocene, coinciding with permanent changes in calcareous plankton (Aubry 1992; 1998; Wade 2004; Aubry and Bord 2009). Unfortunately, this period is poorly documented in expanded well-preserved succession (Fornaciari et al., 2010) and this lack is particularly evident in the material recovered from the Equatorial Pacific Ocean (ODP Leg 199; Fig.1), where Middle to Upper Eocene sediments can be broadly described as radiolarian ooze and clay (Lyle and Wilson, 2006). However, PEAT program recently carried out in IODP Exp. 320-321 recovered a continuous record of this interval, suggesting a very dynamic and shallow CCD during the Eocene, with several excursions of ca. 500m (Lyle et al., 2010; Pälike et al., 2010). This material represents an exceptional archive in which modifications of nannoplankton assemblages can be thoroughly investigated. Relative abundance and semiquantitative counts of calcareous nannofossils were performed during the Middle Eocene to Early Oligocene interval with the two-fold aim to provide a robust biostratigraphic framework and point out any possible environmental-forced change in nannoplankton assemblages.

2.Materials nd Methods

2.1. Materials

IODP Site U1333 is located in the Equatorial Pacific (12°04.0892’N, 142°09.720’W; 5113 mbsl; Fig. 1) and represents the third oldest and deepest component of the Exp. 320 depth transect. At Site U1333C, seafloor basalt is overlain by ca.183 m of pelagic sediment, dominated by nannofossil and radiolarian ooze with varying amounts of clay (Pälike et al. 2010). The IODP Site 1333C was sampled in the interval from 192.06 to

124.80 rmcd at an average spacing of 20-40 cm from 178 to 159 rmcd and ca.100 cm in the basal and upper parts of the study succession. The study material consists of biogenic sediments comprising clayey nannofossil ooze, nannofossil radiolarian ooze, nannofossil ooze, radiolarian nannofossil ooze, and porcellanite in the Middle to Upper Eocene and alternating very pale brown nannofossil ooze and yellowish brown nannofossil ooze with radiolarians in the Upper Eocene-Lower Oligocene. Mean accumulation rates are about 4-5 m/Myr from 45 to 31 Ma (Middle Eocene to Early Oligocene) and increase up to ca. 12 m/Myr from the Early Oligocene. In the Eocene time $CaCO_3$ contents vary abruptly between <1 and 74 wt% because of variations of Equatorial CCD. The Eocene paleodepth for IODP Site U1333C is estimated to have been ca. 3800m and preliminary notes report high carbonate content–bearing sediments around the MECO event, suggesting the possibility to study the high-carbonate preservation events (CAEs) in relation to global modification in Earth's climate (Lyle et al., 2005; Pälike et al. 2010).

2.2. Methods

Calcareous Nannofossils

An amount of 109 samples was prepared for calcareous nannofossil analysis from unprocessed material as smear slides using standard techniques described in Bown and Young (1998). Smear slides were then analyzed with a Zeiss Axiophot optical microscope, at 1250X magnification. Calcareous nannofossils were determined using taxonomy of Perch-Nielsen (1985) and Aubry (1984; 1988; 1989; 1990; 1999), except for sphenoliths for which we have followed Fornaciari et al. (2010). The biostratigraphic standard schemes of Martini (1971) and Okada and Bukry (1980) were applied and compared with the mid latitude zonal scheme recently published by Fornaciari et al. (2010). Age calibration of calcareous nannofossil biohorizons is based on magnetostratigraphic and ciclostratigraphic data available for Site U1333C.

The state of preservation, the degree of dissolution and/or overgrowth of calcareous nannofossil assemblages largely vary throughout the study interval. We thus decided to describe every sample following the qualitative classification proposed by Roth and Thierstein (1972) and Roth (1983). This approach provides three main subgroups of samples, that are defined as follows: 1) goodly preserved (G) for samples with slightly etched and/or overgrown coccoliths; 2) moderately preserved (M) for samples with moderate etching and/or overgrowth, 3) poorly preserved (P) for strongly etched and/or overgrown coccoliths assemblages with reduced diversity. Additionally a specific

classification for etching and overgrowth is also provided. (see supplementary data of Pacific in the attached CD).

Relative abundance analyses were carried out by determining the relative abundances of species and genera, expressed in percentage, based on at least 300 specimens. Semiquantitative data are determined counting all calcareous nannofossil specimens present in a prefixed area (1 mm^2, 50 fields of view). To monitor the species abundance within to the same genus, a total of 100 specimens belonging to *Discoaster* and *Sphenolithus* were counted (Rio et al. 1990). To provide a more reliable biostratigraphic framework, additional countings were carried out in a prefixed area of 9 mm^2 (three transects) for *Chiasmolithus solitus, C. grandis, C. oamaruensis* and *Isthmolithus recurvus*, index species very rare to virtually missing in the study material.

Magnetostratigraphy and cyclostratigraphy

Cleaned paleomagnetic data provide a series of distinct ~180° alternations in declination and subtle changes in inclination, which, when combined with biostratigraphic age constraints, allow a continuous magnetostratigraphy to be constructed that correlates well with the geomagnetic polarity timescale (Pälike et al. 2010; Acton, personal communication). In Table 1, we reported ages and relative positions of bioevents in relation to magnetochrons based the cyclostratigraphic framework available for this Site (Westerhold, personal communication).

3. Results and Discussion

Calcareous nannofossils are present and moderately to poorly preserved through most of the study material. However, we have observed some short barren/very impoverished intervals in the middle/upper Eocene. The study interval spans a complete sequence of nannofossil zones from middle Eocene Zone NP15 to lower Oligocene Zone NP22 in which fossil assemblages are mainly composed of discoasterids, placoliths and sphenoliths. The relative abundance of *Discoaster* and *Sphenolithus* is highly variable and anti-covariant, alternating phases in which *Discoaster* dominates the assemblage and *Sphenolithus* shows low relative abundances to phases in which *Sphenolithus* is very common and *Discoaster* decreases its abundance percentages. Placoliths are well represented in the assemblages with *Dictyococcites* showing a relative abundance pattern similar to that of *Discoaster* and opposite to the other placoliths (*Reticulofenestra, Coccolithus, Ericsonia*).

3.1. Dissolution and preservation

The preservation of carbonate microfossils is mainly affected by primary and export productivity as well as by water-column and seafloor chemistry. In particular, at Site U1333C, the strength of dissolution is in direct ratio to the depth/paleodepth and fluctuations of the CCD of the drilling site (Pälike et al. 2010). Estimations of Eocene Equatorial CCD return a result of depths shallower than 3.5 km (Lyle et al., 2005), with several CCD swallowing phases occurring during the middle to late Eocene. However, the most outstanding change in carbonate sedimentation is represented by the CCD deepening at the Eocene–Oligocene transition which produces a shift from siliceous prevailing sediments to calcareous plankton oozes (Pälike et al. 2010).

Overall, coccoliths are considered to be less susceptible to dissolution than planktic foraminifera (e.g.; Hay, 1970; McIntyre and McIntyre 1971) and they are often present even in very low carbonate sediments. Within the nannofossil assemblages, however, certain taxa are more resistant than others to dissolution and their abundance can be investigated with the aim of reconstructing the degree of dissolution through time (Toffanin et al, 2011). At IODP Site U1333C, the preservation of the calcareous nannofossil assemblages varies throughout the study succession, from moderate to bad. In particular, 13 barren samples are found during the MECO (ca. 172-170 rmcd). In the same interval, between 174.40 and 165.15 rmcd, an overall decrease in preservation is observed with samples showing strong dissolution. In general, calcareous nannofossil assemblages are strongly affected by dissolution, ranging from moderate (etching level E-2) below and above the critical interval to strong (etching level E-3) during the event.

The degree of preservation of an assemblage is affected by two main factors, calcite overgrowth and dissolution (Roth and Thiestein, 1972; Roth, 1983). In our samples, overgrowth processes are sporadically occurring only in large specimens of heavy-calcified genera as for instance *Discoaster, Reticulofenestra* and *Dictyococcites*. In general, overgrowth blurs species specific features making a correct determination difficult. The overgrowth process is thus able to modify the relative abundance of some taxa within the assemblage, because of wrong determination, but do not significantly alter the absolute abundance of calcareous nannofossil taxa. On the contrary, dissolution, which is by far the most common process affecting calcareous nannofossil assemblages in our material is species preferential and therefore alters both the relative and absolute abundance of calcareous nannofossil taxa (Roth and Thierstein, 1972). The way by which

dissolution modifies calcareous nannofossil assemblages is twofold. Firstly, it lowers the total number of taxa observed (species richness), dissolving the more fragile species almost completely. This mechanism eventually results in higher relative abundances of dissolution-resistant taxa and lower relative abundance or even absence of more delicate species (Bornemann and Mutterlose, 2008). Secondly, it causes the decrease of the absolute abundance of calcareous nannofossils taxa, even the more resistant and robust ones. The stronger the dissolution, the lower the number of specimens in a prefixed area.

Looking back over our data, if dissolution would have severely affected nannofossil taxa, the assemblage should be dominated by dissolution-resistant taxa, such as for instance *Discoaster* (Adelseck et al., 1973). Actually, at Pacific Equatorial Site 1333C we observed changes in the nannofossil assemblages, that are consistent with strong dissolution, during the MECO. As we go into greater detail, a remarkable decrease of the number of specimens/mm^2 is clearly visible (Fig. 2). *Reticulofenestra umbilicus* and *Sphenolithus* show a terrific decrease in the total number of specimens observed for mm^2. These genera have a low to intermediate resistance to dissolution, their prominent decrease is thus consistent with an increased dissolution. Additionally, *Discoaster*, considered to be one of the most resistant taxa (Roth and Thiestein,1972; Roth,1983), show a prominent decrease, if counted in a prefixed area (mm^2), and a remarkable increase if counted in the total assemblage (relative abundance in %). These patterns, that seem apparently irreconcilable, are on the contrary easily explained if we considered the fossil calcareous nannofossil assemblage as the result of a pristine assemblage altered/biased by preferential dissolution.

Changes in the absolute and relative abundance of calcareous nannofossils observed during the MECO are correlated with an episode of CCD shallowing (Fig. 2; Bohaty et al., 2009; Pälike et al. 2010). Very similar modifications are found to recur at least two more times before the end of the Eocene virtually mirroring $CaCO_3$ contents and CCD reconstruction. At the base of the Rupelian, a final augment in the absolute abundance of calcareous nannofossils is associated with a long-lasting increase in carbonate content suggesting a permanent deepening of the Pacific Equatorial CCD (Fig. 2; Pälike et al. 2010).

3.2. Calcareous nannofossil biostratigraphy

Calcareous nannoplankton first appeared in the Late Triassic as low diversity assemblages and rapidly radiated during the Early Jurassic. From that time they have colonized the Oceans and their abundance, wide geographic distribution and rapid evolution have been used in biostratigraphy for a long time. In fact, the stratigraphic distributions of calcareous nannofossil taxa are utilized to construct a number of standard biozonations. For the Paleogene interval these biostratigraphic frameworks have been assembled by Martini (1971) and Okada and Bukry (1980) but more recently, other authors (i.e.; Catanzariti et al. 1997; Fornaciari et al., 2010) have proposed new biostratigraphic schemes for the middle Eocene-Early Oligocene interval.

Here, we determined the biohorizons of the Paleogene standard zonations of Martini (NP; Martini, 1971) and Okada and Bukry (CP; Okada and Bukry, 1980), besides we checked the mid latitude biostratigraphic zonal scheme of Catanzariti et al. (1997), integrated by Fornaciari et al. (2010).

The following biohorizons were used: Lowest Rare Occurrence (LRO), Lowest Occurrence (LO), Lowest Common Occurrence (LCO), Highest Common Occurrence (HCO) and Highest Occurrence (HO) and Crossover (CO).

Abundance patterns of the index species adopted in considered zonal schemes are reported in Fig. 3. Microphotos of standard markers and several calcareous nannofossil taxa are provided in Plates I-II. The taxonomic list of taxa observed during the study is available in Appendix A.

4.2.1. Standard calcareous nannofossil biohorizons

The LO of *Reticulofenestra umbilicus*

The LO of *R. umbilicus* defines the base of CP14a Zone of Okada and Bukry (1980) and are used to approximate the base of NP16 Zone of Martini (1971) when *Blackites gladius* is missing (Perch-Nielsen, 1985). At ODP Site 1333C *R. umbilicus* >14µm has its Lowest Occurrence (LO), within Chron C19r (183.35 ± 0.45 rmcd; Table 1) consistently with some previous findings (Wei and Wise; 1989; Jovane et al., 2007; Fornaciari et al., 2010). The taxonomic concept of *R. umbilicus* proposed by Backman and Hermelin (1986), which includes all the specimens larger than 14µm, is now commonly accepted and the more recent calibrations based on this morphometric definition seem to minimize the large discrepancies existing in previous age estimations.

The HO of *Blackites gladius*

The HO of the *B. gladius* defines the base of NP16 Zone of Martini (1971). This species is thought to be facies controlled (Bukry et al., 1971) and is seldom reported from deep-sea settings (Wei and Wise, 1989). In our material, the species is absent likely because of the bad preservation or ecological exclusion, thus preventing its use for biostratigraphic aims.

The HO of *Chiasmolithus solitus*

The HO of *Chiasmolithus solitus* defines base of NP17 and CP14b Zones (Martini, 1971; Okada and Bukry, 1980). The species is reported to be scarce in low latitude sediments and diachronous at different latitudes (Perch-Nielsen, 1985; Wei and Wise, 1992; Aubry, 1992; Villa et al., 2008; Fornaciari et al., 2010). At IODP Site 1333C, *C. solitus* is present but very rare up to 160 rmcd (159.95 $\pm$ 0.20; Table 1), in the upper part of Chron C18n.1n. This datum is quite consistent with recent findings from mid-high latitudes (Villa et al., 2008; Fornaciari et al, 2010) even if some previous studies observed an anticipated disappearance in low-mid latitude areas (Poore et al. 1984; Wei and Wise 1989; 1990a).

The HO of *Discoaster bifax*

The HO of *D. bifax* is used by Okada and Bukry (1980) to mark the base of CP14b Zone. This species is usually common in equatorial sediments (e.g., Bukry, 1973) and rare/absent at middle to high latitudes (Percival 1984; Proto Decima et al. 1975; Nocchi et al. 1988; Wei and Wise 1989; 1992; Wei and Thierstein 1991; Marino and Flores 2002a; b; Fornaciari et al., 2010). At IODP Site 1333C, only very few, sporadic specimens of *D. bifax* were observed during the analysis within CP16 Zone, at higher stratigraphic levels with respect to predicted position of this biohorizon. The HO of *D. bifax* is not used in this study.

The LO of *Chiasmolithus oamaruensis*

The LO of this species defines the base of NP18 Zone and is secondarily used to define the CP15a Zone as a secondary biohorizon (Martini, 1971; Okada and Bukry 1980). Previous authors reported a rare presence of *C. oamaruensis* from low latitude areas (e.g., Wei and Wise, 1989). These data are confirmed by the absence of this taxon at IODP Site 1333C.

The HO of *Chiasmolithus grandis*

The HO of *C. grandis* defines the base of CP15a Zone (Okada and Bukry, 1980). The species is previously reported to be common at low to middle latitudes (Wei and Wise, 1990a) but shows low frequencies and discontinuous presence, albeit counted in 9mm^2, at

IODP Site 1333C. At this Site, *C. grandis* is present from the base of the section up to the upper part of Chron C18n.1n (158.55 ± 0.20 rmcd; Table 1). Recent data from middle latitudes evidenced for a significant decrease in abundance of this taxon, that the authors named Highest Common Occurrence (HCO), just in the upper part of Chron C18n.1n (Fornaciari et al., 2010). Our results on the HO of *C. grandis* seem to be consistent with this datum, but provide a decisively older age estimation with respect to the last presence of this species, observed at Chron C17n.2n by the same authors. At IODP Site 1333C, the extinction of *C. grandis* thus occurs well before most of the available calibrations, except for findings of Monechi and Thierstein (1985), which observed the final presence of this taxon in the upper part of Chron C18n in the Mediterranean area. On this basis, we retain that this biohorizon is highly controversial and should be used with extreme caution.

The LO and LCO of *Isthmolithus recurvus*

The LO of *I. recurvus* defines the base of NP19-NP20 Zone and CP15b Subzone (Martini, 1971; Okada and Bukry 1980). Data available from literature provide a peculiar abundance pattern for this species, a first presence (LO) lying within Chron C17n.1n is followed by a temporary absence and eventually by a common and continuous presence (LCO) of this taxon (Backman, 1987; Catanzariti et al., 1997; Villa et al., 2008; Fornaciari et al., 2010). At IODP Site 1333C, *I. recurvus* is extremely rare and the first specimens ascribable to this taxon was recorded only in basal part of Chron C16n.2n (142.75 ± 0.50 rmcd; Table 1), where the LCO of this species was usually found to occur (Fornaciari et al., 2010). The absence of this taxon before Chron C16n.2n can likely be explained by its unevenly distribution in Equatorial Pacific.

The HO of *Discoaster saipanensis*

The HO of *Discoaster saipanensis* marks the base of NP21 Zone (Martini, 1971), whereas the HOs of *D. saipanensis* and *D. barbadiensis,* defines the base of CP16a Subzone (Okada and Bukry 1980). At IODP Site 1333C, the HOs of the latter two species are neatly recorded at 136.92 rmcd (136.92 ± 0.08 rmcd; Table I) within Chron C13r. The extinction of rosette-shaped discoasterids is clearly diachronous if high and low-middle latitude data are compared (Wei and Wise, 1990a; Arney and Wise, 2003; Persico and Villa, 2004; Villa et al., 2008). In fact, this event has an age of ca. 40 Ma at ODP Site 748 (Villa et al., 2008) but is found consistently within Chron C13r at low-middle latitudes (Berggren et al., 1995). Our data from IODP Site 1333C support the idea that the disappearance of rosette-shaped discoasterids at high latitudes was environmentally

controlled and considerably precedes the final presence of these taxa at low-middle latitudes.

The Acme of *Clausicoccus subdistichus/Clausicoccus obrutus*

The Acme End (AE) of *Clausicoccus subdistichus* defines the base of CP16b Subzone (Okada and Bukry, 1980). *C. subdistichus* is reported to be quite common in the basal Oligocene of some sections while it can be very rare or absent in others (Perch-Nielsen, 1985). Following the reasoning of Backman (1987), we instead use the AB of *Clausicoccus obrutus* both to subdivide NP21 Zone and mark the base of CP16b Subzone. This biohorizon seems to represent the best available nannofossil marker to approximate the base of the Oligocene being consistently found in the upper part of Chron C13r (e.g., Backman, 1987; Coccioni et al., 1988; Berggren et al., 1995, Marino and Flores, 2002; Hyland et al., 2009). At IODP Site 1333C, *C. obrutus* and *Clausicoccus* in general show a remarkable increase in abundance at 134.45 rmcd (134.45 ± 0.40 rmcd; Table 1) and remains abundant up to the top of the studied section. The AB is thus a clear event that can serve to approximate the Eocene-Oligocene boundary; on the contrary, the AE is not well defined, because specimens ascribable to this taxon are still present and common even after the HO of *Ericsonia formosa* (128.17 ± 1.53 rmcd), well above the base of the Oligocene.

The HO of *Ericsonia formosa*

The HO of *E. formosa* defines the base of NP22 Zone and CP16c Subzone (Martini, 1971; Okada and Bukry 1980). This event is considered diachronous between low-mid latitudes (Nocchi et al., 1986; Premoli et al. 1988; Backman, 1987; Berggren et al., 1995; Marino et al., 2002b), where it was found to occur from the uppermost part of Chron C13n and lower part of Chron C12r, and southern high latitudes, where it is present up to Chron C18 (Berggren et al., 1995).

At IODP Site 1333C, the species was quite common and its final presence was observed at the base of Chron C12r rmcd (128.17 ± 1.53 rmcd; Table 1) consistently with most of low-mid latitude data available.

4.2.2. Additional calcareous nannofossil biohorizons

In the Equatorial Pacific, bad preservation of study material and low abundances of a number of marker species utilized in standard zonations prevent from a full recognition of standard biohorizons, which thus implies a poor biostratigraphic resolution. To improve this crucial point, we have integrated standard bioevents with some additional calcareous

nannofossil datums recently proposed by Catanzariti et al. (1997) and Fornaciari et al. (2010). Comments on these additional biohorizons are provided in the following in stratigraphic order:

The LO, LCO and HO of *Cribrocentrum reticulatum*

The appearance and disappearance datums of this species have been employed in Middle-Late Eocene regional biostratigraphy (Wei and Wise, 1989, 1990a, Berggren et al., 1995; Catanzariti et al., 1997, Marino e Flores, 2002, Fornaciari et al., 2010) and its first appearance have been proposed for approximating the base of the Bartonian (Berggren et al., 1995; Flugeman, 2007). Actually, calibrations available for the first appearance of *C. reticulatum* are not consistent, ranging from Chron C20r to Chron C18n, likely because of rare and discontinuous presence of *C. reticulatum* in its initial stratigraphic distribution (see discussion in Fornaciari et al., 2010). However, the LCO of *C reticulatum* has been consistently found at the base of Chron C18r and seem to be a more reliable biohorizon (Berggren et al., 1995; Fornaciari et al., 2010), unfortunately at IODP Site 1333C phenomena of strong dissolution in calcareous nannofossil specimens often produces the partial/total loss of the central area, which inhibits from a straightforward recognition and a reliable abundance pattern of this taxon. The same reasoning holds true even for the HO of this taxon at least in Equatorial Pacific material preventing from a useful use of this biohorizon.

The HO of *Sphenolithus furcatolithoides*

The HO of *S. furcatolithoides* is one of the most neat biohorizon of the late part of the Middle Eocene and it is consistently found in the upper part of Chron C18r shortly preceding the LCOs of *D. bisectus* and *D. scrippsae* (Proto Decima et al. 1975; Perch-Nielsen 1977; Parisi et al.1988; Nocchi et al. 1988; Firth 1989; Wei and Wise 1989; 1992; Okada 1990; Bralower and Mutterlose 1995; Mita 2001; Marino and Flores 2002a; b). At IODP Site 1333C, *S. furcatolithoides* decreases abruptly in abundance in the upper part of Chron C18r (174.49 $\pm$ 0.1 rmcd; Table 1) just before the LCOs of *D. bisectus* and *D. scrippsae* thus maintaining the same stratigraphic position even in this area.

The LCO of *Dictyococcites bisectus*

The taxonomic ambiguities in defining *D. bisectus* essentially derive from different morphometric definitions. Here, we have decided to follow the generally accepted advice of Bralower and Mutterlose (1995), who proposed 10 µm as lower limit for the size of this taxon. This clarification makes the biostratigraphic use of *D. bisectus* more useful. Although some specimens of *D. bisectus* have been found before Chron C18r (Mita, 2001;

Larrasoaña et al.2008), the remarkable increase in abundance in the upper part of Chron C18r is considered to be a very promising datum since it is associated with others two neat biohorizons (i.e., the LCO of *D. scrippsae* and the HO of *S. furcatolithoides*). At IODP Site 1333C, the LCO of *D. bisectus* have been observed in the upper part of Chron C18r (172.69 ± 0.1 rmcd; Table 1) consistently with previous results (e.g., Backman, 1987; Bralower and Mutterlose, 1995; Fornaciari et al., 2010) and very close to the onset of the MECO event. This large dataset indicates that this biohorizon is one of the more reliable bioevents of this interval.

The LCO of *Dictyococcites scrippsae*

The LCO of the *D. scrippsae* is one of the biohorizon found to be positioned very close to the LCO of *D. bisectus* in the upper part of Chron C18r, during the MECO event (Backman, 1987; Fornaciari et al., 2010). At IODP Site 1333C this taxon shows a common a continuous abundance from the upper part of Chron C18r (172.69 ± 0.1 rmcd; Table 1) in coincidence with the prominent increase in abundance of *D. bisectus*. This datum represents a good biohorizon especially if used together with the LCO of *D. bisectus* and the HO of *S. furcatolithoides.*

The HCO of *Sphenolithus spiniger*

The HCO of *S. spiniger* has been recently considered by Fornaciari et al (2010) in their new biozonation. This taxon shows a rare and discontinuous presence in the bad preserved material recovered at IODP Site 1333C. This unevenly distribution in the Equatorial Pacific is likely attributable to its fragile structure that makes *S. spiniger* very prone to dissolution and completely unusable for biostratigraphic aims, at least at this site.

The LO and HO of *Sphenolithus obtusus*

The stratigraphic distribution of *S. obtusus* has been constrained in the Middle Eocene by a number of previous works (Bukry 1973; Nocchi et al. 1988; Wei and Wise 1989; 1992; Okada 1990). In particular, Fornaciari et al. (2010) in their new mid-latitude zonal scheme use the LO and HO of this taxon to redefine and subdivide the NP17 Zone of Martini (1971). These authors report the first appearance of *S. obtusus* in the lower part of Chron C18n and last occurrence at the transition between Chron C18n.1n and Chron C17r. Our data from IODP Site 1333C substantially confirm the same positions with respect to the GPTS, which are the lower part of Chron C18n1n for the LO (164.15 ± 0.2 rmcd; Table 1) and uppermost part of Chron C18n.1n for the HO (158.15 ± 0.2 rmcd; Table 1) respectively.

The Acme of *Cribrocentrum erbae* and the LO of *Cribrocentrum isabellae*

The Acme of *Cribrocentrum erbae* and the LO of *Cribrocentrum isabellae* has been proposed by Fornaciari et al. (2010) to redefine and subdivide the NP18 Zone of Martini (1971). These biohorizons seem to be extremely reliable at least at low-mid latitudes, however, the strong dissolution in the Equatorial Pacific Site 1333C biased the pristine assemblage virtually erasing all the specimens belonging to genus *Cribrocentrum* and thus preventing from using these biohorizons.

The Acme of *Sphenolithus intercalaris*

Martini formally describes *S. intercalaris* from sediments recovered during DSDP Leg 33 in the Central Pacific giving a biostratigraphic distribution restricted between NP16 Zone and NP21 Zone (Middle-Late Eocene to Early Oligocene; 1976). Perch-Nielsen (1985) reports an even more limited distribution, that is NP17-NP18 Zones, however, more recently Bown (2005) found this taxon to be present in the Upper Eocene-Early Oligocene sediments recovered at the Shatsky Rise (Northwest Pacific). Our data from IODP Site 1333C are consistent with previous results from the Pacific Ocean (Martini, 1976; Bown, 2005) and evidenced for a remarkable increase of *S. intercalaris* between 142.75 and 135.35 rmcd (NP21 Zone or MNP21A Zone; Table 1), where this taxon represents more than 50% of the total assemblage of the sphenoliths. This interval is here referred to as the Acme of *S. intercalaris* and correlates with the late part of the Priabonian just preceding the Eocene - Oligocene boundary. This new biohorizon is very prominent at Site 1333C but should be tested over wider area in order to be used for regional correlations.

4.Conclusions

A high-resolution calcareous nannofossil biostratigraphy was carried out at IODP Site 1333C in the Equatorial Pacific Ocean. The Middle Eocene-Early Oligocene study section encompasses nannofossil Zones NP15–NP22 and Chrons C20r–C12r. We have analyzed more than 20 biohorizons in an 11 Myr time interval, from ca 44 Ma to 33 Ma. A number of these biohorizons are used in standard zonations (Martini, 1971; Okada and Bukry, 1980) but are not usable in our material because of the unevenly distribution of some marker species. For this reason we decided to test some additional calcareous nannofossil bioevents proposed in the new zonal scheme of Fornaciari et al. (2010) for the Middle Eocene to Early Oligocene interval. Some of these biohorizons are proved to be reliable and reproducible over wide areas (i.e., The HO of *S. furcatolithoides*, the LO and HO of *S. obtusus*, the LCO of *D. scrippsae* and *D. bisectus*), but some others are affected by the

strong dissolution pervading the study material, which has profoundly altered the pristine abundance of taxa, especially that of the index species more prone to dissolution. The preservation of carbonate sediments is a main issue in the Equatorial Pacific because it is highly variable during the Eocene, where several shallowing events of the CCD, mirroring the $CaCO_3$ content, are found to occur. Calcareous nannofossil absolute and relative abundance can be used as a proxy of degree of dissolution of the assemblage/changes and thus of carbonate preservation through time.

FIGURES

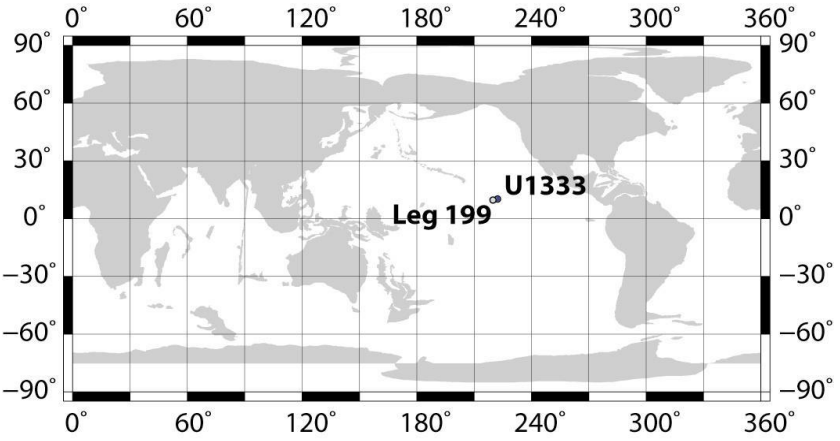

Figure 1. Locations of IODP Leg 199 drilling sites and IODP Site 1333 (http://www.odsn.de/odsn/services/paleomap/paleomap.html).

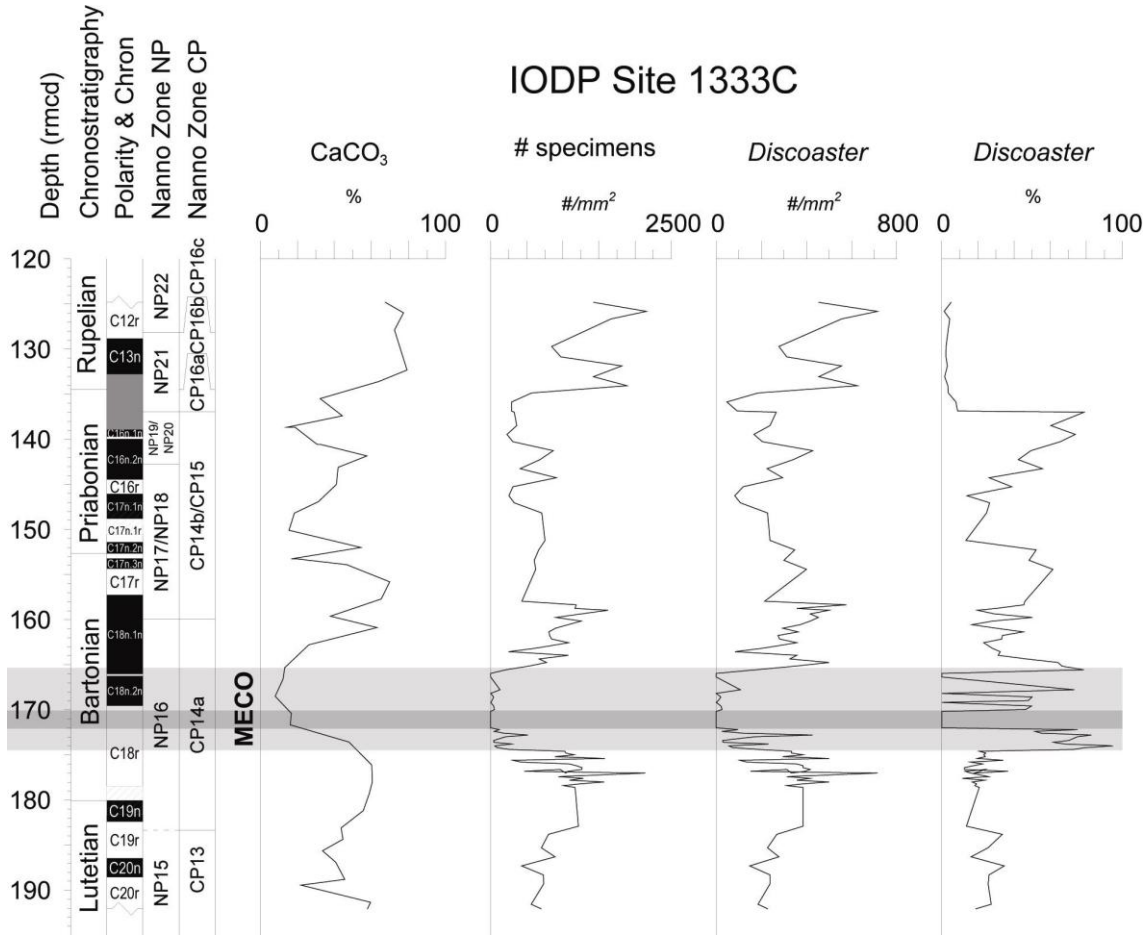

Figure 2. Abundance patterns of *Discoaster*, total number of specimens in a prefixed area (#/mm2) and $CaCO_3$ content (after Pälike et al., 2010) from the IODP Site 1333C are plotted against magnetostratigraphy and biostratigraphy (NP—Martini, 1971; Okada and Bukry, 1980). The light grey shaded bar emphasizes the MECO event that correlates with one of the episodes of CCD shallowing during the Eocene. The Eocene/Oligocene boundary is placed in correspondence with the AB of *C. obrutus*.

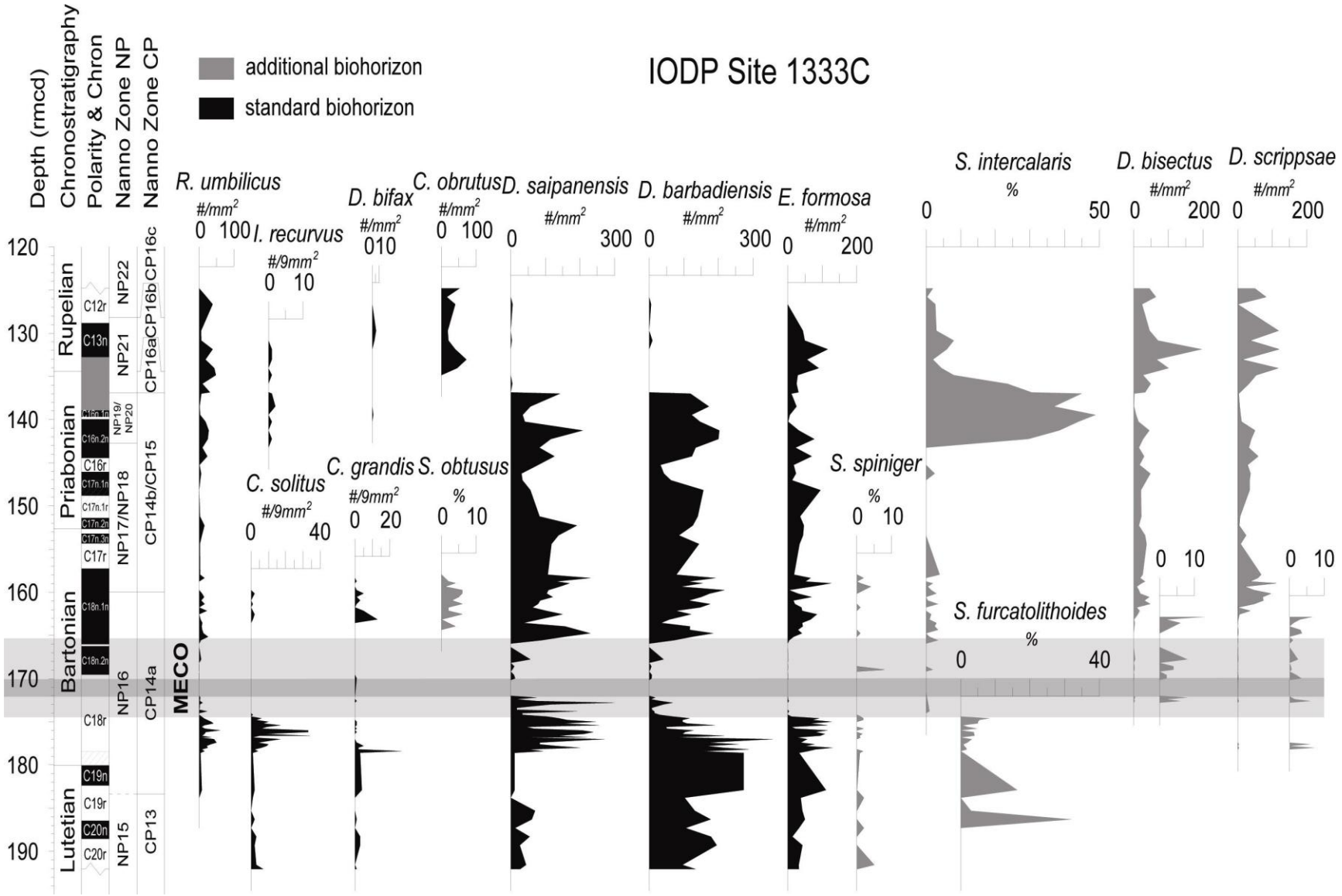

Figure 3. Abundance patterns of standard and additional calcareous nannofossil index taxa from the IODP Site 1333C are plotted against magnetostratigraphy and biostratigraphy (NP—Martini, 1971; Okada and Bukry, 1980). The light grey shaded bar emphasizes the MECO event that correlates with one of the episodes of CCD shallowing during the Eocene. The Eocene/Oligocene boundary is placed in correspondence with the AB of *C. obrutus*.

TABLES

Biohorizon	Sample Base		Sample Top		Depth (rmcd) +	Error (m)	Chron	Age Top (Ma) *	Age Base (Ma) *
E. formosa HO	U1333C-14H-1	135	U1333C-13H-7	70	128,17	± 1,53	C12r	33,3198	32,9443
C. obrutus AB	U1333C-14H-5	35	U1333C-14H-4	85	134,45	± 0,4	C13r	/	/
D. saipanensis HO	U1333C-14H-5	135	U1333C-14H-5	35	136,92	± 0,08	C13r	/	/
I. recurvus LCO	U1333C-15H-4	45	U1333C-15H-3	95	142,750	± 0,5	C16n.2n	36,1601	36,0029
S. intercalaris AB	U1333C-15H-4	45	U1333C-15H-3	95	142,750	± 0,5	C16n.2n	36,1601	36,0029
S. obtusus HO	U1333C-17H-2	5	U1333C-17H-1	115	158,150	± 0,2	C18n.1n	38,5872	38,5371
C. grandis HO	U1333C-17H-2	45	U1333C-17H-2	5	158,550	± 0,2	C18n.1n	38,6373	38,5872
C. solitus HO	U1333C-17H-3	35	U1333C-17H-2	145	159,950	± 0,2	C18n.1n	38,8127	38,7626
S. obtusus LO	U1333C-17H-6	5	U1333C-17H-5	115	164,150	± 0,2	C18n.1n	39,3389	39,2888
D. scrippsae LCO	U1333C-18H-5	105	U1333C-18H-5	85	172,69	± 0,1	C18r	40,4316	40,4102
D. bisectus LO	U1333C-18H-5	105	U1333C-18H-5	85	172,69	± 0,1	C18r	40,4316	40,4102
S. furcatolithoides HO	U1333C-18H-6	137	U1333C-18H-6	115	174,490	± 0,1	C18r	40,6181	40,5947
R. umbilicus LO	U1333C-20H-3	25	U1333C-20H-2	25	183,350	± 0,45	C19r	42,0115	41,6472

*using amcd & revised u-chan magstrat (Acton pers. comm.)
+ Westerhold (pers. comm.)

Table 1: The position of biohorizons are reported together with their chron notations and age estimations.

Chron Base	Hole	Core	Section	Interval (cm)	Depth (rmcd) *	Mean (rmcd)*	Age CK95+ (Ma)
c12n	U1333C U1333C	10H 12H	7 2	83 4	104,59 113,77	**109,18**	30,939
c12r	U1333C U1333C	14H 14H	1 1	45 49	128,80 128,84	**128,82**	33,058
c13n c16n.1n	U1333C U1333C	14H 15H	3 1	146 43	132,76 138,93	**135,85**	33,545
c13r c15n c15r							34,655 34,940 35,343
c16n.1n	U1333C U1333C	15H 15H	1 1	116 122	139,66 139,72	**139,69**	35,526
c16n.1r	U1333C U1333C	15H 15H	2 2	13 19	139,93 139,99	**139,96**	35,685
c16n.2n	U1333C U1333C	15H 15H	5 5	15 23	144,45 144,53	**144,49**	36,341
c16r	U1333C U1333C	15H 15H	6 6	45 49	146,03 146,07	**146,05**	36,618
c17n.1n	U1333C U1333C	15H 16H	6 1	146 66	147,03 150,57	**148,80**	37,473
c17n.1r	U1333C U1333C	16H 16H	2 2	6 11	151,37 151,42	**151,40**	37,604
c17n.2n	U1333C U1333C	16H 16H	2 2	134 138	152,65 152,69	**152,67**	37,848
c17n.2r	U1333C U1333C	16H 16H	3 3	23 28	153,19 153,24	**153,22**	37,920
c17n.3n	U1333C U1333C	16H 16H	3 3	136 141	154,32 154,37	**154,35**	38,113
c17r	U1333C U1333C	17H 17H	1 1	43 47	157,23 157,27	**157,25**	38,426
c18n.1n	U1333C U1333C	17H 17H	7 7	23 28	165,99 166,04	**166,02**	39,552
c18n.1r	U1333C U1333C	17H 18H	7 1	67 5	166,43 167,06	**166,75**	39,631
c18n.2n	U1333C U1333C	18H 18H	3 3	59 63	169,51 169,55	**169,53**	40,130
c18r	U1333C U1333C	19H 20H	3 1	96 41	178,41 181,60	**180,01**	41,257
c19n	U1333C U1333C	20H 20H	1 1	117 123	182,36 182,42	**182,39**	41,521
c19r	U1333C U1333C	20H 20H	4 4	89 93	186,44 186,48	**186,46**	42,536
c20n	U1333C U1333C	20H 20H	5 6	145 5	188,49 188,60	**188,55**	43,789

*Westerhold (pers. comm.)
+from GPTS of Cande and Kent (1995; CK95)

Table 2: The positions of Chron base are reported.

PLATES

Plate I. Microphotographs of calcareous nannofossil from the ODP Leg 320, Site U1333 in the middle and late Eocene interval. All specimens × 1000.

1-2. *Coccolithus eopelagicus.* Sample 320-U1333-16H-3W, 45 1 Crossed nicols. 2 Parallel light, 3-4. *Coccolithus pelagicus*. Sample 320-U1333-18H-8W, 15. 3 Crossed nicols. 4 parallel light. 5-6. Ericsonia formosa. Sample 320-U1333-14H-1W, 135. 5 Crossed nicols. 6 parallel light. 7-8. *Coccolithus cachaoi* Sample 320-U1333-20H-6W, 75. 7 Crossed nicols. 8 parallel light. 9-10. *Chiasmolithus solitus.* Sample 320-U1333-17H-3W, 35. 9 Crossed nicols. 10 Parallel light. 11-12. *Chiasmolithus grandis.* Sample 320-U1333-17H-3W, 35. 11 Crossed nicols. 12 Parallel light. 13-14. *Chiasmolithus grandis.* Sample 320-U1333-17H-2W, 45. 13 Crossed nicols. 14 Parallel light. 15-16. *Dictyococcites bisectus.* Sample 320-U1333-18H-5W, 65. 15 Crossed nicols. 16 Parallel light. 17. *Dictyococcites scrippsae* affinis. Sample 320-U1333-15H-5W, 95. Crossed nicols. 18. *Cyclicargolithus floridanus*. Sample 320-U1333-20H-2W, 25. Crossed nicols. 19-20. *Reticulofenestra umbilicus.* Sample 320-U1333-18H-8W, 75. 19 Crossed nicols. 20 Parallel light.

PLATE I

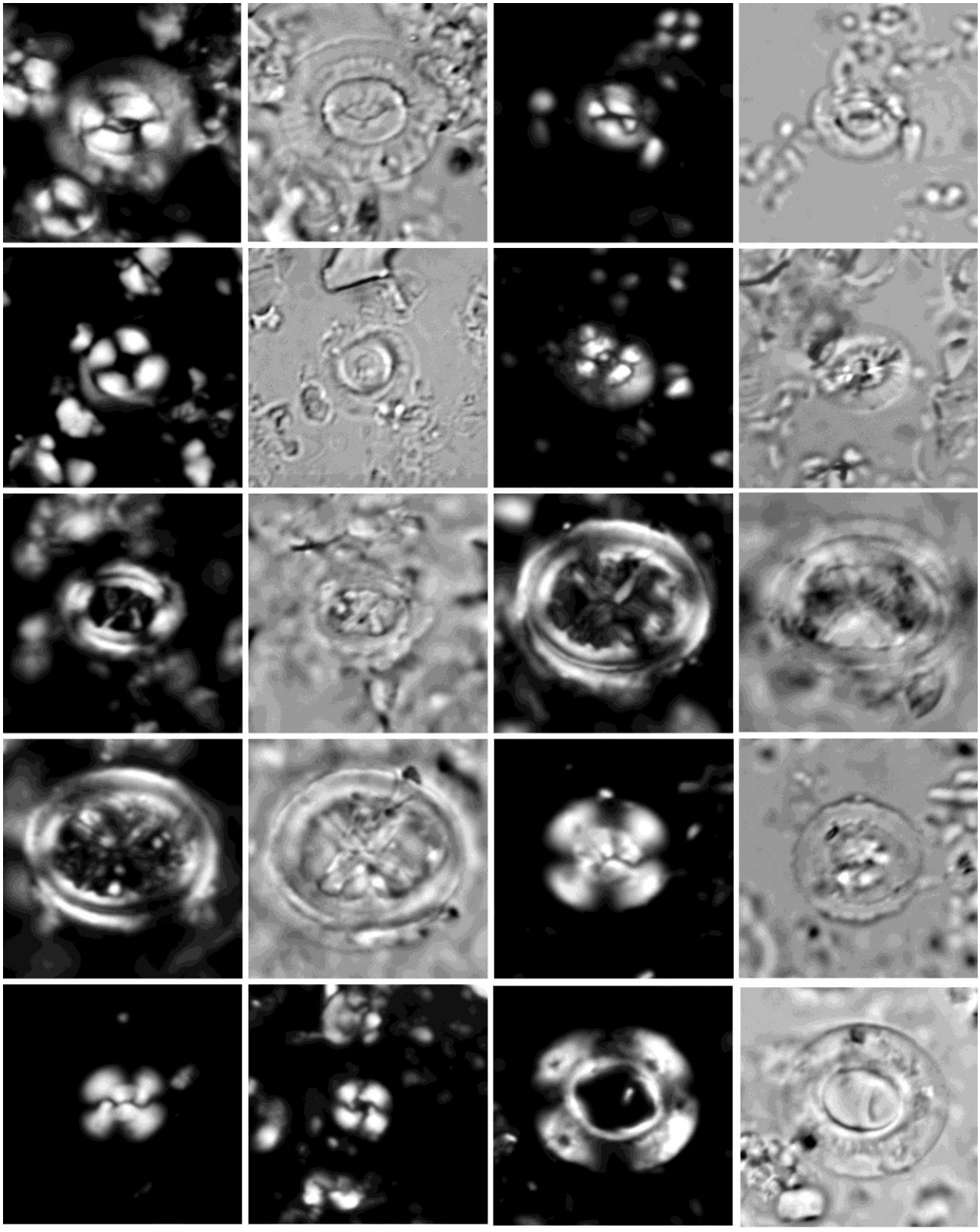

Plate II. Microphotographs of calcareous nannofossil from the ODP Leg 320, Site U1333 in the middle and late Eocene interval. All specimens × 1000.

1. *Clausicoccus subdistichus*; Sample 320-U1333-14H-4W, 5. Crossed nicols. 2–4. *Sphenolithus furcatolithoides*. Sample 320-U1333-18H-6W, 137. 2. Crossed nicols 0°. 3. Crossed nicols 30°. 4. Crossed nicols 45°. 5. *Sphenolithus moriformis*. Sample 320-U1333-18H-8W, 35. Crossed nicols 0°. 6–8. *Sphenolithus* cf *predistentus.* Sample 320-U1333-18H-7W, 145. 6. Crossed nicols 0°. 7. Crossed nicols 30°. 8. Crossed nicols 45°. 9–11. *Sphenolithus predistentus distentus.* Sample 320-U1333-13H-7W, 70. 9. Crossed nicols 0°. 10. Crossed nicols 30°. 11. Crossed nicols 45°. 12. *Thoracosphaera sp*.; Sample 320-U1333-17H-4W, 125. Crossed nicols. 13–15. *Sphenolithus obtusus.* Sample 320-U1333-17H-5W, 115. 13. Crossed nicols 0°. 14. Crossed nicols 30°. 15. Crossed nicols 45°. 16. *Discoaster saipanensis*; Sample 320-U1333-4H-1W, 135. Crossed nicols. 17. *Discoaster barbadiensis*; Sample 320-U1333-4H-1W, 135. Crossed nicols. 18. *Discoaster deflandrei*; Sample 320-U1333-14H-3W, 55. Crossed nicols. 19-20. *Isthmolithus recurvus*. Sample 320-U1333-14H-7W, 65. 19 Crossed nicols. 20 Parallel light.

PLATE II

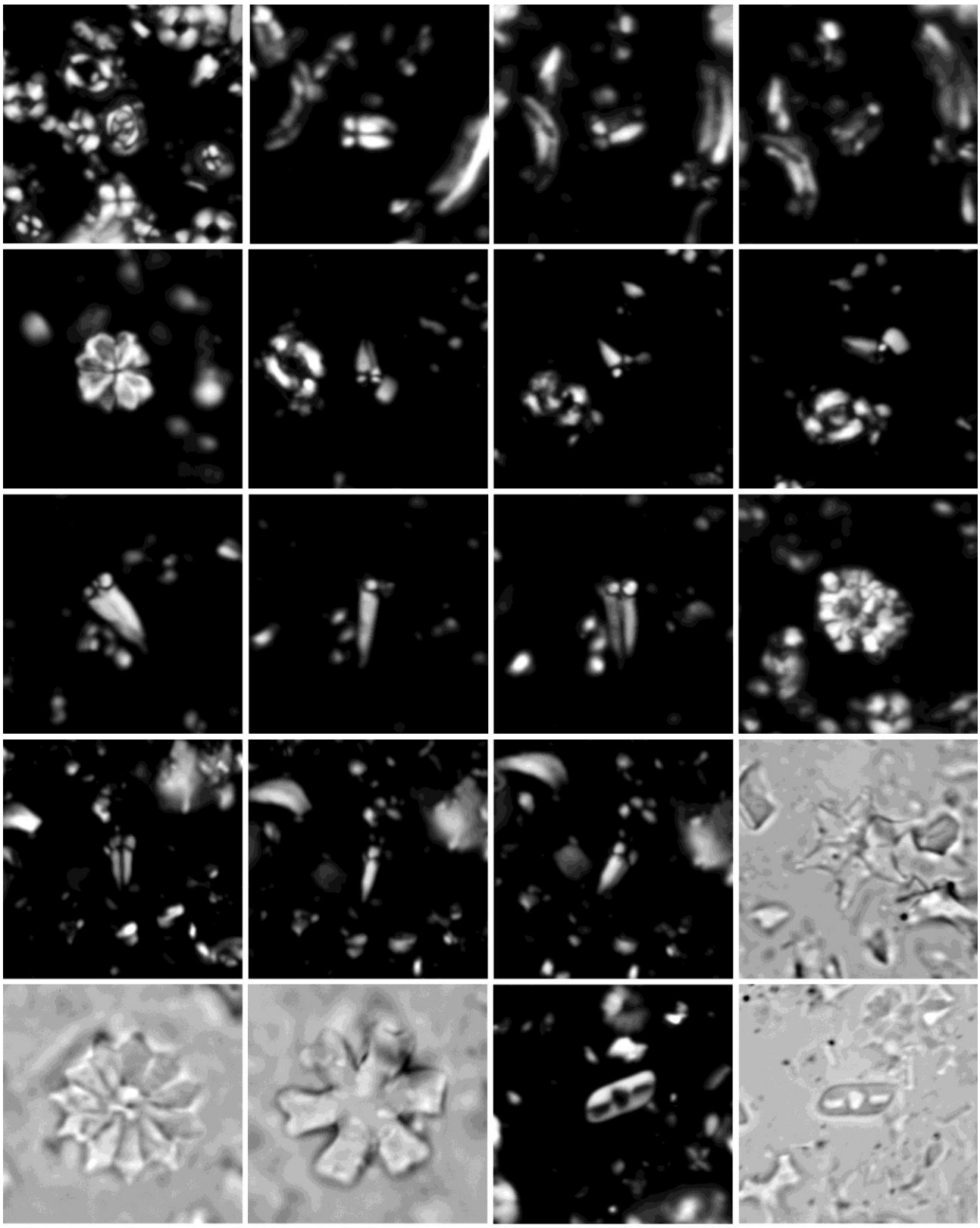

Appendix A:Taxonomic List

Blackites gladius (Locker 1967) Varol, 1989
Chiasmolithus altus Bukry and Percival, 1971
Chiasmolith consuetus (Bramlette and Sullivan) Hay and Mohler, 1967
Chiasmolithus oamaruensis (Deflandre, 1954) Hay et a., 1966
Chiasmolithus grandis (Bramlette and Riedel) Radomski, 1968
Chiasmolithus solitus (Bramlette and Sullivan) Locker, 1968
Clausicoccus subdistichus (Roth and Hay, in Hay et al., 1967) Prins, 1979
Clausicoccus obrutus (Perch-Nielsen 1971) Prins, 1979
Coccolithus cachaoi (Bown, 2005)
Coccolithus eopelagicus (Bramlette and Riedel) Bramlette and Sullivan, 1961
Coccolithus pelagicus (Wallich) Schiller, 1930
Cribrocentrum erbae (Fornaciari et al., in Fornaciari et al., 2010)
Cribrocentrum isabellae (Catanzariti et al., in Fornaciari et al., 2010)
Cyclicargolithus (Bukry, 1971)
Dictyococcites (Black, 1967)
Dictyococcites bisectus (Hay, Mohler and Wade, 1966) Bukry and Percival, 1971
Dictyococcites scripsae Bukry and Percival 1971
Discoaster barbadiensis Tan, 1927
Discoaster bifax Bukry, 1971
Discoaster binodosus Martini, 1958
Discoaster deflandrei Bramlette and Riedel, 1954
Discoaster gemmifer Stradner, 1961
Discoaster lenticularis Bramlette and Sullivan, 1961
Discoaster lodoensis Bramlette and Riedel, 1954
Discoaster mirus Deflandre, 1969
Discoaster saipanensis Bramlette and Riedel, 1954
Discoaster strictus Stradner, 1961
Discoaster subodoensis Bramlette and Sullivan, 1961
Discoaster tanii Bramlette & Riedel, 1954
Discoaster tanii var*. nodifer* (Bramlette and Riedel 1954)
Discoaster wemmelensis Achuthan and Stradner, 1969
Ericsonia formosa (Kamptner 1963) Hai 1971
Ericsonia subpertusa Hay and Mohler, 1967
Helicosphaera bramlettei (Müller) Jafar and Martini, 1975
Helicosphaera compacta Bramlette and Wilcoxon, 1967
Helicosphaera dinesenii Perch-Nielsen, 1971
Helicosphaera heezenii (Bukry) Jafar and Martini, 1975
Hughesius (Varol, 1989)
Isthmolithus recurvus Deflandre, 1954
Lanternithus minutus Stradner, 1962
Neococcolithes minutus (Perch-Nielsen) Perch-Nielsen, 1971
Pontosphaera multipora (Kamptner) Roth, 1970
Pseudotriquetrorhabdulus Wise in Wise and Constans, 1976
Reticulofenestra Hay et al., 1966
Reticulofenestra daviesii (Haq) Haq, 1971
Reticulofenestra umbilicus (Levin), Martini and Ritzkowski, 1968
Rhabdolitus Kamptner ex Deflandre in Grass, 1952
Sphenolithus distentus (Martini) Bramlette and Wilcoxon, 1967
Sphenolithus furcatolithoides Locker, 1967
Sphenolithus intercalaris Martini, 1976
Sphenolithus moriformis (Brönnimann and Stradner) Bramlette and Wilcoxon, 1967
Sphenolithus obtusus Bukry, 1971
Sphenolithus predistentus Bramlette and Wilcoxon, 1967
Sphenolithus radians Deflandre, 1952
Sphenolithus spiniger Bukry, 1971
Thoracosphaera Kamptner, 1927
Toweius eminens Bramlette and Sullivan, 1961
Transversopontis Hay, Mohler and Wade, 1966
Watznaueria Reinhardt 1964

References

Adelseck, C.G. Jr., Geehan, G.W. and Roth, P.H., 1973. Experimental Evidence for the Selective Dissolution and Overgrowth of Calcareous Nannofossils During Diagenesis, Geological Society of America Bulletin 84, 2755-2762.

Agnini C., Fornaciari E., Giusberti L., Grandesso P., Lanci L., Luciani V., Muttoni G., Rio D., Stefani C., Pälike H. and Spofforth D.J.A, 2011 Integrated bio-magnetostratigraphy of the Alano section (NE Italy): a proposal for defining the Middle-Late Eocene boundary, Geological Society of America Bulletin. Arney and Wise, 2003

Arney, J.E., and Wise, S.W., Jr., 2003. Paleocene-Eocene nannofossil biostratigraphy of ODP Leg 183, Kerguelen Plateau. In Frey, F.A., Coffin, M.F., Wallace, P.J., and Quilty, P.G. (Eds.), Proc. *ODP, Sci. Results,* 183 [Online].

Aubry, M.-P., 1984. Handbook of Cenozoic Calcareous Nannoplankton, book 1, Ortholithae (Discoaster). Am. Mus. of Nat. Hist. Micropaleontol. Press, New York. 263 pp.

Aubry, M.-P., 1988. Handbook of Cenozoic Calcareous Nannoplankton, book 2, Ortholithae (Holococcoliths, Ceratoliths, Ortholiths and Other). Am. Mus. of Nat. Hist.Micropaleontol. Press, New York. 279 pp.

Aubry, M.-P., 1989. Handbook of Cenozoic Calcareous Nannoplankton, book 3, Ortholithae (Pentaliths and Other), Heliolithae (Fasciculiths, Sphenoliths and Others). Am. Mus. of Nat. Hist. Micropaleontol. Press, New York. 279 pp.

Aubry, M.-P., 1990. Handbook of Cenozoic Calcareous Nannoplankton, book 4, Heliolithae (Helicoliths, Cribriliths, Lopadoliths and Other). Am. Mus. of Nat. Hist. Micropaleontol. Press, New York. 381 pp.

Aubry, M.-P., 1992. Late Paleogene calcareous nannoplankton evolution: a tale of climatic deterioration, in Eocene–Oligocene climatic and biotic evolution. In: Prothero, D.R., Berggren, W.A. (Eds.), Eocene–Oligocene Climatic and Biotic Evolution. Princeton Univ. Press, Princeton, NJ, pp. 272–309.

Aubry M.-P.,1998, Early Paleogene calcareous nannoplankton evolution: a tale of climatic amelioration, in late Paleocene and early Eocene climatic and biotic evolution. In: M.-P. Aubry, S. Lucas and W. Berggren, Editors, Late Paleocene–early Eocene climatic and biotic events in the marine and terrestrial record, Columbia University Press (1998), pp. 158–203.

Aubry, M.-P., 1999. Handbook of Cenozoic Calcareous Nannoplankton, book 5, Heliolithae (Zygoliths and Rhabdoliths). Am. Mus. of Nat. Hist.Micropaleontol. Press, New York. 368 pp.

Aubry, M.-P., and Bord, D., 2009. Reshuffling the Cards in the Photic Zone at the Eocene/Oligocene Boundary. Geological Society of America Special Paper (GSA-SP), 452, p. 279-301

Backman J,Hermelin JO (1986) Morphometry of the Eocene nannofossil Reticulofenestra umbilicus lineage and its biochronological consequences. Palaeogeography, Palaeoclimatology, Palaeoecology 57, 103–116.

Backman, J., 1987. Quantitative calcareous nannofossil biocronology of middle Eocene through early Oligocene sediments from DSDP Sites 522 and 523. Abhandlungen Der Geologischen Bundesanstalt, 39:21-31.

Berggren, W. A., Kent, D. V., Swisher, C. C., Aubry M.P., 1995. A revised Cenozoic geochronology and chronostratigraphy. Geochronology, Time Scales and Global Stratigraphic Correlation: Soc. Econ. Paleontol. Mineral., Spec. Publ. 54, 212 pp.

Bohaty, S.M., Zachos, J.C., 2003. Significant Southern Ocean warming event in the late middle Eocene. Geology 31(11), 1017– 1020, doi:10.1130/G19800.1

Bohaty, S.M., Zachos, J.C., Florindo, F., Delaney, M.L. 2009. Coupled greenhouse warming and deep-sea acidification in the middle Eocene Paleoceanography 24 , PA2207.

Bornemann, A., Mutterlose, J., 2008. Calcareous Nannofossil and $\delta^{13}C$ Records from the Early Cretaceous of the Western Atlantic Ocean: Evidence for Enhanced Fertilization across the Berriasian–Valanginian Transition. Palaios 23, 821-832.Bosellini, F.R.

Bown, P.R., and Young, J.R., 1998. Techniques. In Bown, P.R. (Ed.), Calcareous Nannofossil Biostratigraphy: London, Chapman & Hall, pp. 16–28.

Bown, P.R., 2005. Early to mid-Cretaceous calcareous nannoplankton from the northwest Pacific Ocean, Leg 198, Shatsky Rise. /In/ Bralower, T.J., Premoli Silva, I., and Malone, M.J. (Eds.), /Proc. ODP, Sci. Results,/ 198: College Station, TX (Ocean Drilling Program), 1--82. doi:10.2973/odp.proc.sr.198.103.2005

Bralower, T. J., and Mutterlose, J., 1995. Calcareous nannofossil biostratigraphy of ODP Site 865, Allison Guyot, Central Pacific Ocean: a tropical Paleogene reference section: in Winterer, E. L., Sager, W. W., Firth, J. V., et al., Proceedings of the Ocean Drilling Program Scientific Results, v. 143, p. 31-72.

Bukry, D., 1971. Cenozoic calcareous nannofossils from the Pacific Ocean. Transactions of the San Diego Society of Natural History 16, 303–328.

Bukry, D. 1973. Coccolith stratigraphy, eastern equatorial Pacific, Leg 16, Deep Sea Drilling Project.. Initial Reports of the Deep Sea Drilling Project. 16:653-711.

Cande, S.C., Kent, D.V., 1995. Revised calibration of the geomagnetic polarity time scale for the Late Cretaceous and Cenozoic. J. Geophys. Res. 100 (B4), 6093–6096. doi:10.1029/94JB03098.

Catanzariti R., Rio D., Martelli L.. 1997 – Late Eocene to Oligocene Calcareous Nannofossil Biostratigraphy in Northern Apennines: the Ranzano Sandstones. Mem. Sc. Geol., 49, 207-253.

Coccioni R. (1988)- The genera Hantkenina and Cribrobantkenina (Foraminifera) in the Massignano section (Ancona, Italy). In: Premoli Silva I., Coccioni R. and Montanari A. (Eds.): 81 - 96.

Coxall, H.K., Wilson, P.A., Pälike, H., Lear, C.H., and Backman, J., 2005. Rapid stepwise onset of Antarctic glaciations and deeper calcite compensation in the Pacific Ocean. Nature (London, U. K.), 433(7021):53–57. doi:10.1038/nature03135

DeConto, R.M., Pollard, D., Wilson, P.A., Palike, H., Lear, C.H., and Pagani, M., 2008. Thresholds for Cenozoic bipolar glaciation. Nature (London, U. K.), 455(7213):652–656. doi:10.1038/nature07337

Edgar, K.M., Wilson, P.A., Sexton, P.F. Suganuma, Y., 2007. No extreme bipolar glaciation during the main Eocene calcite compensation shift. Nature, 448:908-911.

Firth, J V (1989): Eocene and Oligocene calcareous nannofossils from the Labrador Sea, ODP Leg 105. In: Srivastava, SP; Arthur, M; Clement, B; et al. (eds.), Proceedings of the Ocean Drilling Program, Scientific Results, College Station, TX (Ocean Drilling Program), 105, 263-286, doi:10.2973/odp.proc.sr.105.131.1989

Fluegeman, R. H., 2007. Unresolved issues in Cenozoic chronostratigraphy. Stratigraphy, 4:109-116.

Fornaciari, E., Agnini, C., Catanzariti, R., Rio, D., Bolla, E.M., Valvasoni, E., 2010, Mid-latitude calcareous nannofossil biostratigraphy, biochronology and evolution across the middle to late Eocene transition. Stratigraphy 7, (4) 229-264.

Hay, W.W., 1970, Sedimentation Rates: Calcium Carbonate Compensation: Deep Sea Drilling Proj. Initial Repts, Vol. 4, p 668-672.

Hyland, E.; Murphy; B.; Varela, P.; Marks, K.; Colwell, L.; Tori, F.; Monechi, S.; Cleaveland, L.; Brinkhuis, H:; van Mourik, C.A.; Coccioni, R.; Bice, D.; Montanari, A.;

2009: Integrated stratigraphic and astrochronologic calibration of the Eocene-Oligocene transition in the Monte Cagnero section (northeastern Apennines, Italy): A potential parastratotype for the Massignano global stratotype section and point (GSSP) GSA Special Papers, v. 452, p. 303-322

Jovane L., Florindo, F., Coccioni, R., Dinare`s-Turell, J., Marsili, A., Monechi, S., Roberts, A. P. and Sprovieri, M., 2007, The middle Eocene climatic optimum event in the Contessa Highway section, Umbrian Apennines, Italy, Geol. Soc. Am. Bull., 119 (3 – 4), 413 – 427, doi:10.1130/B25917.1Lyle, Wilson, Janecek, et al., 2002

Larrasoaña, J.C., Gonzalvo, C., Molina, E., Monechi, S., Ortiz, S., Tori, F. & Tosquella, J. 2008: Integrated magnetobiochronology of the Early/Middle Eocene transition at Agost (Spain): Implications for defining the Ypresian/Lutetian boundary stratotype. *Lethaia*,Vol. 41, pp. 395–415

Lyle, M., Olivarez Lyle, A., Backman, J., and Tripati, A., 2005. Biogenic sedimentation in the Eocene equatorial Pacific—the stuttering greenhouse and Eocene carbonate compensation depth. In Lyle, M., Wilson, P.A., Janecek, T.R., et al., Proc. ODP, Init. Repts., 199: College Station, TX (Ocean Drilling Program), 1–35. doi:10.2973/odp.proc.sr.199.219.2005

Lyle, M., and Wilson, P.A., 2006 Leg 199 Synthesis: Evolution of the equatorial Pacific in the early Cenozoic, in Lyle, M., Wilson, P., and Firth, J., eds., Proceedings of the Ocean Drilling Program, Scientific Results, Volume 199: College Station TX, Ocean Drilling Program, p. 1-35, doi:10.2973/odp.proc.sr.199.219.2005 http://www-odp.tamu.edu/publications/199_SR/synth/synth.htm

Lyle, M., Palike, H., Nishi, H, Raffi, I., Gamage, K., Klaus, A. and the IODP Expedition320/321 Scientific Party, 2010. The Pacific Equatorial Age Transect, IODP Expeditions 320 and 321: Building a 50-million-year-long environmental record of the Equatorial Pacific. Sci. Drill. 9, 4-15.

Marino M., Flores J.A ,(2002a) -Miocene to Pliocene calcareous nannofossil biostratigraphy at ODP Leg 177 Sites 1088 and 1090. Marine Micropaleontology, 45: 291-307.

Marino M., Flores J.A. (2002b) -Middle Eocene to early Oligocene calcareous nannofossil stratigraphy at Leg 177 Site 1090. (2002) - Marine Micropaleontology, 45: 383-398.

Martini E., 1971, Standard Tertiary and Quaternary calcareous nannoplankton zonation, in Farinacci, A., ed., Proceedings, International Conference on Planktonic Microfossils, second, Rome, Volume 2: Rome, Italy, Tecnoscienza Edizione, p. 739-785.

Martini E., 1976. Cretaceous to Recent calcareous nannoplankton from the central Pacific Ocean (DSDP Leg 33). In: S.O. Schlanger and E.D. Jackson (Eds.), Init. Rep. DSDP, 33: 439-450.

Miller, K.G., Wright, J.D., Fairbanks, R.G., 1991. Unlocking the Ice House: Oligocene–Miocene oxygen isotopes, eustasy, and margin erosion. J. Geophys. Res. 96, 6829–6848.

Mita, I., 2001. Data Report: Early to late Eocene calcareous nannofossil assemblages of Sites 1051 and 1052, Blake Nose, northwestern Atlantic Ocean. *In* Kroon, D., Norris, R.D., and Klaus, A. (Eds.), *Proc. ODP, Sci. Results,* 171B, 1–28 [Online]. Available from www: <http://wwwodp.tamu.edu/publications/171B_SR/VOLUME/CHAPTERS/SR171B07.PDF>

Monechi S., Thierstein H.R., 1985, Late Cretaceous-Eocene nannofossil and magnetostratigraphic correlations near Gubbio, Italy. Mar. Micropal., 9: 419-440.

Nocchi, M., Parisi, G., Monaco, P., Monechi, S., Madile, M., Napoleone, G., Ripepe, M., Orlando, M., Premoli Silva, I. and Bice, D.M., 1986. The Eocene-Oligocene boundary in the umbrian pelagic sequences, Italy. In: Pomerol, Ch., Premoli Silva, I., Eds., Terminal Eocene Events, 25-40. Amsterdam: Elsevier. Developments in Palaeontology and Stratigraphy, vol. 9.

Nocchi, M., Parisi, G., Monaco, P., Monechi, S., Madile, M., 1988. Eocene and Early Oligocene micropaleontology and paleoenvironments in SE Umbria, Italy. Palaeogeography, Palaeoclimatology, Palaeoecology, 67:181-124.

Okada, H., 1990. Quaternary and Paleogene calcareous nannofossils, Leg 115. In: Duncan, R.A., Backman, J., Peterson, L.C., et al.,Eds., Proceedings of the Ocean Drilling Program, Scientific Results, 115: 129--174. College Station, TX: Ocean Drilling Program.

Okada, H., Bukry, D., 1980. Supplementary modification and introduction of code numbers to the low-latitude Coccolith biostratigraphic zonation, (Bukry, 1973; 1975). Mar. Micropaleontol. 5, 321-325

Pälike, H., Nishi, H., Lyle, M., Raffi, I., Klaus, A., Gamage, K., and the Expedition 320/321 Scientists, 2009. Pacific Equatorial Transect. IODP Prel. Rept., 320. doi:10.2204/iodp.pr.320.2009.

Pälike, H., Nishi, H., Lyle, M., Raffi, I., Gamage, K., Klaus, A., and the Expedition 320/321 Scientists, 2010. Expedition 320/321 summary. In Pälike, H., Lyle, M., Nishi, H., Raffi, I., Gamage, K., Klaus, A., and the Expedition 320/321 Scientists, Proc. IODP,

320/321: Tokyo (Integrated Ocean Drilling Program Management International, Inc.). doi:10.2204/iodp.proc.320321.101.2010).

Perch-Nielsen, K. 1985, Cenozoic calcareous nannofossils. In Bolli H.M., Saunders J.B., Perch-Nielsen K. Plankton Stratigraphy. Cambridge University Press, p. 427-554.

Parisi, G., Guerrera, F., Madile, M., Magnoni, G., Monaco, P., Monechi, S. and Nocchi, M., 1988. Middle Eocene to early Oligocene calcareous nannofossil and foraminiferal Biostratigraphy in the Monte Cagnero section, Piobbico (Italy).In: Premoli Silva. I., Coccioni. R., Montanari, A., Eds., The Eocene-Oligocene boundary in the Marche-Umbria Basin (Italy), 119-235. Ancona: Fratelli Anniballi. International Union of Geological Sciences International Subcommission on Paleogene Stratigraphy. Special Publication.

Percival, S.F., 1984; Late Cretaceous to Pleistocene calcareous nannofossils from the South Atlantic oxygen and carbon isotope record from South Atlantic Deep Sea Drilling Project, 73, in Hsu, K.J., La Brecque, J.L., et al., Initial reports of the Deep Sea Drilling Project, Volume 73, Washington D.C., U.S. Government Printing Office, p. 725-736.

Persico, D., Villa G., 2004. Eocene-Oligocene calcareous nannofossils from Maud Rise and Kerguelen Plateau (Antarctica): palaeoecological and palaeoceanographic implications. Mar. Micropaleontol. 52, 153-179.

Poore, R:Z:, and Matthews, R:K:, 1984, Late Eocene-Oligocene oxygen and carbon isotope record from South Atlantic Ocean DSDP Site 522, in Hsu, K.J., La Brecque, J.L., et al., Initial reports of the Deep Sea Drilling Project, Volume 73, Washington D.C., U.S. Government Printing Office, p. 725-736.

Premoli Silva, I., Coccioni, R. and Montanari, A., 1988.The Eocene-Oligocene Boundary in the Marche-Umbria Basin (Italy). Ancona: Fratelli Anniballi. International Union of Geological Sciences International Subcommission on Paleogene Stratigraphy. Special Publication, 268 pp.

Proto Decima, F.; Roth, P.H.; Todesco, L. Nannoplancton calcareo del Paleocene e dell'Eocene della sezione di Possagno, in: H.M. Bolli (Ed.), Monografia Micropaleontologica sul Paleocene e l'Eocene di Possagno, Provincia di Treviso, Italia, Schweiz. Pala?ontol. Abh., vol. 97, 1975, pp. 35-- 55.

Rio, D., Raffi, I., Villa, G., 1990. Pliocene–Pleistocene calcareous nannofossil distribution patterns in the western Mediterranean. Proc. Ocean Drill. Program Sci. Results 107, 513–533.

Robertson, A.H.F., Emeis, K.-C., Richter, C., and Camerlenghi, A. (Eds.), 1998 Proceedings of the Ocean Drilling Program, Scientific Results, Vol. 160).

Roth, P.H., 1983. Jurassic and Lower Cretaceous calcareous nannofossils in the Western North Atlantic (Site 534): biostratigraphy, preservation, and some observations on biogeography and paleoceanography. Initial Reports of the Deep Sea Drilling Project 76, 587-621.

Roth, P.H., Thierstein, H.R. 1972. Calcareous nannoplankton: Leg XIV of the Deep Sea Drilling Project. In D. E. Hayes & A. C. Pimm (Eds.), Initial Reports of the Deep Sea Drilling Project 14, :421-486.

Salisbury, Matthew H; Shinohara, Masanao; Richter, Carl; et al (2002): Proceedings of the Ocean Drilling Program, Initial Reports. College Station, Texas (Ocean Drilling Program), 195, online, doi:10.2973/odp.proc.ir.195.2002).

Sexton, P.F., Wilson, P.A., Norris, R.D., 2006. Testing the Cenozoic multisite composite $\delta^{18}O$ and $\delta^{13}C$ curves: New monospecific Eocene records from a single locality, Demerara Rise (Ocean Drilling Program Leg 207). Paleoceanography 21, PA2019, doi:10.1029/2005PA001253.

Sexton, P.F.; Norris, R.D.; Wilson, P.A.; Pälike, H.; Westerhold, T.; Röhl, U.; Bolton, C. T. and Gibbs, S., 2011. Eocene global warming events driven by ventilation of oceanic dissolved organic carbon. Nature, 471 pp. 349–352.

Toffanin, F., Agnini, C., Fornaciari, E., Rio, D., Giusberti, L., Luciani, V., Spofforth, D.J.A., Pälike, H., 2011 Changes in calcareous nannofossil assemblages during the Middle Eocene Climatic Optimum: Clues from the central-western Tethys (Alano section, NE Italy), Marine Micropaleontology, Volume 81, 1–2, p 22-31, ISSN 0377-8398, 10.1016/j.marmicro.2011.07.002.

Tripati, A., Elderfield, H., 2005a. Deep-Sea Temperature and Circulation Changes at the Paleocene-Eocene Thermal Maximum. Science 308(5729), 1894-1898.

Vonhof, H.B.,| Smit, J., Brinkhuis, H., Montanari, A., Nederbragt, A.J., 2000. Global cooling accelerated by early late Eocene impacts? Geology 28 (8), 687-690.

Villa, G., Fioroni, C., Pea, L., Bohaty, S. M., Persico, D., 2008. Middle Eocene– late Oligocene climate variability: Calcareous nannofossil response at Kerguelen Plateau, Site 748. Mar. Micropaleontol. 69, 173–192, doi:10.1016/ j.marmicro.2008.07.006.

Wade, BS (2004) Planktonic foraminiferal biostratigraphy and mechanisms in the extinction of Morozovella in the late middle Eocene, Mar. Micropaleontol, **51**, pp.23-38.

Wei, W. and Wise JR., S.W., 1989. Paleogene calcareous nannofossil magnetobiostratigraphy: results from South Atlantic DSDP 516. Marine Micropaleontology, 14:119–152.

Wei, W., Wise, S.W., 1990a, Biogeographic gradients of middle Eocene-Oligocene calcareous nannoplankton in the South Atlantic Ocean. Palaeogeogr. Palaeoclimatol. Palaeoecol. 79, 29– 61.

Wei, W., Thierstein, H.R., 1991. Upper Cretaceous and Cenozoic calcareous nannofossils of the Kerguelen Plateau (southern Indian Ocean) and Prydz Bay (East Antarctica). In: Barrow, B., Larsen, B., et al. (Eds.), Proc. ODP, Sci. Results, vol. 119, 467– 492.

Wei, W., and Wise, S.W., Jr., 1992. Oligocene–Pleistocene calcareous nannofossils from Southern Ocean Sites 747, 748, and 751. In Wise, S.W., Jr., Schlich, R., et al., Proc. ODP, Sci. Results, 120: College Station, TX (Ocean Drilling Program), 509–521. doi:10.2973.odp.proc.sr.120.201.1992

Zachos, J.C., Pagani, M., Sloan, L., Thomas, E., Billups, K., 2001, Trends, rhythms, and aberrations in global climate 65 Ma to present: Science 292, 686–693.

Zachos, J.C., Dickens, G.R., Zeebe, R.E., 2008. An early Cenozoic perspective on greenhouse warming and carbon-cycle dynamics. Nature 451, 279-283.

CHAPTER 4 - Change in calcareous nannofossil assemblages during the Middle Eocene Climatic Optimum at ODP Site 1051A: Gradual biotic modifications are the response to gradual climatic perturbations?

Abstract

Here, we investigated the response of calcareous nannofossil assemblages of ODP Site 1051A to the Middle Eocene Climatic Optimum (MECO), a significant temporary warming phase interrupting the Middle-Late Eocene long-term cooling trend. This event is characterized by an increase in surface and deep-sea temperatures of about 4-6 C°, testified by a gradual negative shift in oxygen stable isotopes; this perturbation occurred at Chron C18r-C18n transition (ca. 40 Ma) and lasted ca. 500-600 kyr (Bohaty et al., 2009). In this study, our main aim was to investigate the calcareous nannofossil response to the MECO by means of semi-quantitative analyses on calcareous nannofossil. Our results point out that modifications in calcareous nannoflora are not correlated with the onset of the $\delta^{18}O$ negative excursion and started well after the increase in sea temperature, where no clear evidence for a paleoenvirontal perturbations was found to occur. However, during this long warming phase we observed several changes, which include the increase in the number of specimen/mm^2 and small reticulofenestrids, the LCO of large *Dictyococcites,* the gradual decrease of sphenolihs and discoasterids and a major reorganization within genus *Sphenolithus*. All these lines of evidence not only depict a shift toward more eutrophic conditions in sea surface waters, they also suggest a scenario in which abiotic and biotic changes seem not to mirror one each other, the first considerably predating the latter.

1.Introduction

The Cenozoic has been characterized by an articulated evolution of the Earth climate system. Warm temperatures persisted from the Cretaceous and reached their peaks during the Early Eocene Climatic Optimum 50 Ma (EECO), this entire long interval has been usually referred to as the greenhouse world (Zachos et al., 2001). This phase is followed by a long–term cooling trend, the doubthouse world (50-33.4 Ma), that eventually led the Earth to the so called icehouse world of the Oligocene, with the permanent presence of the Antarctic ice sheet (O1 event, 33,4 Ma; Miller et al., 1991). The doubthouse world represents a transitional interval that is not yet completely understood. Based on current general knowledge, this Middle to Late Eocene cooling trend was not monotonic, but has instead revealed climatic variability and repeated transient warming/cooling events (Diester Haas and Zahn, 1996; Wade and Kroon, 2002; Bohaty and Zachos, 2003). The most pronounced of these short-lived events, the Middle Eocene Climatic Optimum (MECO) has been first described at Maud Rise and Kerguelen Plateau in Southern Ocean (Bohaty and Zachos, 2003), with an estimated age of ca.~ 41.5 Ma. This extreme warming event is defined based on a negative gradual shift in $\delta^{18}O$ values (~1‰), which is interpreted as an increase in surface and deep waters of about 4-6°C. A parallel shoaling in the Carbonate Compensation Depth (CCD), lasted ca. 500 Kyr, was observed to occur in correspondence with this phase both in the Atlantic and Pacific Oceans (Bohaty et al., 2009; Pälike et al., 2010). High resolution $\delta^{18}O$ data from different areas indicate that a gradual bottom-water increase in temperature culminated with a peak warming lasting ca. 100 Kyr. The return to pre-event temperatures is testified by a quite rapid $\delta^{18}O$ shift toward more positive values (Bohaty et al., 2009).

Since the MECO has became the focus of much research, robust chronologic studies have been also carried out that evidenced big discrepancies between the age estimation provided from Southern Ocean, ca. 41.5 Ma (Bohaty and Zachos, 2003), and the most recent evaluations coming from several areas, ca. 40.0 Ma (Sexton et al, 2006, Jovane et al, 2007; Bohaty et al., 2009; Agnini et al., 2011), and based on solid magnetostratigraphic frameworks. The conundrum about the age of the MECO event has been eventually solved placing the MECO event at Chron C18r/Chron C18n.2n transition (ca. 40.0 Ma), where it is found to occur in the mid to equatorial Atlantic latitudes (ODP Sites 1051, 1263 and 1258) as well as in the Thetyan domain (Sexton et al, 2006, Jovane et al, 2007; Bohaty et al., 2009; Agnini et al., 2011)

A transient rise in pCO_2 levels is considered the most plausible cause for the MECO warming event. This slow increase in pCO_2 values (500 kyr) has been tentatively linked to a prolonged pulse of metamorphic decarbonation during an initial ‘‘Eohimalayan’’ phase of prograde metamorphism (Kerrick and Caldeira, 1999; Bohaty et al., 2009). Alternative hypotheses took into account the role that an increased extrusive arc volcanism around the Pacific rim or an episode of increased carbonatite magmatism in the East Africa Rift zone. could have played (Bailey, 1992; 1993; Cambray and Cadet, 1996). Another trigger mechanism considered for the MECO event is the input of methane hydrates in the ocean-atmosphere system, the main problem with this hypothesis is the gradual long-lasting warming documented by the $\delta^{18}O$ values that more likely suggests a constant long-lived source of CO_2.

In this contest, we have decided to study the calcareous nannofossil assemblages before, during and after the MECO. In fact, calcareous nannofossil assemblages have been used for a long time to trace paleoenviromental changes (e.g., Haq and Lohmann, 1976; Wei and Wise, 1990a; Aubry, 1998; Bralower, 2002; Erba, 2006) because their abundances are thought to be controlled by temperature, nutrient availability and salinity (e.g., Bralower, 2002; Gibbs et al., 2006; 2010; Tremolada and Bralower, 2004; Agnini et al., 2007). Our main aim in this study is thus to provide a better understand of paleoenviromental perturbations and biotic changes occurred during this Middle Eocene Hyperthermal correlating our results with those available from different areas (Villa et al., 2008; Egdar et al., 2010; Luciani et al., 2010; Toffanin et al. 2011; in prep.).

2. Location and Geological Setting

During the Ocean Drilling Program (ODP) Leg 171B, an expanded sedimentary succession of Maastrichtian through Eocene age was recovered from a transect of the Florida Continental Margin (Blake Nose) (Ogg and Bardot, 2001). These sediments record a well-preserved magnetostratigraphic signal and contain abundant, highly diversified calcareous nannofossils assemblages (Ogg and Bardot, 2001; Mita, 2001). In particular, Hole 1051A is located at 30°3.1740´N, 76°21.4580´W and has an estimated palaeodepth of ca. 1000–2000 mbsl for the middle Eocene (Shipboard Scientific Party, 1998) with a paleolatitude of ca. 25°N (Figure 1; Ogg and Bardot, 2001). Sediments drilled at this site encompass nannofossil Zones NP4–NP18 (equivalent to CP3–CP15) and Chrons C27r–C16r and consist of light green and yellow siliceous chalk and ooze,

with a mean accumulation rate of ca. 2-6 cm/Kyr (Norris et al., 2001). A complete and expanded documentation of the MECO event is present at ODP Site 1051A as already demonstrated by Bohaty et al. (2009).

3. Materials and Methods

3.1. Calcareous nannofossils

At ODP Site 1051A, the study interval extends from 99,85 to 63,25 mbsf, that is within NP16 Zone (or CP14a Subzone; Martini, 1971, Okada and Bukry, 1980) at Chron 18r/Chron 18n transition. The peak phase of the MECO has been recognized by Edgar et al., (2010) at ca. 72 mbsf. An amount of 72 samples was prepared from unprocessed material as smear slides for nannofossil analysis using standard techniques (Bown and Young, 1998), the average sampling resolution was of ca. 50 cm. Smear slides were analyzed with Zeiss Axiophot optical microscope, at 1250X magnification. Calcareous nannofossils were determined using taxonomy of Perch-Nielsen (1985) and Aubry (1984; 1988; 1989; 1990; 1999), except for sphenoliths that were classified following Fornaciari et al. (2010). The biostratigraphic schemes adopted are those of Martini (1971) and Okada and Bukry (1980).The preservation of calcareous nannofossils was estimated following Roth and Thierstein (1972) and Roth (1983):

G = good; no dissolution or overgrowth;

M = moderate; slight to moderate dissolution or overgrowth;

P = poor; considerable dissolution or overgrowth.

After a qualitative analysis of each study sample, semi quantitative counting methods were carried out by determining the relative abundances of species and genera, expressed in percentage, on at least 300 specimens. The abundance of species belonging to genera *Discoaster* and *Sphenolithus* were determined by counting a prefixed number of taxonomically related forms, 100 sphenoliths and 100 discoasterids (Rio et al., 1990). Additional countings were performed for very rare taxa, as species belonging to genus *Chiasmolithus*, in order to provide a more reliable biostratigraphic framework, which is essentially based on *C. solitus* presence. A dataset was created and graphs of calcareous nannofossil taxa were generated to investigate the changes, if any, occurring before, during and after the MECO at Site 1051A.

3.2. Magnetostratigraphy and Geochemistry

The revised magnetostratigraphy of Hole 1051A is that recently proposed by Edgar et al. (2010). The carbon and oxygen stable isotope data are those of Bohaty et al (2009) aligned on the new Site 1051 age model of Edgar et al. (2010).

4.Results

4.1. Calcareous nannofossil biostratigraphy results

Here we present calcareous nannofossil data from the interval comprised from 99,85 to 63,25 mbsf, in which the MECO is recorded. Overall calcareous nannofossils are well preserved and do not show any prominent change in the preservation state. Calcareous nannofossil assemblages are mostly dominated by placoliths such as *Coccolithus*, *Cyclicargolithus*, *Dictyococcites* and *Reticulofenestra*; common taxa are also *Braarudosphaera*, *Discoaster* (e.g., *D. barbadiensis, D. saipanensis* and *D. binodusus* gr.) and *Sphenolithus* (e.g., *S. moriformis, S. furcatolithoides; S. obtusus*). Throughout the investigated succession prominent modifications are observed in calcareous nannofossil assemblages, which include the following (Figs. 1-3):

- A long-term increase in the number of specimens/mm^2 starts at 89.15 mbsf (± 0.25m) before the peak phase of the MECO event within Chron C18r. This pattern is highly variable ranging from ca. 1000 to ca 2500 forms per mm^2 and showing at least two temporary decreasing at ca. 89.0-88.0 and 82.0-80.0 mbsf in what we named the second step of the MECO. This interval is comprised from 90.65 (± 0.25m) to ca. 74.0 mbsf and is defined by the presence of several calcareous nannofossil biohorizons and/or modifications in the relative abundance of some taxa within the assemblage (Figs. 2-3).
- Large *Dictyococcites*, which include *D. scrippsae* and *D. bisectus*, show an abrupt increase in their relative abundance (ca. 5-10%) at 90.65 mbsf (±0.25m) and remain abundant throughout the study section. The lowest presence of these morphotypes is reported well before the MECO interval in the Early/Middle Eocene (Mita; 2001; Agnini et al, 2006; Larrasoaña et al., 2008), being usually followed by temporary disappearance and final massive re-enter in the paleontologic record in the upper part of Chron C18r (Backman, 1987; Fornaciari et al., 2010). This peculiar abundance pattern allows a definition of a lowest common and continuous occurrence (LCO) for these two taxa that serve as a good biostratigraphic marker and, in our case, to define the base of second step of the MECO interval.

- Overall genus *Reticulofenestra* gradually increases in abundance from ca. 89.65 mbsf (±0.25m) and shows a second remarkable increase at Chron C18/C18n transition (79.12 mbsf ± 0.25m). The abundance pattern of the genus is in fact controlled by the abundance of small reticulofenstrids (4-8 µm), which, in contrast with large reticulofenestrids (e.g. *Reticulofenestra umbilicus*), progressively increase during the investigated interval (Fig. 2-3).
- *Zyghrablithus bijugatus* rises in abundance from 91.60 mbsf (±0.25m), just preceding the LCO of *Dictyococcites,* and show a continuous presence up to the top of the section (Fig.3).
- Though *Helicosphaera* is quite rare in our material, it shows an increase in abundance lasting for the entire second step of the MECO, from 91.13 mbsf (±0.23m) to 73.87 mbsf (±0.40m).
- Genus *Sphenolithus* is quite common in the assemblages and shows little variation in its abundance pattern. Nevertheless, if observed at species level, we recognized several biohorizons such as the HO of *S. furcatolithoides*, the temporary presence of *S.* predistentus and LO of *S. obtusus* from 90.65 mbsf (±0.25m) upward.
- *Sphenolithus furcatolithoides* disappears at 90.65 mbsf (±0.25m) and its highest occurrence correlates with the LCO of large *Dictyococcites* and thus with the onset of the second step of the MECO (Fig. 2). This biohorizon is used in biostratigraphy (Perch-Nielsen, 1985; Marino and Flores 2002; Fornaciari et al., 2010) and is consistently found in the upper part of Chron C18r, where we also observed its final presence.
- *D. saipanensis* shows an abrupt decrease starting from 90.65 mbsf (±0.25m), persisting throughout the entire section (Fig.2).
- In the investigated section, *Braarudosphaera* represents a common component of the calcareous nannofossil assemblage and is characterized by an interval of low abundances during the entire second step of the MECO (Fig. 3).
- *Cribrocentrum* is characterized by low abundances during the second step of the MECO interval from from 90.65 (± 0.25m) to ca. 74.0 mbsf.
- *Discoaster* evidences a progressive decrease in its relative abundance during the second step of the MECO interval from 90.65 (± 0.25m) to ca. 74.0 mbsf.
- *Ericsonia, Coccolithus* and *Discoaster* show a gradual decrease in their relative abundance throughout the study section.

5.Discussion

In the studied section, the MECO interval, as originally defined by Bohaty and Zachos (2003) starts, based on the onset of the long-term negative $\delta^{18}O$ trend, at ca. 120 mbsf (Fig.2); in addition, the onset of the second step of the MECO, as defined in this study, is placed at 90.65 mbsf (± 0.25m), predating the Chron C18r/C18n boundary. Our results also indicate that major modifications among calcareous nannofossils occurred between the onset of the second step of the MECO and the top of MECO, as defined by Bohaty et al. (2009), that is from 90.65 (± 0.25m) to ca. 74.0 mbsf. The changes observed in the second step of the MECO in calcareous nannofossil assemblage are characterized by two different modes:

- The LCO of large *Dictyococcites*, the HO of *S. furcatolithoides*, The LO of *S. obtusus*, the increase of *Z. bijugatus*, the decrease of *D. saipanensis*, the low abundances of *Braarudosphaera* and *Cribrocentrum* occur quite abruptly and starts, except for the LO of *S. obtusus*, in correspondence with the onset of the second step of the MECO, well before the MECO peak (74.0 mbsf) (Fig. 2, 3).
- The increase of reticulofenestrids, especially the smaller specimens, the decrease of sphenoliths, *Coccolithus*, *Ericsonia* and *Discoaster* are also recorded from the onset of the second step of the MECO but they are more gradual and enduring, lasting even after the MECO interval.

5.1.Main modifications in calcareous nannofossil assemblages

Changes in calcareous nannofossils are described below and tentatively used to reconstruct, based on previous paleoecologic affinity and together with carbon and oxygen stable isotopes, the paleoenviromental evolution during the study interval. A series of taxa generally shows an increase during the MECO:

- *Reticulofenestra* is thought to be a temperate/mesotrophic, taxon (Wei and Wise, 1990a; Persico and Villa, 2004; Villa et al., 2008); in particular, small reticulofenestrids (4-5.8μm) are able to adapt to stressed conditions (Okada, 2000; Hagino and Okada, 2001) and thus their increase recorded from 90.65 mbsf (± 0.25m) upward might represent an evidence of a long-term eutrophication of sea surface water at Site 1051A beginning after the onset of the second step of the MECO (Fig. 3).

- *Dictyococcites* has been previously interpreted as a temperate water taxon (Haq and Lohmann, 1976; Villa and Persico, 2006; Wei and Wise, 1990a) adapted to eutrophic conditions (Spofforth et al., 2010; Toffanin et al., 2011). In a context of a long term gradual warming, the increase of this genus from the beginning of the second step of the MECO reconciles with a paleonviromental evolution toward more eutrophic conditions (Figs. 2, 3).
- *Helicosphaera* prefers eutrophic upwelling areas (Edward and Perch-Nielsen, 1975; Perch-Nielsen, 1985), its temporary increase during the second step of the MECO matches with an increase in nutrient availability during the second step of the MECO.
- *Zyghrablithus* is thought to be a warm oligotrophic taxon during the Early Paleogene (Wei and Wise, 1990a; Aubry, 1998; Bralower, 2002; Gibbs at al., 2006; Agnini et al., 2007) but a more eutrophic affinity was suggested for this taxon during the middle to Late Eocene interval (Persico and Villa, 2004; Villa and Persico, 2006 and Villa et al. 2008). The suddenly increase of *Z. bijugatus* could indicate more eutrophic conditions (Fig. 3).

All these changes are consistent with more eutrophic conditions at least during the second step of the MECO. A second group of taxa is instead characterized by a gradual irreversible decrease from the base of the second step of the MECO upward in the section. These taxa are *Sphenolithus, Discoaster*, *Cribrocentrum, Braarudosphaera*, *Coccolithus* and *Ericsonia* (Fig.3):

- *Sphenolithus* and *Discoaster* are generally considered to be warm/oligotrophic taxa, (e.g., Wei and Wise, 1990a; Aubry, 1998; Young, 1994; Bralower, 2002; Agnini et al., 2007). Their decrease in abundance throughout the section is likely related to a gradual eutrophication during the second step of the MECO and to the gradual decrease in sea surface temperate after the end of the MECO. This articulated explanation finally resulted in a continuous decrease in abundance from ca. 90.0 mbsf to the end of the study section (Fig. 3).
- *Braarudosphaera* is interpreted as a cold shallow water taxon (Bramlette and Martini, 1964; Bukry et al., 1971; Kelly et al., 2003) and thus its temporary decline during the second step of the MECO together with that of *Cribrocentrum reticulatum* can be interpreted as a natural response to the warming phase documented by the negative trend of the oxygen isotope curve (Fig. 3).

- *Coccolithus* and *Ericsonia* are considered a temperate-water taxa (Wei and Wise, 1990a; Persico and Villa; 2004; Villa and Persico, 2006; Villa et al., 2008), changing its paleecological preferences from warm/oligotrophic to cold/eutrophic waters from the Eocene-Oligocene transition (Haq and Lohmann, 1976, Wei and Wise, 1990a). Aubry (1998) suggested a eurytopic affinity. The decrease in abundance of *Coccolithus* and *Ericsonia* during the studied interval suggests that these two taxa suffered, although slightly, for the increase in water temperature during the second step of the MECO interval.

5.1.1. Sphenolithus

Sphenolithus and *Discoaster* are usually used in paleoecologial reconstruction because they are thought to have a strong warm/oligotrophic affinity (e.g., Bralower, 2002; Wei and Wise, 1990a; Gibbs et al., 2004; Gibbs at al., 2006; Agnini et al., 2007; Persico and Villa, 2004; Villa and Persico, 2006; Villa et al. 2008).

At genus level *Sphenolithus* shows a very slight decrease throughout the section but, if we observe sphenoliths at the species level, the scenario substantially changes. In fact, this group shows a species specific affinity more than an homogeneous behavior. *S. moriformis*, the main constituent of this genus, shows a slight decrease in concomitance with the MECO interval, but the other species of this genus are instead characterized by a short-term profound modification that eventually led to a major reorganization within sphenoliths. In particular, species ascribable to *Sphenolithus* appear/disappear and increase/decrease in abundance during the second step of the MECO. From the onset of the second step of the MECO, we observed a series of interesting changes such as the extinction of *S. furcatolithoides*, the relative increase in abundance of *S. spiniger* and *S. predistentus* and *S. radians*, the relative decrease of *S. moriformis* and the appearance of *S. obtusus*. If we try to interpret these data in a different perspective with respect to most of previous literature, sphenoliths can be considered a kind of heterogeneous taxa characterized by different paleoecological affinity. This alternative view is essentially based on a different paleoecological behavior of species within *Sphenolithus*. In particular, sphenoliths with a prominent apical spine are found to increase their abundance during phases of enhanced eutrophication, like that observed in the MECO Alano section and in the Eocene/Oligocene Tanzania succession (Dunkley Jones et al., 2008; Toffanin et al., 2011). By contrast, *S. moriformis*, in which apical spine is not present, shows a decrease in abundance in the Alano and Tanzania successions suggesting that it prefers more

oligotrophic condition. A similar behavior of *S. moriformis* is documented during the Paleocene Eocene Thermal Maximum and the Pliocene suggesting that an increase in nutrient availability results in a decrease of this taxon (Gibbs et al., 2006; Agnini et al., 2007). On this basis, we can hypothesize a different response within spenoliths that is likely related to a distinct ecological adaptations within the genus.

6.Conclusions

At ODP Site 1051A, we have performed a high resolution study on calcareous nannofossil assemblages during the MECO event. Our data highlight that modifications in calcareous nannoflora are not correlated with the onset of the $\delta^{18}O$ negative excursion and in fact started well after the increase in sea temperature, where no clear evidence for a paleoenvirontal perturbations was found to occur. The integration of calcareous nannofossil and stable isotopes data indicates that $\delta^{18}O$ changes foresee the biotic modifications by ca. 400 kyr possibly suggesting two different scenarios: 1- a large delay of the biotic component with respect to the abiotic one or 2- a nonexistence relationship between the changes in the physical enviroment and the response of the calcareous nannoflora. However, during this long warming phase we observed several changes, which include the increase in the number of specimen/mm^2 and small reticulofenestrids, the LCO of large *Dictyococcites,* the gradual decrease of sphenolihs and discoasterids and a major reorganization within genus *Sphenolithus*.

Figures

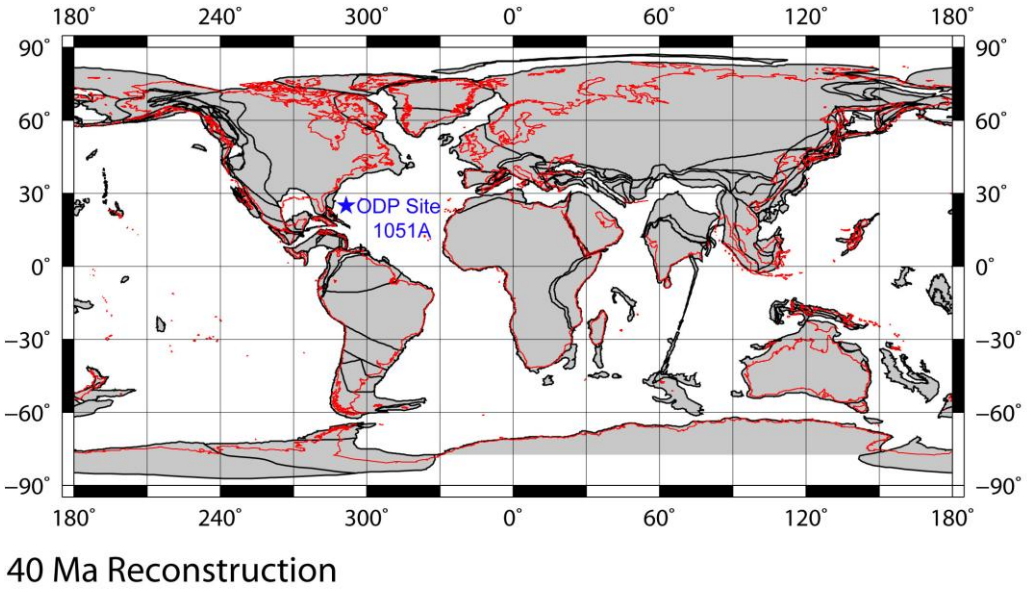

Figure 1. Map projection indicates the location of ODP Site 1051A shown on paleogeographic map at 40 Ma (http://www.odsn.de/odsn/services/paleomap/paleomap.html).

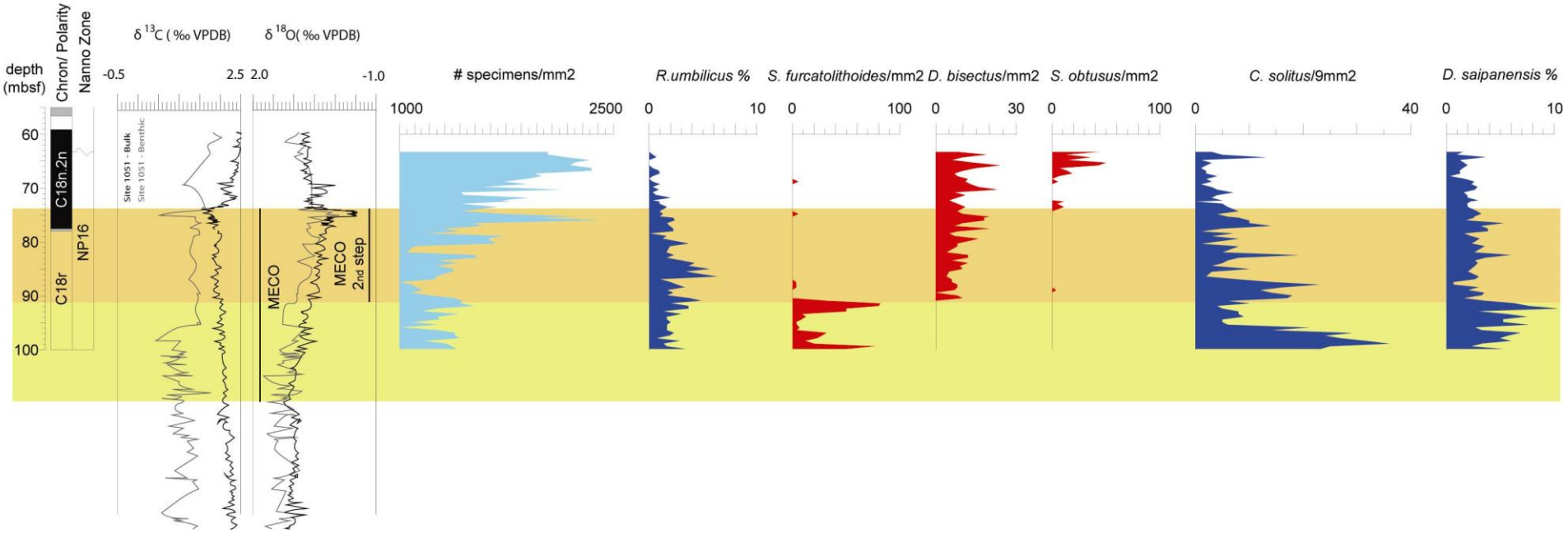

Figure 2. Abundance patterns of selected calcareous nannofossil index species used in biostratigraphy are reported against revised magnetostratigraphy (Edgar et al., 2010) and calcareous nannofossil biostratigraphy in ODP Site 1051A. Shown here are also $\delta^{18}O$ and $\delta^{13}C$ records (Bohaty et al., 2009). The shaded orange band indicates the position of the MECO, as defined by Bohaty et al. (2009). The shaded yellow band indicates the MECO 2nd step, in which most of changes in calcareous nannofossil assemblages are found to occur.

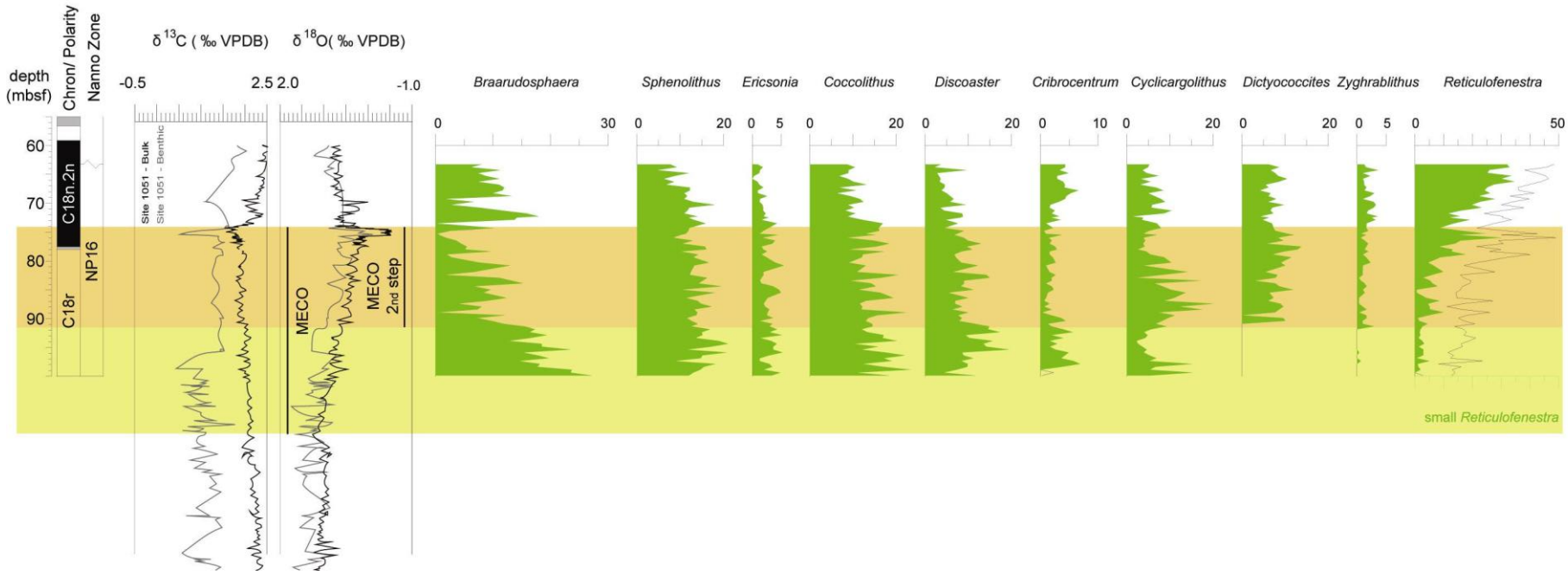

Figure 3. Abundance patterns of selected calcareous nannofossil taxa are reported against revised magnetostratigraphy (Edgar et al., 2010) and calcareous nannofossil biostratigraphy in ODP Site 1051A. Shown here are also $\delta^{18}O$ and $\delta^{13}C$ records (Bohaty et al., 2009). The shaded orange band indicates the position of the MECO, as defined by Bohaty et al. (2009). The shaded yellow band indicates the MECO 2nd step, in which most of changes in calcareous nannofossil assemblages are found to occur.

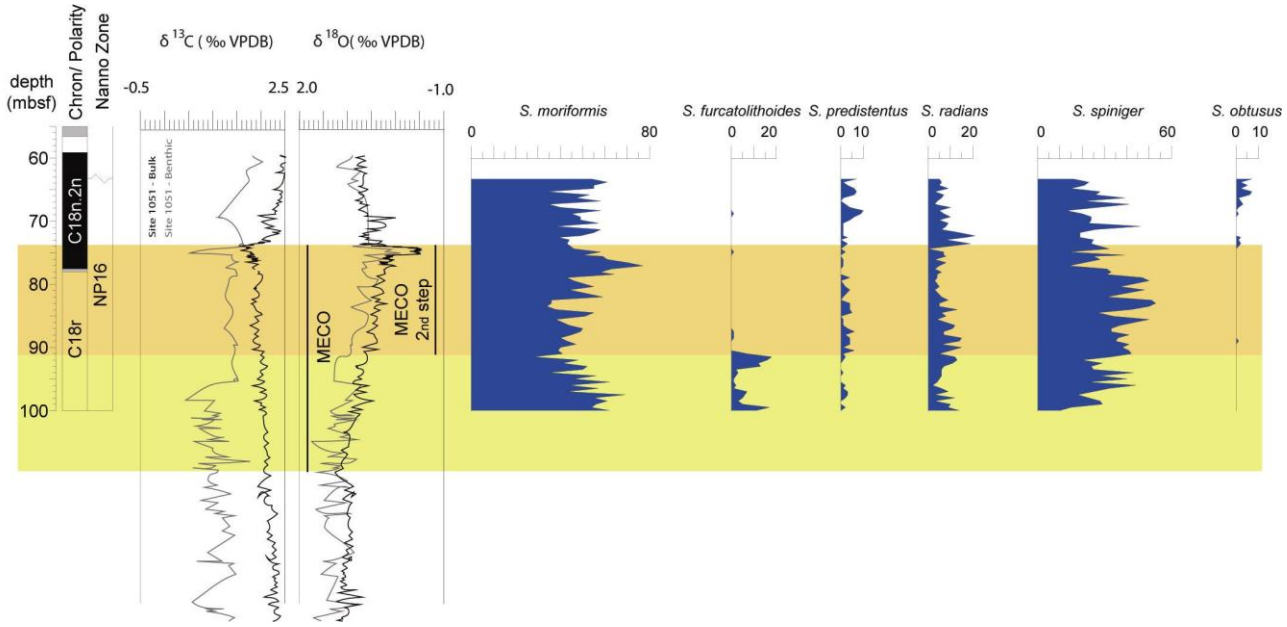

Figure 4. Abundance patterns of relative abundance (%) of selected species of *Sphenolithus* (%) calculated among sphenoliths on at least 100 are reported against revised magnetostratigraphy (Edgar et al., 2010) and calcareous nannofossil biostratigraphy in ODP Site 1051A. Shown here are also $\delta^{18}O$ and $\delta^{13}C$ records (Bohaty et al., 2009). The shaded orange band indicates the position of the MECO, as defined by Bohaty et al. (2009). The shadedyellow band indicates the MECO 2nd step, in which most of changes in calcareous nannofossil assemblages are found to occur.

Table

Biohorizon	**Sample**							**Depth**	**Chron Notation**[+]		**Age (Ma)**
	Leg	Site	H	Core	Sect	Int.	(cm)	(mbsf)			CK95*
Chron 18n.1r base								59,12 59,14			
S. obtusus LO	171 171	1051 1051	A A	8H 8H	5 6	117 17	119 19	68,76 69,26	C18n.2n	0.49	39.88
Chron 18n.2n base								78,54 79,64			
D. bisectus LCO	171 171	1051 1051	A A	10H 10H	6 7	110 10	112 12	90,40 90,90	C18r	0.23	40.39
S. furcatolithoides HO	171 171	1051 1051	A A	10H 10H	6 7	110 10	112 12	90,40 90,90	C18r	0.23	40.39
Chron 18r base								128,70 128,72			

° Revised magnetostratigraphy is after Edgar et al. (2010).

*Ages are based on the GPTS of Cande and Kent (1995; CK95).

[+]The relative positions of calcareous nannofossil biohorizons within magnetochrons follow the advice of Hallam et al. (1985) and Cande and Kent (1992).

Table 1. Depth (mbsf), Chron notation and Age (Ma) of calcareous nannofossil biohorizons from ODP Site 1051A using the GPTS of Cande and Kent (1995; CK95).

Plate I. Microphotographs of calcareous nannofossil from the ODP Leg 171B, Site 1051A in the middle and late Eocene interval of Blake Nose Transect, Florida Continental Margin. All specimens × 1000. 1-2. *Coccolithus eopelagicus.* Sample 171B-1051A-8H-6W, 17 1 Crossed nicols. 2 Parallel light, 3-4. *Coccolithus cachaoi*. Sample 171B-1051A-8H-3W, 116. 3 crossed nicols. 4 parallel light. 5-6. *Ericsonia formosa*. Sample 171B-1051A-8H-3W, 116. 5 crossed nicols. 6 parallel light. 7-8. *Chiasmolithus consuetus* Sample 171B-1051A-8H-3W, 116. 7 crossed nicols. 8 parallel light. 9-10. *Chiasmolithus grandis.* Sample 171B-1051A-8H-3W, 116. 9 Crossed nicols. 10 Parallel light. 11-12. *Chiasmolithus solitus.* Sample 171B-1051A-9H-1W, 57. 11 Crossed nicols. 12 Parallel light. 13. *Dictyococcites bisectus.* Sample 171B-1051A-9H-4W, 70. Crossed nicols. 14. *Dictyococcites bisectus.* Sample 171B-1051A-8H-3W, 116. Parallel light. 15-16. *Reticulofenestra umbilicus.* Sample 171B-1051A-8H-6W, 17. 15 Crossed nicols. 16 Parallel light. 17-18. *Cribrocentrum reticulatum*. Sample 171B-1051A-8H-3W, 116. 17 Crossed nicols. 18. Parallel light. 19-20. *Clausicoccus obrutus*. Sample 171B-1051A-8H-3W, 116. 19 Crossed nicols. 20. Parallel light. 21-22. *Braarudosphaera* spp. Sample 171B-1051A-8H-3W, 116. 21 Crossed nicols. 22. Parallel light. 23-24. *Thoracosphaera* spp. Sample 171B-1051A-8H-3W, 35. 23 Crossed nicols. 24. Parallel light.

PLATE I

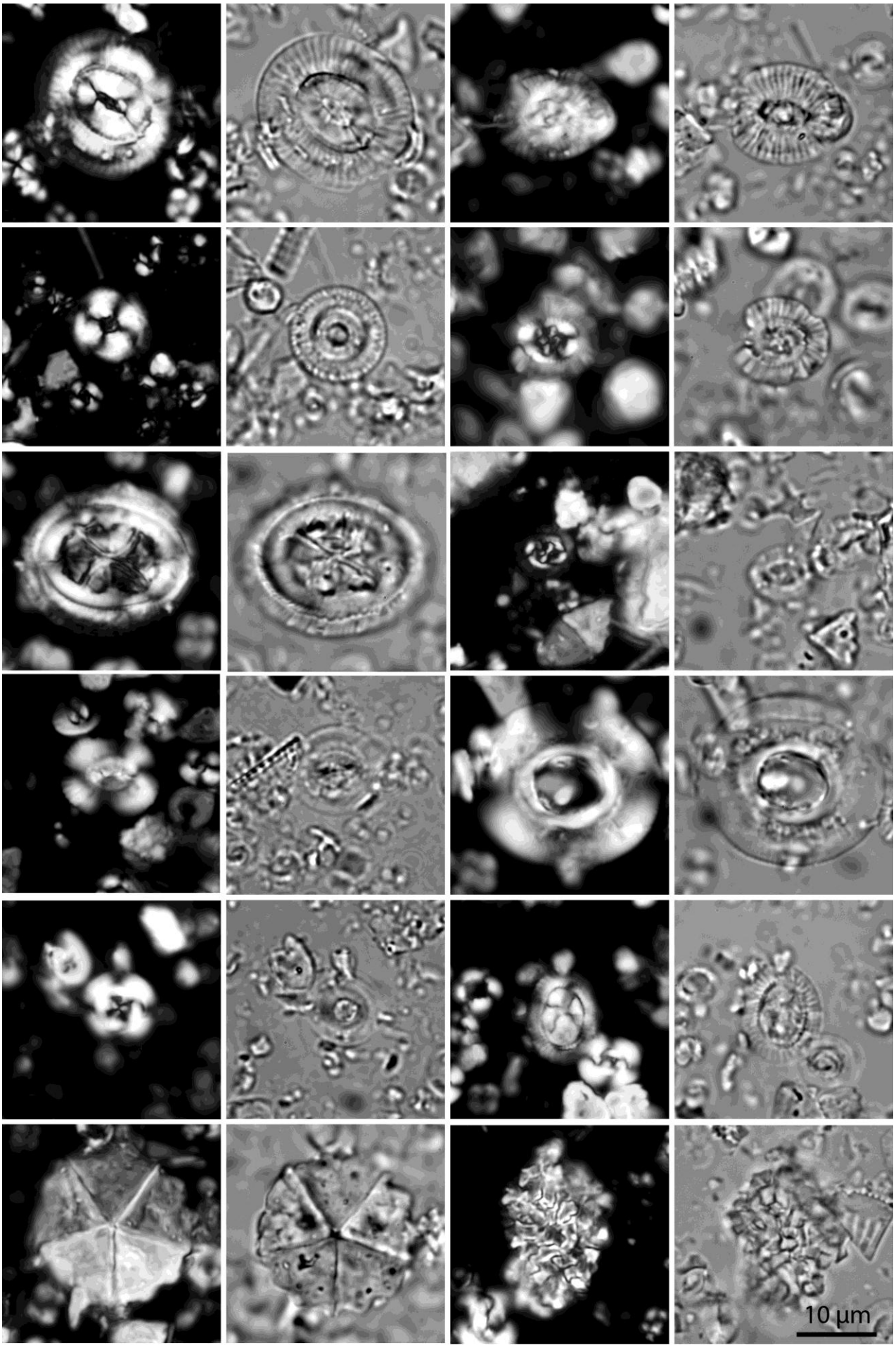

Plate II. Microphotographs of calcareous nannofossil from the ODP Leg 171B, Site 1051A in the middle and late Eocene interval of Blake Nose Transect, Florida Continental Margin. All specimens × 1000. 1-3. *Sphenolithus furcatolithoides.* Sample 171B-1051A-11H-5W, 55 1. Crossed nicols 0°. 2. Crossed nicols 30°. 3. Crossed nicols 45°. 5-7. *Sphenolithus spiniger.* Sample 171B-1051A-11H-5W, 55 5. Crossed nicols 0°. 6. Crossed nicols 30°. 7. Crossed nicols 45°, 4 and 8. *Sphenolithus radians*. Sample 171B-1051A-8H-3W, 116. 4. Crossed nicols 0°. 8. Crossed nicols 45°. 9–11. *Sphenolithus predistentus.* Sample 171B-1051A-8H-5W, 67. 9. Crossed nicols 0°. 10. Crossed nicols 30°. 11. Crossed nicols 45°. 12. *Sphenolithus moriformis.* Sample 171B-1051A-9H-1W, 57. Crossed nicols. 13-15. *Sphenolithus predistentus-distentus.* Sample 171B-1051A-8H-5W, 67. 13. Crossed nicols 0°. 14. Crossed nicols 30°. 15. Crossed nicols 45°. 17-19. *Sphenolithus obtusus.* Sample 171B-1051A-8H-3W, 116. 17. Crossed nicols 0°. 18. Crossed nicols 30°. 19. Crossed nicols 45°. 16. *Discoaster tanii*; Sample 171B-1051A-8H-3W, 116. Parallel light.. 20. *Discoaster binodosus* gr. *hirundinus*; Sample 171B-1051A-10H-5W, 110. Parallel light. 21. *Discoaster saipanensis*; Sample 171B-1051A-11H-2W, 5. Parallel light.. 22. *Discoaster barbadiensis*; Sample 171B-1051A-10H-5W, 110. Parallel light. 23-24 *Zyghrablithus bijugatus*; Sample 171B-1051A-11H-2W, 5. 23. Crossed nicols. 24. Parallel light.

PLATE II

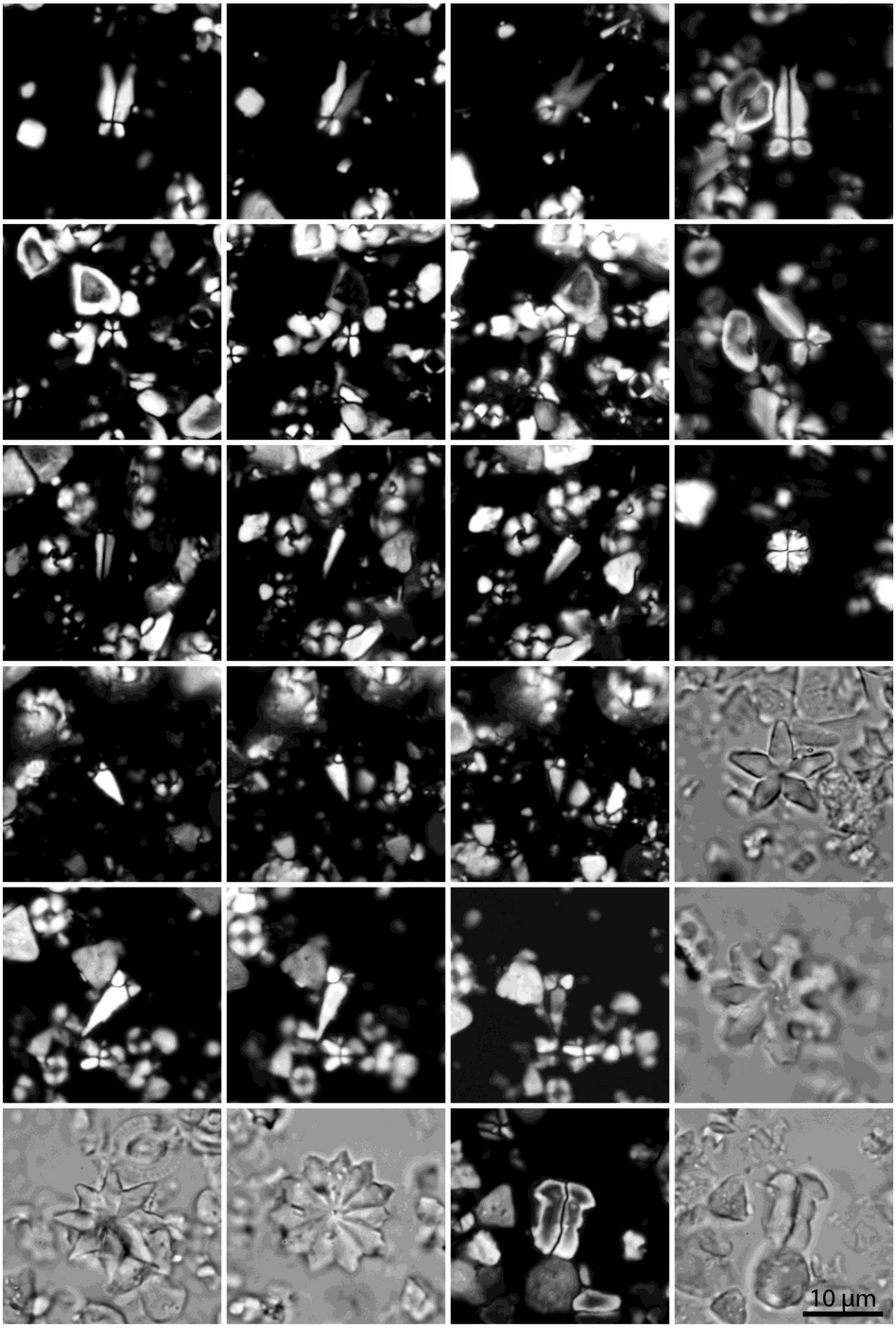

References

Agnini, C., Muttoni, G., Kent, D.V., and Rio D., 2006, Eocene biostratigraphy and magnetic stratigraphy from Possagno, Italy: The calcareous nannofossil response to climate variability, Earth Planet. Sci. Lett., 241, 815–830, doi:10.1016/j.epsl.2005.11.005.

Agnini, C., Fornaciari, E., Raffi, I., Rio, D., Röhl, U., Westerhold, T., 2007b. High resolution nannofossil biochronology of middle Paleocene to early Eocene at ODP Site 1262: Implications for calcareous nannoplankton evolution, Mar. Micropaleontol., 64, 215 – 248, doi:10.1016/j.marmicro. 2007.05.003.

Agnini C., Fornaciari E., Giusberti L., Grandesso P., Lanci L., Luciani V., Muttoni G., Rio D., Stefani C., Pälike H. and Spofforth D.J.A, 2011 Integrated bio-magnetostratigraphy of the Alano section (NE Italy): a proposal for defining the Middle-Late Eocene boundary, Geological Society of America Bulletin.

Aubry M.-P.,1998, Early Paleogene calcareous nannoplankton evolution: a tale of climatic amelioration, in late Paleocene and early Eocene climatic and biotic evolution. In: M.-P. Aubry, S. Lucas and W. Berggren, Editors, Late Paleocene–early Eocene climatic and biotic events in the marine and terrestical record, Columbia University Press (1998), pp. 158–203.

Aubry, M.-P., 1984. Handbook of Cenozoic Calcareous Nannoplankton, book 1, Ortholithae (Discoaster). Am. Mus. of Nat. Hist. Micropaleontol. Press, New York. 263 pp.

Aubry, M.-P., 1988. Handbook of Cenozoic Calcareous Nannoplankton, book 2, Ortholithae (Holococcoliths, Ceratoliths, Ortholiths and Other). Am. Mus. of Nat. Hist.Micropaleontol. Press, New York. 279 pp.

Aubry, M.-P., 1989. Handbook of Cenozoic Calcareous Nannoplankton, book 3, Ortholithae (Pentaliths and Other), Heliolithae (Fasciculiths, Sphenoliths and Others). Am. Mus. of Nat. Hist. Micropaleontol. Press, New York. 279 pp.

Aubry, M.-P., 1990. Handbook of Cenozoic Calcareous Nannoplankton, book 4, Heliolithae (Helicoliths, Cribriliths, Lopadoliths and Other). Am. Mus. of Nat. Hist.Micropaleontol. Press, New York. 381 pp.

Aubry, M.-P., 1999. Handbook of Cenozoic Calcareous Nannoplankton, book 5, Heliolithae (Zygoliths and Rhabdoliths). Am. Mus. of Nat. Hist.Micropaleontol. Press, New York. 368 pp.

Backman, J., 1987. Quantitative calcareous nannofossil biocronologyof middle Eocene through early Oligocene sediments fromDSDP Sites 522 and 523. Abhandlungen Der GeologischenBundesanstalt 39, 21-31.

Bailey, D. K. (1992), Episodic alkaline igneous activity across Africa: Implications for the causes of continental break-up, Geol. Soc. Spec. Publ., 68, 91-- 98, doi:10.1144/GSL.SP. 1992.068.01.06.

Bailey, D. K. (1993), Carbonate magmas, J. Geol. Soc. London, 150(4), 637 -- 651, doi:10.1144/gsjgs.150.4.0637.

Bohaty S. M., and Zachos, J. C., 2003. Significant Southern Ocean warming event in the late middle Eocene, Geology, 31(11), 1017– 1020, doi:10.1130/G19800.1

Bohaty S. M., Zachos J. C., Florindo F., Delaney M. L. 2009, Coupled greenhouse warming and deep-sea acidification in the middle Eocene, Paleoceanography, 24 , PA2207.

Bown, P.R., and Young, J.R., 1998. Techniques. *In* Bown, P.R. (Ed.), Calcareous Nannofossil Biostratigraphy: London, Chapman & Hall, 16–28.

Bralower T. J., 2002, Evidence for surface water oligotrophy during the Paleocene-Eocene Thermal Maximum: Nannofossil assemblage data from Ocean Drilling Program Site 690, Maud Rise, Weddell Sea, Paleoceanography, v. 17, no. 2, 10.1029/2001PA000662.

Bukry, D., 1971. Cenozoic calcareous nannofossils from the Pacific Ocean. Transactions of the San Diego Society of Natural History, 16:303–328.

Bramlette, M.N. and Martini, E.; 1964, The great ch’ange in calcareous nannoplankton fossils between the Maestrichtian and Danian; Micropaleontology, v. 10, p. 291-322. do:10.2307/1484577.

Cambray, H., and J. P. Cadet (1996), Synchronisme de l'activite volcanique d'arc: Mythe ou realite?, C. R. Acad. Sci., Ser. IIa Sci. Terre Planetes, 322(3), 237 - 244.

Cande, S.C., Kent, D.V., 1992. A new geomagnetic polarity timescale for the Late Cretaceous and Cenozoic. J. Geophys. Res. 97, 13917–13951.

Cande, S.C., Kent, D.V., 1995. Revised calibration of the geomagnetic polarity time scale for the Late Cretaceous and Cenozoic. J. Geophys. Res. 100 (B4), 6093–6096. doi:10.1029/94JB03098.

Diester-Haass, L., and Zahn, R., 1996, Eocene–Oligocene transition in the Southern Ocean: History of water mass circulation and biological productivity: Geology, v. 24, p. 163–166.

Dunkley Jones, T., Bown, P.R., Pearson, P.N., Wade, B.S., Coxall, H.K., Lear, C.H. 2008. Major shifts in calcareous phytoplankton assemblages through the Eocene-Oligocene transition of Tanzania and their implications for low-latitude primary production. Paleoceanography 23, PA4204, doi:10.1029/2008PA001640.

Edwards, A.R. and Perch-Nielsen, K., 1975. Calcareous nannofossils from the southwest Pacific, D.S.D.P., Leg 29. In Kenneth, J. P., Houtz, R. A., et al., Init. Rep. of the D. S. D. P., vol. 29, pp. 469-539.

Edgar, K.M.; Wilson, P.A. Sexton, P.F.; Gibbs, S.J.; Roberts, A.P.; Norris, R.D., 2010; New biostratigraphic, magnetostratigraphic and isotopic insights into the Middle Eocene Climatic Optimum in low latitudes Original Research Article Palaeogeography, Palaeoclimatology, Palaeoecology, Volume 297, Issues 3--4, 20, Pages 670-682

Erba, E., 2006. The first 150 million years history of calcareous nannoplankton: biosphere-geosphere interactions. Palaeogeography, Palaeoclimatology, Palaeoecology, 232: 237-250.

Fornaciari, E., Agnini, C., Catanzariti, R., Rio, D., Bollad, E.M., Valvasoni, E., 2010. Mid-latitude calcareous nannofossil biostratigraphy, biochronology and evolution across the middle to late Eocene transition. Stratigraphy, vol. 7, no. 4, text-figures 1-16, tables 1-3, plates 1-2, pp. 229-264.

Gibbs, S. J., Shackleton, N. J., and Young, J. R., 2004, Orbitally forced climate signals in mid-Pliocene nannofossil assemblages, Mar. Micropaleontol., 51, 39 – 56, doi:10.1016/ j.marmicro.2003.09.002.

Gibbs, S.J., Bralower, T.J., Bown, P.R., Zachos, J.C., Bybell, L.M., 2006. Shelf and open-ocean calcareous phytoplankton assemblages across the Paleocene–Eocene thermal maximum: implications for global productivity gradients. Geology 34 (4), 233–236.

Gibbs, S. J., Stoll, H. M., Bown, P. R., and Bralower, T. J.,2010: Ocean acidification and surface water carbonate production across the Paleocene-Eocene Thermal Maximum, Earth Planet Sci. Lett., 295, 583--592, doi:10.1016/j.epsl.2010.04.044

Hagino, K., Okada, H., 2001. Morphological observations of living Gephyrocapsa crassipons, J. Nannoplankton Res. 23, 3–7.

Hallam, A., Hancock, J.M., LaBreque, J.L., Lowrie, W., Channell, J.E.T., 1985. Jurassic to Palaeogene magnetostratigraphy. In: Snelling, N.J. (Eds.), The Chronology of the Geological Record. Geol. Soc. London, vol. 10, pp. 118–140.

Haq, B.U. and Lohmann, G.P., 1976. Early Cenozoic Calcareous nannoplankton biogeography of the Atlantic Ocean: Marine Micropaleo., v. 1, p. 120-197.

Jovane L., Florindo, F., Coccioni, R., Dinare`s-Turell, J., Marsili, A., Monechi, S., Roberts, A. P. and Sprovieri, M., 2007, The middle Eocene climatic optimum event in the Contessa Highway section, Umbrian Apennines, Italy, Geol. Soc. Am. Bull., 119 (3 – 4), 413 – 427, doi:10.1130/B25917.1Lyle, Wilson, Janecek, et al., 2002

Kelly, D.C.; Norris, R.D.; Zachos, J.C., 2003; Deciphering the paleoceanographic significance of Early Oligocene Braarudosphaera chalks in the South Atlantic Marine Micropaleontology 49 49-63

Kerrick, D. M., and K. Caldeira (1999), Was the Himalayan orogen a climatically significant coupled source and sink for atmospheric CO2 during the Cenozoic?, Earth Planet. Sci. Lett., 173, 195 -- 203, doi:10.1016/S0012-821X(99) 00229-0.

Larrasoaña, J.C., Gonzalvo, C., Molina, E., Monechi, S., Ortiz, S., Tori, F. & Tosquella, J. 2008: Integrated magnetobiochronology of the Early/Middle Eocene transition at Agost (Spain): Implications for defining the Ypresian/Lutetian boundary stratotype. *Lethaia*,Vol. 41, pp. 395–415

Luciani, V., Giusberti, L., Agnini, C. Fornaciari, E., Rio, D., Spofforth, D.J.A., Pälike, H.. 2010. Ecological and evolutionary response of Tethyan planktonic foraminifera to the middle Eocene climatic optimum (MECO) from the Alano section (NE Italy), Palaeogeography, Palaeoclimatology, Palaeoecology 292 (2010) 82–95.

Marino M., Flores J.A. (2002) -Middle Eocene to early Oligocene calcareous nannofossil stratigraphy at Leg 177 Site 1090. (2002) - Marine Micropaleontology, 45: 383-398.

Martini E., 1971, Standard Tertiary and Quaternary calcareous nannoplankton zonation, in Farinacci, A., ed., Proceedings, International Conference on Planktonic Microfossils, second, Rome, Volume 2: Rome, Italy, Tecnoscienza Editzione, p. 739-785.

Miller, K.G., Wright, J.D., and Fairbanks, R.G., 1991. Unlocking the Ice House: Oligocene–Miocene oxygen isotopes, eustasy, and margin erosion. J. Geophys. Res., 96:6829–6848.

Mita, I., 2001. Data Report: Early to late Eocene calcareous nannofossil assemblages of Sites 1051 and 1052, Blake Nose, northwestern Atlantic Ocean. *In* Kroon, D., Norris, R.D., and Klaus, A. (Eds.), *Proc. ODP, Sci. Results,* 171B, 1–28 [Online]. Available from www: <http://wwwodp.tamu.edu/publications/171B_SR/VOLUME/CHAPTERS/SR171B07.PDF>

Norris, R.D.; Kroon, D.; Klaus, A. 2001 Introduction: Cretaceous---Paleogene Climatic Evolution of the Western North Atlantic, Results from ODP Leg 171B, Blake Nose doi:10.2973/odp.proc.sr.171B.101.2001

Okada, H., 2000. Neogene and Quarternary calcareous nannofossils from the Blake Ridge, Sites 994, 995, and 997. *In* Paull, C.K., Matsumoto, R., Wallace, P.J., and Dillon, W.P. (Eds.), Proc. ODP, Sci. Results*,* 164: College Station, TX (Ocean Drilling Program), 331-341.

Okada, H., and Bukry, D., 1980. Supplementary modification and introduction of code numbers to the low-latitude Coccolith biostratigraphic zonation, (Bukry, 1973; 1975). Mar. Micropaleontol., 5:321-325

Ogg, J.G., and Bardot, L., 2001. Aptian through Eocene magnetostratigraphic correlation of the Blake Nose Transect (Leg 171B), Florida continental margin. *In* Kroon, D., Norris, R.D., and Klaus, A. (Eds.), *Proc. ODP, Sci. Results,* 171B, 1–58 [Online]. Available from World Wide Web: <http://www-odp.tamu.edu/ publications/171B_SR/VOLUME/ CHAPTERS/SR171B09.PDF>.

Pälike, H., Lyle, M., Nishi, H., Raffi, I., Gamage, K., Klaus, A., and the Expedition 320/321 Scientists, 2010. Proc. IODP, 320/321: Tokyo (Integrated Ocean Drilling Program Management International, Inc.). doi:10.2204/iodp.proc.320321.105.2010

Perch-Nielsen, K. 1985, Cenozoic calcareous nannofossils. In Bolli H.M., Saunders J.B., Perch-Nielsen K. Plankton Stratigraphy. Cambridge University Press.

Persico, D. and Villa G., 2004, Eocene-Oligocene calcareous nannofossils from Maud Rise and Kerguelen Plateau (Antarctica): palaeoecological and palaeoceanographic implications. Mar. Micropaleontol. 52, 153-179.

Rio, D., Raffi, I., Villa, G., 1990. Pliocene–Pleistocene calcareous nannofossil distribution patterns in the western Mediterranean. Proc. Ocean Drill. Program Sci. Results 107, 513–533.

Roth, P.H., 1983. Jurassic and Lower Cretaceous calcareous nannofossils in the Western North Atlantic (Site 534): biostratigraphy, preservation, and some observations on biogeography and paleoceanography. Initial Reports of the Deep Sea Drilling Project 76, 587-621.

Roth, P.H., Thierstein, H.R. 1972. Calcareous nannoplankton: Leg XIV of the Deep Sea Drilling Project. In D. E. Hayes & A. C. Pimm (Eds.), Initial Reports of the Deep Sea Drilling Project 14, :421-486. Schlanger, S.O., and Jenkins, H.C., 1976*,* Cretaceous anoxic events: Causes and consequences: Geologie en Mjinbouw*,* v. 55p. 179-184.

Sexton, P.F., Wilson, P.A., Norris, R.D., 2006. Testing the Cenozoic multisite composite $\delta^{18}O$ and $\delta^{13}C$ curves: New monospecific Eocene records from a single locality, Demerara Rise (Ocean Drilling Program Leg 207). Paleoceanography 21, PA2019, doi:10.1029/2005PA001253.

Spofforth D.J.A., Agnini C., Pälike H., Rio D., Fornaciari E., Giusberti L:, Luciani V., Lanci L., and Muttoni G., 2010. Organic carbon burial following the middle Eocene climatic optimum in the central western Tethys. Paleoceanography 25, PA3210, doi:10.1029/2009PA001738.

Toffanin, F., Agnini, C., Fornaciari, E., Rio, D., Giusberti, L., Luciani, V., Spofforth, D.J.A., Pälike, H., 2011 Changes in calcareous nannofossil assemblages during the Middle Eocene Climatic Optimum: Clues from the central-western Tethys (Alano section, NE Italy), Marine Micropaleontology, Volume 81, Issues 1–2, November 2011, Pages 22-31, ISSN 0377-8398, 10.1016/j.marmicro.2011.07.002.

Toffanin, F., Agnini, C., Rio, D., Acton, G., Westerhold, T. In prep. Middle Eocene to Early Oligocene calcareous nannofossil biostratigraphy at Site U1333C (Pacific Equatorial)

Tremolada, F., Bralower, T.J., 2004. Nannofossil assemblage fluctuations during the Paleocene–Eocene Thermal Maximum at Sites 213 (Indian Ocean) and 401 (North Atlantic Ocean): palaeoceanographic implications. Mar. Micropaleontol. 52, 107–116.

Villa G. Persico D., 2006. Late Oligocene climatic changes: Evidence from calcareous nannofossils at Kerguelen Plateau Site 748 (Southern Ocean). Palaeogeogr., Palaeoclimatol., Palaeoecol. 231(1-2), 110-119.

Villa, G., Fioroni, C., Pea, L., Bohaty, S. M., Persico, D., 2008. Middle Eocene– late Oligocene climate variability: Calcareous nannofossil response at Kerguelen Plateau, Site 748. Mar. Micropaleontol. 69, 173–192, doi:10.1016/ j.marmicro.2008.07.006.

Wade, B.S. and Kroon, D. 2002 Middle Eocene regional climate instability: Evidence from the western North Atlantic. Geology, 30 (11): 1011-1014.

Wei, W., Wise, S.W., 1990a, Biogeographic gradients of middle Eocene-Oligocene calcareous nannoplankton in the South Atlantic Ocean. Palaeogeogr. Palaeoclimatol. Palaeoecol. 79, 29– 61.

Young, J.R., 1994. Functions of coccoliths. In: Winter, A, Siesser, W.G., Eds., *Coccolithophores*, p. 63–82. Cambridge: Cambridge University Press.

Zachos, J.C., Pagani, M., Sloan, L., Thomas, E., Billups, K., 2001, Trends, rhythms, and aberrations in global climate 65 Ma to present: Science 292, 686–693.

CHAPTER 5 – Conclusions

In this PhD thesis, we investigated the response of calcareous nannofossil assemblages to the MECO event in three different sections, located in different areas and depositional settings.

ODP Site 1051A, located at low-mid latitudes in the NW Atlantic, is one of the reference section for this interval. Our data on calcareous nannofossil assemblages evidence for several modifications during this long warming phase starting from the mid part of Chron C18r and ending within Chron C18.2n. At this site, the onset of the MECO is very expanded and the $\delta^{18}O$ negative shift, which defines the event, is well documented allowing a precise placing for the base of the event (Bohaty et al., 2009). The integration of calcareous nannofossil and stable isotopes data indicates that $\delta^{18}O$ changes foresee the biotic modifications by ca. 400 kyr possibly suggesting two different scenarios: 1- a large delay of the biotic component with respect to the abiotic one or 2- a nonexistence relationship between the changes in the physical enviroment and the response of the calcareous nannoflora.

The Alano section, located at mid latitudes of the paleo-Tethyan domain, is a middle-bathial on-land section in which the post-MECO event is particularly well documented. The post-MECO phase is defined and described in previous works carried out in the Alano section (Luciani et al., 2010; Spofforth et al, 2010; Agnini et al., 2011). This interval represents the recovery of the system and return to pre-event conditions. At Alano, the post-MECO is characterized by a prominent change in lithology from grey marls to laminated organic-enriched sediments. Calcareous nannofossil assemblages are integrated with geochemical (e.g., $\delta^{13}C$ and TOC) and lithologic (e.g., $CaCO_3$ content) proxies, which together suggest a scenario of enhanced weathering and high productivity, which, in turn, imply that the silicatic and biotic pumps could have played an important role in the restablisment of a new equilibrim in the aftermath of the MECO.

The IODP Site U1333C, located in the Equatorial Pacific, is a deep-sea site (paleodepth ca. 3800m). During the MECO event the sedimentation experienced a virtual collapsing of the carbonate sediments, intepreted as a CCD shoaling (Lyle et al. , 2005; Pälike et al., 2010). The strong dissolution and the almost complete absence of calcareous nannofossils prevented from any paleoecological recostruction. However, the correlation

with the other two study sections, indicate that the CCD shoaling had profoundly altered the pristine sediments in the deep-sea U1333C Site but was not so large to affect the shallower Alano section and ODP 1051A Site, in which there are no evidence for strong dissolution in sediments/rocks.

Thought the distinctive features of the three study section, a number of mofications in calcareous nannofossil assemblages have been observed worldwide during the MECO and post-MECO. These global changes are listed as follows:

1- The global long-lasting LCO of large *Dyctiococcites* (i.e., *D. bisectus* and *D. scrippsae*)

2- The global long-lasting profound reorganization among genus *Sphenolithus* (e.g., the HO of *S. furcatolithoides,* the LOs of *S. predistentus* and *S. obtutus*).

3- The global increase in the relative abundance of reticulofenestrids, especially the smaller ones.

However, we have also observed many changes in the relative abundance of calcareous nannofossil taxa within the assemblages that are not global in nature and instead represent a local/regional response to a global perturbation.

References

Agnini C., Fornaciari E., Giusberti L., Grandesso P., Lanci L., Luciani V., Muttoni G., Rio D., Stefani C., Pälike H., Spofforth D.J.A , 2011. Integrated bio-magnetostratigraphy of the Alano section (NE Italy): a proposal for defining the Middle-Late Eocene boundary, Geological Society of America Bulletin, 123, (5/6) 841-872. doi:10.1130/B30158.1.

Bohaty, S.M., Zachos, J.C., Florindo, F., Delaney, M.L. 2009. Coupled greenhouse warming and deep-sea acidification in the middle Eocene Paleoceanography 24 , PA2207.

Luciani, V., Giusberti, L., Agnini, C. Fornaciari, E., Rio, D., Spofforth, D.J.A., Pälike, H.. 2010. Ecological and evolutionary response of Tethyan planktonic foraminifera to the middle Eocene climatic optimum (MECO) from the Alano section (NE Italy), Palaeogeogr., Palaeoclimatol., Palaeoecol. 292, 82–95.

Lyle, M., Olivarez Lyle, A., Backman, J., and Tripati, A., 2005. Biogenic sedimentation in the Eocene equatorial Pacific—the stuttering greenhouse and Eocene carbonate compensation depth. In Lyle, M., Wilson, P.A., Janecek, T.R., et al., Proc. ODP, Init. Repts., 199: College Station, TX (Ocean Drilling Program), 1–35. doi:10.2973/odp.proc.sr.199.219.2005

Pälike, H., Nishi, H., Lyle, M., Raffi, I., Gamage, K., Klaus, A., and the Expedition 320/321 Scientists, 2010. Expedition 320/321 summary. In Pälike, H., Lyle, M., Nishi, H., Raffi, I., Gamage, K., Klaus, A., and the Expedition 320/321 Scientists, Proc. IODP, 320/321: Tokyo (Integrated Ocean Drilling Program Management International, Inc.). doi:10.2204/iodp.proc.320321.101.2010).

Spofforth D.J.A., Agnini C., Pälike H., Rio D., Fornaciari E., Giusberti L:, Luciani V., Lanci L., and Muttoni G., 2010. Organic carbon burial following the middle Eocene climatic optimum in the central western Tethys. Paleoceanography 25, PA3210, doi:10.1029/2009PA001738.